New Solutions of an Amplitude Equation Describing Transition in a Laminar Shear Flow

Thesis by
Michael J. Landman

In Partial Fulfillment of the Requirements

for the Degree of

Doctor of Philosophy

California Institute of Technology

Pasadena, California

June, 1987

(Submitted April 14, 1987)

Acknowledgments

I am much indebted to Prof. P. G. Saffman, whose great knowledge, guidance and encouragement have made this thesis not only possible, but an enjoyable experience. Thanks also go to Prof. E. Doedel for use of and assistance with the invaluable AUTO continuation software.

During my study at Caltech I have benefited from the help of many of the members of the Applied Math Department, and to them I am grateful for both friendship and many hours toiling at the blackboard. In particular I thank Jeff Aguilera, whose THEME macro package in TEX and great patience allow him to take the credit for how nice the words and equations look.

To my parents and sisters, I will always be grateful for their constant love and support, which despite vast distances has always been a source of encouragement.

In addition to my thanks to Caltech for financial support, I acknowledge the support of the Office of Naval Research (N00014-85-K-0205).

Abstract

In order to better understand the process of laminar-turbulent transition in parallel shear flows, the study of the stability of viscous flow between parallel plates, known as plane Poiseuille flow, is found to be a good prototype. For Reynolds number near the critical value at which a linear instability first appears, Stewartson and Stuart (1971) developed a weakly nonlinear theory for which an amplitude equation is derived describing the evolution of a disturbance in plane Poiseuille flow in two space dimensions. This nonlinear partial differential equation is now commonly known in the literature as the Ginzburg-Landau equation, and is of the form

$$\frac{\partial A}{\partial t} = (a_r + ia_i)\frac{\partial^2 A}{\partial x^2} + (Re - Re_c)A + (d_r + id_i)A|A|^2.$$

This dissertation concentrates on analyzing quasi-steady solutions of the Ginzburg-Landau equation, where

$$A = e^{-i\Omega t}\Phi(x - ct).$$

These solutions describe modulations to the wave of primary instability, with amplitude which is steady in an appropriate moving coordinate system. The ordinary differential equation describing the spatial structure of quasi-steady solutions is viewed as a low-dimensional dynamical system. Using numerical continuation and perturbation techniques, new spatially periodic and quasi-periodic solutions are found which bifurcate from the laminar state and undergo a complex series of bifurcations. Moreover, solitary waves and

other solutions suggestive of laminar transition are found numerically for Reynolds number on either side of Re_c, connecting the laminar state to finite amplitude states, some of the latter corresponding to known solutions of the full fluid equations. The existence of these new spatially quasi-periodic and transition solutions suggests the existence of a similar class of solutions in the Navier Stokes equations, describing pulses and fronts of instability, as observed experimentally in parallel shear flows.

Table of Contents

List of Figures

List of Tables

CHAPTER 1

Introduction

Since the Navier-Stokes equations were first formulated early last century, scientists have been investigating their ability to describe real fluid flow phenomena. In particular, the theoretical understanding of the nonlinear processes of laminar-turbulent transition through these equations is of fundamental importance. This thesis is motivated by the hope that the study of solutions of a simplified equation approximating the Navier-Stokes equations can lead to new insight into the still poorly understood nonlinear structure of the full fluid equations.

The equation on which this study concentrates is of the form

$$\frac{\partial A}{\partial t} = a\frac{\partial^2 A}{\partial x^2} + (Re - Re_c)A + dA|A|^2. \tag{1.1}$$

The coefficients a and d are complex, and the equation has become widely known in the literature as the (generalized) Ginzburg-Landau (GL) equation and has been studied in a variety of contexts. For a list of references see Keefe (1985). Of most interest here is that this amplitude equation was derived by Stewartson and Stuart (1971) to describe the weakly nonlinear evolution of 2-dimensional disturbances to plane Poiseuille flow at Reynolds numbers close to the critical Reynolds number Re_c of linear instability.

Plane Poiseuille flow can be regarded as a prototype for many parallel shear flows, and describes the driven flow of a fluid of viscosity ν bounded by parallel plates separated a distance $2h$, as illustrated in Figure 1.1. At all Reynolds numbers $Re = U_0 h/\nu$, a basic laminar parabolic flow exists, where U_0 is chosen to be the maximum velocity determined by the strength of the forcing (an applied pressure gradient or

flux condition). At a finite value Re_c this base flow becomes linearly unstable to infinitesimal disturbances in the channel. By developing a weakly nonlinear theory in a vicinity of this instability, the GL equation is derived. A describes the amplitude of the envelope modulating the marginally stable waves given by linear theory, as viewed in the reference frame moving with the group velocity. This relationship between the GL equation and the Navier-Stokes equations is explained further in the following section.

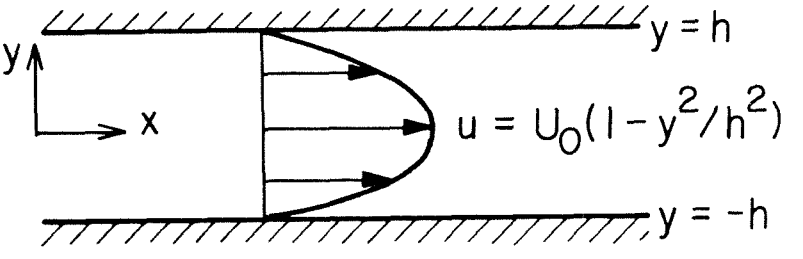

FIGURE 1.1. Geometry of plane Poiseuille flow.

In the study of the GL equation, most investigators have concentrated on the case when the real part of the coefficient of the nonlinear term, d_r, is negative. A negative value of d_r arises when the GL equation is derived as the amplitude equation describing a supercritical bifurcation as in convection problems (Newell and Whitehead, 1969). In this case the GL equation has been shown to exhibit a large variety of behaviors, including chaotic behavior both temporally (Moon *et al.* (1983), Keefe (1985)) and spatially (Deissler (1985), C. Holmes and Wood (1985), P. Holmes (1986)).

For 2-dimensional plane Poiseuille flow and other systems with a subcritical bifurcation, d_r is positive however, in which case the GL equation has quite different behavior. The analysis in the literature for this case is chiefly concerned with seeking time dependent singularities of solutions of (1.1) (Hocking and Stewartson 1972);

however their analysis and numerical studies failed to find singular bursts in finite time for the Poiseuille parameters. Nevertheless the large quantity of recent literature studying the initial value problem of the GL equation concentrates on having $d_r < 0$ due to the common belief that having the nonlinearity of the opposite sign leads to singularities in the numerical integration. Our experience with integrating the GL equation for Poiseuille flow does confirm this when periodic boundary conditions are applied, though given an infinite domain with localized initial conditions (as simulated by Hocking and Stewartson), the amplitude may remain bounded and the time dependent behavior appears to be very complicated. In preference to solving the initial value problem with a variety of initial and boundary conditions, however, the main aim of this dissertation is to discover the more fundamental underlying structure of the Ginzburg-Landau equation.

This thesis is concerned with the structure of solutions of the Ginzburg-Landau equation (1.1) with the simple time dependence

$$A = e^{-i\Omega t}\Phi(x - ct). \tag{1.2}$$

We shall call solutions of this form quasi-steady, where the function Φ satisfies a second order complex ordinary differential equation of the form of a damped Duffing equation. We concentrate on studying this equation for the coefficient values applicable to 2-dimensional plane Poiseuille flow.

Solutions of the form (1.2) with $c = 0$ have been studied by several authors for the GL equation with d_r negative (Sirovich and Newton (1986), C. Holmes and Wood (1985)). These studies have primarily concentrated on a single branch of spatially periodic solutions ($\Phi(x) = \Phi(x + L)$) which bifurcates supercritically from the nontrivial stable uniform solution of the GL equation as an appropriate parameter is varied. P. Holmes (1986) has also studied quasi-steady solutions with

$c = 0$ for the perturbed nonlinear Schrödinger equation which is of the form of the GL equation.

We have found a large class of solutions of the form (1.2) for the GL equation with d_r positive which are applicable to plane Poiseuille flow. A previously known subset of solutions is those of the plane waves

$$A = Be^{i(kx-\Omega t)}. \tag{1.3}$$

These correspond to the well known finite amplitude travelling wave solutions of the full fluid equations for flow between parallel plates. Bifurcations from the plane wave solutions (1.3) and the trivial solution have recently been discussed by C. Holmes (1985) using center manifold theory.

We have been able to find other spatially periodic and quasi-periodic solutions of the GL equation. When $Re > Re_c$ a third branch of periodic envelope solutions bifurcates from the Orr-Sommerfeld neutral curve in addition to the pair of plane wave solutions. This new family of solutions has amplitude greater than the amplitude B of the solutions (1.3). When $Re < Re_c$ other periodic solutions are found to exist for d_r positive which are analogous to those studied by other investigators for d_r negative. We continued these branches numerically in the parameters Ω and c, and find a complex structure of other spatially periodic and quasi-periodic solutions bifurcating from them. These solutions all describe slow spatial modulations to the neutrally stable waves.

One of the main contributions of this thesis is that by using a dynamical systems approach, a wide variety of solitary wave solutions have been discovered, which connect the physically attainable states of the plane waves and the zero amplitude undisturbed laminar state. These solutions can be of breather type decaying at plus and minus infinity, front-like describing a transition from disturbed to laminar flow or hole-like describing localized modulations of the plane wave states. They may

exist for either a discrete or a continuous spectrum of c and Ω, and augment some of the previously known exact solutions of the GL equation (Nozaki and Bekki, 1984). Other more general transitions from the laminar or plane wave states to spatially quasi-periodic or apparently chaotic states in space and time have also been found numerically.

The remainder of this introduction briefly describes how the GL equation is derived in the stability theory of plane Poiseuille flow. We then consider in Chapter 2 a complex second order ordinary differential equation of the form of a complex damped Duffing equation, which arises in the study of quasi-steady solutions of the form (1.2). This 4-dimensional dynamical system may in some instances be reduced to a 3-dimensional first order system, which is similar to systems recently discussed by other authors but in different parameter regimes. We analyze the stability and bifurcation structure of the 4- and 3-dimensional systems in Chapters 3 and 4 which is preliminary to the perturbation theory and numerical investigations which follow. Chapters 5 and 6 explore the structure of spatially periodic and quasi-periodic solutions of the GL equation using these dynamical systems. We have found that families of such solutions bifurcate from known exact solutions of the GL equation, and in Chapter 5 we show how these solutions may be described perturbatively. In Chapter 6 numerical continuation is used to show that these solutions are part of a very complex structure of finite amplitude solutions of the GL equation. Chapter 7 investigates the possible quasi-steady solitary wave solutions of the GL equation, with a description of the previously known exact solutions in the setting of the 3-dimensional equations. A numerical search reveals a far larger class of solitary waves and their generalization to other transitions from the trivial and plane wave solutions. Chapter 7 is thus of most interest to the shear flow problem and the description of the transition of undisturbed flow.

Real shear flow instability is of course fully 3-dimensional in space and is often found to occur well below the critical Reynolds number of linear theory. In accordance with this, numerical evidence suggests that the quasi-steady solutions of the GL equation for Poiseuille flow are unstable, as described in Chapter 8. Nevertheless, corresponding branches of solutions may exist for the Navier-Stokes equations for Poiseuille flow which stabilize at finite amplitude and lower Re than the critical Re_c of 5772. This scenario is in fact true for the continuation of the plane wave solutions in the space of 2-dimensional Navier-Stokes solutions. It is thus our belief that the Stewartson-Stuart weakly nonlinear theory may give rise to solutions which are present in the full Navier-Stokes equations which may be relevant to the process of transition. This conjecture will be further discussed in the last chapter of this work.

1.1 Stability of plane Poiseuille flow and derivation of the GL equation

In parallel shear flow the GL equation arises by considering the weakly nonlinear evolution of a 2-D disturbance to steady laminar incompressible viscous flow between two horizontal plates. We take x in the streamwise direction and y in the vertical direction, where all variables are nondimensionalized with respect to the channel half-width h and maximum velocity U_0 of the parabolic base flow. The boundary conditions imposed are those of constant flux and no slip at the walls. See Figure 1.1.

Before outlining the derivation of the GL equation, it is useful to first describe the well understood linear stability analysis for this flow (Drazin and Reid, 1981). We consider infinitesimal perturbations to the laminar flow stream function

$$\psi_0 = y(1 - \frac{1}{3}y^2),$$

where the velocity components are $(u, v) = (\psi_y, -\psi_x)$. The perturbation stream function may be decomposed into normal modes of the form

$$\psi' = \phi(y)e^{i\alpha(x-ct)},$$

and on substituting $\psi = \psi_0 + \psi'$ into the 2-dimensional incompressible Navier-Stokes equations one finds on linearization

$$\begin{aligned} \frac{i}{\alpha Re}(\phi^{\mathrm{iv}} - 2\alpha^2\phi'' + \alpha^4\phi) + (\psi_0' - c)(\phi'' - \alpha^2\phi) - \psi_0'''\phi = 0 \\ \phi(-1) = \phi(1) = \phi'(-1) = \phi'(1) = 0. \end{aligned} \tag{1.4}$$

This equation is known as the Orr-Sommerfeld equation and is an eigenvalue equation for the complex growth rate $c(\alpha, Re)$. This equation has undergone extensive study for the stability of many basic shear flows.

The Orr-Sommerfeld equation must in general be solved numerically, and for plane Poiseuille flow a curve of marginal stability $c_i(\alpha, Re) = 0$ is found as shown in Figure 1.2. A similar curve is also found for the Blasius boundary layer, for example, though for circular pipe and plane Couette flow it is believed that the flow is linearly stable at all Reynolds numbers.

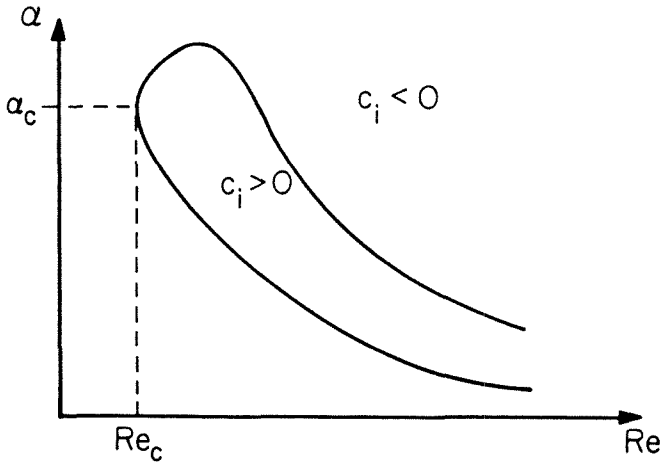

FIGURE 1.2. The Orr-Sommerfeld neutral curve.

From the Orr-Sommerfeld marginal curve one finds that there is a minimum critical Reynolds number Re_c for which there is a linearly unstable disturbance, given by

$$\psi' = \phi_1(y)e^{i\alpha_c(x-c_{cr}t)}$$

with c_{cr} real. We call this marginally stable wave the Tollmien-Schlichting (T-S) wave in analogy to that found in boundary layers. For $Re < Re_c$ linear theory predicts that the base flow is stable, but when $Re > Re_c$ a disturbance exists which has exponential growth in time, up to the point when the assumption that the disturbance is small breaks down. In the case of a boundary layer, the classic experiments of Schubauer and Skramstad (1947) indicate remarkably good agreement with the corresponding Orr-Sommerfeld curve for the Blasius profile, across which instability sets in. Experiments in plane Poiseuille flow are much harder to perform, but by carefully controlling disturbances in the flow Nishioka *et al.* (1975) has results consistent with the curve of Figure 1.2. With less controlled conditions, however, experimentalists find that laminar transition occurs at Reynolds numbers far less than the critical, suggesting the existence of subcritical finite amplitude states for these flows.

In order to extend linear theory to account for small but finite disturbances in the flow, Stewartson and Stuart (1971) used a weakly nonlinear formulation based on the method of multiple time scales. The motivation for such a method is that near Re_c, a continuum of modes of wavenumber α is destabilized. These interact with each other causing variations on slow time and spatial scales. We now briefly outline this method which leads to the Ginzburg-Landau equation.

Following Stewartson and Stuart (1971), the stream function ψ is expanded about the parabolic base flow in both a power series in the small parameter ϵ (proportional to amplitude of the modulation) and in a harmonic series of the most

unstable wave (the Tollmien–Schlichting wave given by linear theory). The lowest order term which describes modulations to the neutrally stable wave is given by

$$\psi - \psi_0 = \epsilon \hat{A}(\xi, \tau)\ \phi_1(y)\ \ e^{i\alpha_c(x - c_{cr}t)} + \text{c.c.} + O(\epsilon^2) \tag{1.5}$$

where ξ and τ are the scaled slow streamwise coordinate and slow time given by

$$\xi = \epsilon(x - c_g t)\ , \qquad \tau = \epsilon^2 t\ .$$

c_g is the group velocity at which the energy of the modulation propagates according to linear theory, and $\phi_1(y)$ is the first Orr-Sommerfeld eigenfunction at the nose of the Orr-Sommerfeld neutral stability curve where $Re = Re_c$. In this way ϵ may also be thought of as being related to the inverse length and time scales of the disturbance.

The Reynolds number is found to scale with ϵ^2 and we write

$$s_r(Re - Re_c) = \epsilon^2 \sigma_r \tag{1.6}$$

where s_r is a fixed positive constant given below and is included for consistency with Stewartson and Stuart. In their original derivation they chose to scale $|\sigma_r| = 1$, whereas for the present we consider σ_r as an order one parameter determining the Reynolds number. We find that this approach has the advantage that the structure of solutions on either side of the critical Reynolds number can be studied without the necessity for ϵ and thus the amplitude to go through zero.

All of the constants above may be calculated from the linear dispersion relation (i.e., the Orr-Sommerfeld neutral stability curve), and from Davey, Hocking and Stewartson (1974) these are given by

$$Re_c = 5772.2 \qquad c_{cr} = 0.264 \qquad \alpha_c = 1.02$$

$$s_r = 0.168 \times 10^{-5} \qquad c_g = 0.383\,.$$

The GL equation for $\hat{A}$ is derived by substituting the expansion (1.5), including higher order corrections to the base flow and harmonics of the T-S wave, into the

Navier-Stokes equations. At order $O(\epsilon^3)$ a solvability condition must be satisfied for the inhomogeneous equation and the GL equation

$$\frac{\partial \hat{A}}{\partial \tau} = b\frac{\partial^2 \hat{A}}{\partial \xi^2} + \frac{s}{s_r}\sigma_r \hat{A} + \kappa \hat{A}|\hat{A}|^2 \tag{1.7}$$

results.

The coefficients relevant to Poiseuille flow have been calculated numerically and we quote these values from Davey *et al.* (1974) as

$$b = 0.187 + 0.0275i \qquad \kappa = 30.8 - 173i \qquad s = (0.168 + 0.811i) \times 10^{-5}. \tag{1.8}$$

On rescaling $\hat{A}$ to A and ξ to x (distinct from the fast scale x) in (1.7) such that

$$A = \sqrt{|\kappa_r|}\exp(-i\sigma_r s_i \tau / s_r)\hat{A}, \qquad x = \xi/\sqrt{b_r},$$

we are able to scale the magnitudes of the real parts of b and κ to unity and make the coefficient of the linear term real. We then get the normal form of the GL equation

$$\frac{\partial A}{\partial t} = (a_r + ia_i)\frac{\partial^2 A}{\partial x^2} + \sigma_r A + (d_r + id_i)A|A|^2 \tag{1.9}$$

where we have also replaced the slow variable τ with t for convenience of notation. Note that $a_r \geq 0$ is necessary for well-posedness, and we will assume this condition throughout. From the relevant values (1.8) the coefficients in equation (1.9) become

$$\begin{aligned} a_r &= 1 & d_r &= 1 \\ a_i &= 0.147 & d_i &= -5.62\ . \end{aligned} \tag{1.10}$$

These coefficients are thus determined solely by the physics and in what follows we will use their values to guide the parameter ranges in which we are interested. Although the above scaling can always be performed provided $b_r\kappa_r \neq 0$, in general we will retain a_r and d_r in our analysis, but use the values (1.10) in our numerical calculations. We will also find it useful to define the quantities

$$a_0 \equiv a_i/a_r, \qquad d_0 \equiv d_i/d_r.$$

CHAPTER 2

Quasi-steady Solutions of the Ginzburg-Landau Equation

In the following chapter we introduce the ordinary differential equations which govern the spatial character of quasi-steady solutions of the GL equation, of the form $A = e^{-i\Omega t}\Phi(x-ct)$. We first discuss plane wave solutions as a special case. We then introduce the complex damped Duffing equation that Φ satisfies, which defines a 4-dimensional dynamical system which can in general be reduced to 3-dimensions. We end with a discussion of some general properties of these systems, which will be of importance to later analysis.

2.1 Plane wave solutions

The simplest and best known exact solutions of the GL equation

$$\frac{\partial A}{\partial t} = (a_r + ia_i)\frac{\partial^2 A}{\partial x^2} + \sigma_r A + (d_r + id_i)A|A|^2 \tag{2.1}$$

are those of constant amplitude plane waves

$$A = Be^{i(kx-\Omega t)} \tag{2.2}$$

where

$$|B| = \sqrt{\frac{a_r k^2 - \sigma_r}{d_r}}\,, \qquad \Omega = (a_i - d_0 a_r)k^2 + d_0\sigma_r$$

and the phase of B is arbitrary. For the Poiseuille coefficients, if $\sigma_r < 0$ ($Re < Re_c$) these wavetrain solutions exist for all wave numbers k and have amplitude bounded above zero. When $\sigma_r > 0$ ($Re > Re_c$) we require $k^2 > \sigma_r/a_r$. For a given σ_r and

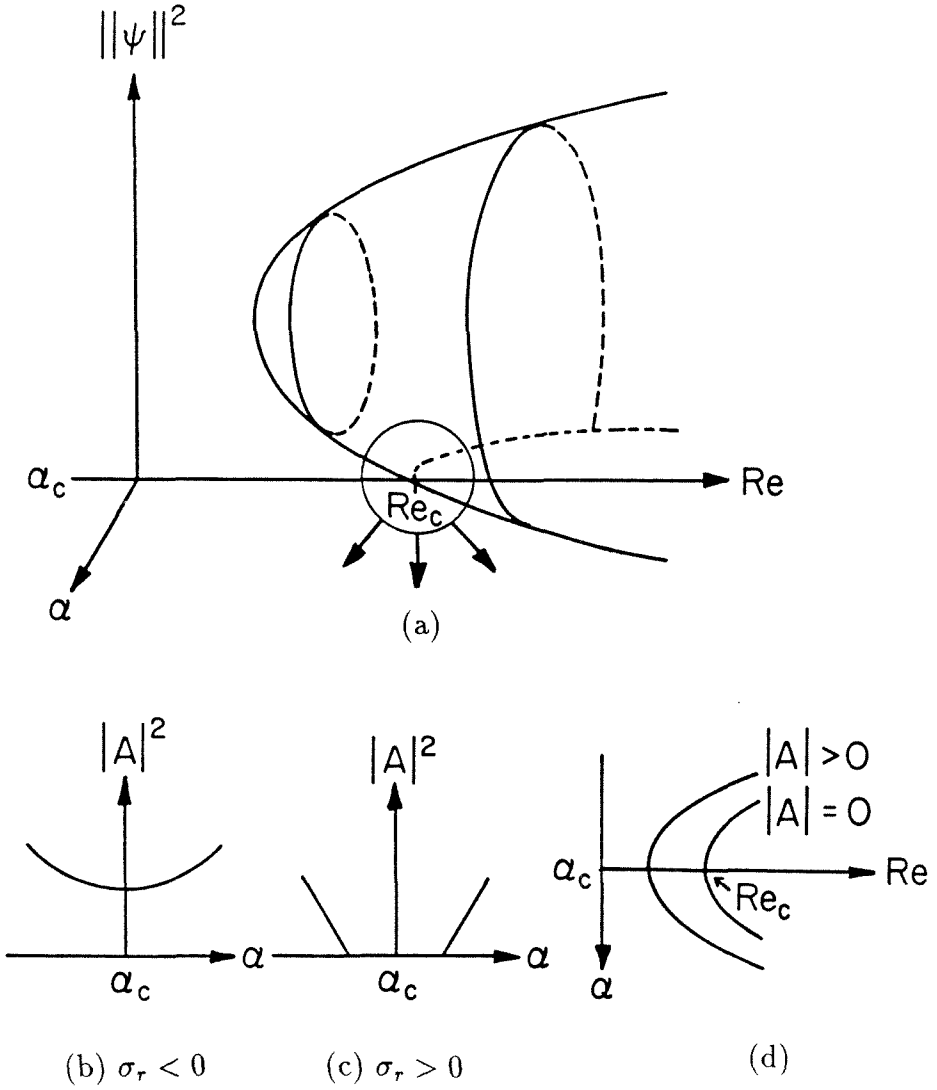

FIGURE 2.1. Solution surface of 2-dimensional travelling waves for plane Poiseuille flow.
(a) Energy surface as a function of Reynolds number and wave number α.
(b)–(d) Small amplitude approximation given by the GL plane wave solutions.

wavenumber a pair of plane waves exists; the solution with wave number $k > 0$ we call T_+, the other with wavenumber $k < 0$ we call T_-.

These wave solutions describe for small amplitude the two-dimensional finite amplitude periodic travelling wave solutions of Poiseuille flow that bifurcate from the undisturbed flow (as predicted by the Orr-Sommerfeld eigenvalue curve). The

stream function of these finite amplitude waves is of the form

$$\psi = F(x - c_p t, y, Re, \alpha),$$

where F is of period $2\pi/\alpha$ in the first variable and satisfies no slip boundary conditions in y. See Figure 2.1. c_p is then determined by a nonlinear dispersion relation for a range of Re and α. These equilibrium states have been studied by several investigators (Zahn *et al.* (1974), Herbert (1981)) and are found to lie on a surface in $(Re, \alpha, Amplitude)$ space which exists down to Reynolds numbers of about 2500. The surface is double valued in amplitude and the upper branch is stable to 2-dimensional superharmonic disturbances (Pugh, 1987).

Note that by allowing σ_r to be an order one parameter we can see that a family of plane waves of equal amplitude exists in a neighborhood of the "nose" of the Orr-Sommerfeld curve on the locus $\sigma_r = a_r k^2 + constant$ which gives a relation between the Reynolds number versus the wavenumber for these waves.

2.2 The complex damped Duffing equation and related dynamical systems

More generally we can seek solutions to the GL equation (2.1) of the form

$$A = e^{-i\Omega t}\Phi(x - ct), \tag{2.3}$$

where the wave speed c provides an order ϵ correction to the group velocity of linear theory if we go back to the derivation of A from the stream function. The modulus of the complex amplitude is therefore steady in a frame of velocity $c_g + \epsilon c$. Substitution of (2.3) into the GL equation gives the ordinary differential equation for $\Phi(X)$ as a function of $X = x - ct$

$$(a_r + ia_i)\Phi'' + c\Phi' + (\sigma_r + i\Omega)\Phi + (d_r + id_i)\Phi|\Phi|^2 = 0.$$

It is convenient to rewrite this equation as

$$\Phi'' + (c_1 + ic_2)\Phi' + (\delta_1 + i\beta)\Phi = (\delta_2 + i\gamma)\Phi|\Phi|^2 \tag{2.4}$$

where from the Poiseuille coefficients (1.10)

$$\begin{aligned} \beta &= \frac{a_r\Omega - a_i\sigma_r}{|a|^2} & \gamma &= \frac{a_i d_r - a_r d_i}{|a|^2} = 5.65 \\ \delta_1 &= \frac{a_r\sigma_r + a_i\Omega}{|a|^2} & \delta_2 &= -\frac{a_r d_r + a_i d_i}{|a|^2} = -0.170 \\ c_1 &= \frac{ca_r}{|a|^2} & c_2 &= -\frac{ca_i}{|a|^2}. \end{aligned} \tag{2.5}$$

Equation (2.4) is a complex version of the damped Duffing equation. This equation has been studied in the undamped case ($c = 0$) by Sirovich and Newton (1986), C. Holmes and Wood (1985) and P. Holmes (1986) although in different parameter regimes than the one in which we are interested.

The 6 parameters above are of course not all independent and they may be reduced in number by rescaling at most two of them. We have sometimes found it convenient to scale the magnitudes of δ_1 and δ_2 to unity, by scaling amplitude and space. In so doing four cases of the complex Duffing equation arise depending on the signs of δ_1 and δ_2. In general we will remain with the parameters (2.5) however, noting that varying Ω is equivalent in scaled parameters to varying β and fixing δ_1.

The equation (2.4) describes the spatial behavior of quasi-steady solutions (2.3) of the GL equation and is the equation on which this study will concentrate. Notice there are two undetermined parameters Ω and c, the temporal frequency of oscillation and the group velocity correction respectively. The coefficients γ and δ_2 in the complex damped Duffing equation are regarded as being determined by the physics of the problem. $c_1 = -c_2/a_0$ is linear in c, and β and δ_1 depend linearly on Ω and also the Reynolds number parameter σ_r.

If we consider the Reynolds number as fixed, then as in Stewartson and Stuart we can set $|\sigma_r| = 1$ through the invariance

$$(\sigma_r, \Omega, c, \Phi, x) \rightarrow (L^2\sigma_r, L^2\Omega, Lc, L\Phi, x/L). \tag{2.6}$$

Thus given any single solution, a family of self-similar solutions exists as σ_r is varied, which become singular as $\sigma_r \rightarrow 0$. This does not exclude the existence of families of solutions in a neighborhood of $\sigma_r = 0$ however, as is true in the instance of the plane wave solutions.

A plane wave solution of wavenumber k, when cast in the framework of quasi-steady solutions, will exist on the line

$$\Omega + kc = (a_i - d_0 a_r)k^2 + d_0\sigma_r \tag{2.7}$$

in Ω–c parameter space. In this way these solutions are redundantly represented, although distinct solutions bifurcate from a given plane wave only for specific values of Ω and c. In Figure 2.2, lines of constant wavenumber (each corresponding to a single plane wave) are shown as a function of the two parameters for the Poiseuille coefficients and $\sigma_r = 1$, which is representative of the supercritical case $\sigma_r > 0$. In this case we see there is a band of excluded k, and specifying Ω and c may result in describing zero (regions I and VI), one (regions IV) or both of the plane waves (elsewhere). For $\sigma_r < 0$ the regions IV and VI disappear and all wavenumbers are present, T_+ and T_- existing everywhere in parameter space except for the parabolic region I.

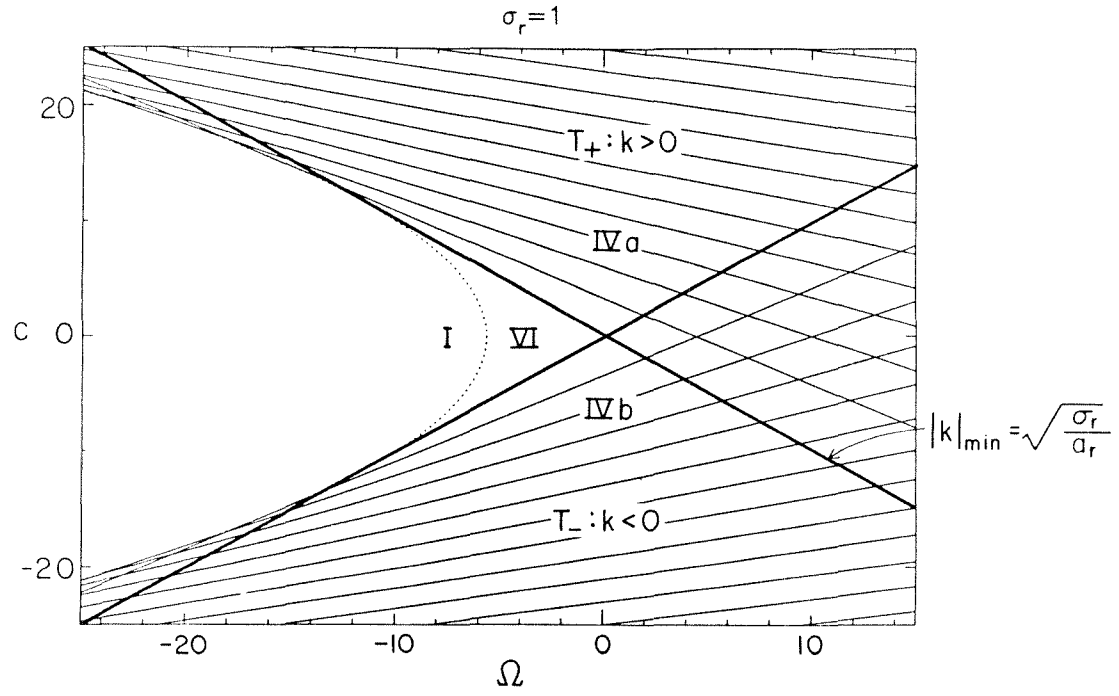

FIGURE 2.2. Lines of constant wavenumber for the plane waves $T_\pm$, $\sigma_r = 1$.

The second order complex O.D.E.'S (2.4) can be written as the first order real system for $\Phi = u + iv$ which is of the form

$$\begin{aligned} u' &= p \\ v' &= q \\ p' &= -\delta_1 u + \beta v + (\delta_2 u - \gamma v)(u^2+v^2) - c_1(p + a_0 q) \\ q' &= -\beta u - \delta_1 v + (\gamma u + \delta_2 v)(u^2+v^2) + c_1(a_0 p - q). \end{aligned} \tag{2.8}$$

Due to the phase invariance of the GL equation

$$A \to Ae^{i\theta} \tag{2.9}$$

this system possesses a rotational symmetry, given by

$$\begin{pmatrix} u \\ v \\ p \\ q \end{pmatrix} \to \begin{pmatrix} \mathrm{Q} & 0 \\ 0 & \mathrm{Q} \end{pmatrix} \begin{pmatrix} u \\ v \\ p \\ q \end{pmatrix} \tag{2.10}$$

where Q is the rotation matrix

$$\begin{pmatrix} \cos\theta & -\sin\theta \\ \sin\theta & \cos\theta \end{pmatrix}$$

with θ arbitrary. This symmetry can be eliminated by writing Φ as an amplitude and phase, thus removing this apparent degree of freedom. Following Sirovich and Newton (1986) it is convenient to use the variables r, s and w where

$$\Phi = r^{1/2} \exp\left[i \int^X s \, dX \right] , \qquad w = \frac{r'}{2r} \tag{2.11}$$

in order to get a system of 3 first order O.D.E.'s. After some algebra we arrive at the reduced equations

$$r' = 2wr \tag{2.12a}$$

$$s' = -\beta + \gamma r - 2sw - c_1(s - a_0 w) \tag{2.12b}$$

$$w' = -\delta_1 + \delta_2 r + s^2 - w^2 - c_1(a_0 s + w) \tag{2.12c}$$

which are a generalization of those of Sirovich and Newton who sought simpler quasi-steady solutions with $c = 0$ (and thus $c_1 = 0$).

Although this reduction to 3 dimensions makes much of the analysis of the complex Duffing equation considerably easier, a coordinate singularity is introduced at amplitude zero, and in general we must return to the 4-dimensional system (2.8) for solutions where the amplitude vanishes at a point.

It is interesting to note that if we write

$$z = \frac{d}{dX} \log \Phi$$

then

$$z = w + is$$

and equations (2.12) may be written

$$\begin{aligned} r' &= 2r\ \mathrm{Re}\{z\} \\ z' &= -(\delta_1 + i\beta) + (\delta_2 + i\gamma)r - c_1(1 - ia_0)z - z^2 \end{aligned} \tag{2.13}$$

which we will find to be a useful representation.

2.3 Some general properties of the complex Duffing sytems

We are primarily interested in classifying the spatial behavior of quasi-steady solutions of the GL equation. In this section we consider some simple properties of the complex damped Duffing equation derived in the previous section and the related 4- and 3-dimensional real systems.

An important property of the quasi-steady O.D.E. systems concerns the divergence of the corresponding flows. For the 4-dimensional system we find

$$\frac{\partial u'}{\partial u} + \frac{\partial v'}{\partial v} + \frac{\partial p'}{\partial p} + \frac{\partial q'}{\partial q} = -2c_1$$

and similarly for a modified reduced system with coordinates (r^2, s, w)

$$\frac{\partial r^{2'}}{\partial r^2} + \frac{\partial s'}{\partial s} + \frac{\partial w'}{\partial w} = -2c_1.$$

Hence as observed by other authors, when $c = 0$, in which case we seek solutions to the GL equation of the form

$$A = \Phi(x)e^{-i\Omega t},$$

the phase spaces are volume preserving and thus no stable attractors can exist. We find that the introduction of the speed correction c acts as a damping on phase volumes and that in the case of positive c solutions may exist which approach an attractor of zero volume in phase space as $X \to \infty$, where $X = x - ct$. Similarly by the reflection symmetry the phase spaces are volume expanding for $c < 0$, and attracting sets may exist as $X \to -\infty$. This phase space contraction does not imply

that phase volumes remain bounded in a region of phase space, however, which occurs in the Lorenz equations for example due to the existence of a Liapunov functional.

The discussion of stability of solutions in the phase space representations for Φ is relevant in determining the class of spatial variations possible for quasi-steady solutions of the GL equation. In particular, by monitoring the stability properties along a branch of solutions as a parameter is varied, one may determine bifurcations to new branches of solutions. Note however that these considerations are independent of the question of time dependent stability of quasi-steady solutions.

In addition to the rotational symmetry (2.9), the GL equation possesses a reflection symmetry which is important in determining the structure of quasi-steady solutions. This $x \to -x$ symmetry of the GL equation manifests itself in the 4-dimensional system (2.8) by the invariance

$$X \to -X \qquad c \to -c \qquad (u, v, p, q) \to (u, v, -p, -q) \tag{2.14}$$

and in the 3-dimensional system (2.12) by

$$X \to -X \qquad c \to -c \qquad (r, s, w) \to (r, -s, -w). \tag{2.15}$$

Introduction of a nonzero wave speed c destroys the reflection symmetry of the steady equations which otherwise exists when $c = 0$. It is easily shown that when $c \neq 0$ the equations cannot support symmetric solutions. However when $c = 0$ both symmetric and nonsymmetric solutions may exist.

When $c = 0$, apart from solutions with the even reflection symmetry

$$\Phi(x) = \Phi(-x), \tag{2.16}$$

the equation can support odd solutions such that

$$\Phi(x) = -\Phi(-x) \tag{2.17},$$

where we have written the axis of symmetry at $x = 0$ although this is of course arbitrary. An important observation to make is that if a solution possesses the odd symmetry, it will be singular in the reduced 3-dimensional phase space (2.12) because $\Phi(0) = 0$. It will therefore be necessary to study some quasi-steady solutions (namely odd periodic and solitary waves) with the 4-dimensional representation (2.8).

Solutions may possess both the odd and even symmetries about different origins, and we have found a fundamental branch of periodic solutions that bifurcates from the zero amplitude state with this double symmetry. This branch and its subsequent symmetry breaking bifurcations are studied in Chapters 5 and 6. This double symmetry is the same as that of the cosine function, being even about 0 and $L/2$ and odd about $L/4$ and $3L/4$.

If we seek periodic solutions in the 3-dimensional reduced representation, solutions of the complex Duffing equation may result which are periodic in 2 frequencies (quasi-periodic), and thus lie on a 2-torus in the 4-dimensional phase space. For periodic solutions obeying the even symmetry (2.15) when $c = 0$ it follows that

$$\bar{s} \equiv \frac{1}{L} \int_0^L s(x)dx = 0 \tag{2.18}$$

and therefore the resulting solutions for Φ, the spatial part of the amplitude A, are also L periodic when reconstructed by the transformation (2.11). Solutions of period L in the 3-dimensional phase space do not have to obey this reflection symmetry however, and we will find such solutions numerically in Chapter 6. Also recall that this symmetry will always be violated for periodic solutions with $c \neq 0$. In these cases the spatial variation of the corresponding GL solutions will be quasi-periodic with 2 spatial frequencies, since $\bar{s} \neq 0$ in general, and thus the resulting spatial

variation of A is

$$\Phi(X) = r^{1/2}(X)\exp(ip(X))\exp(i\bar{s}X)$$

where $r(X)$ and $p(X)$ are of period L. A will have the two spatial frequencies $1/L$ and $\bar{s}/2\pi$, as well as three temporal frequencies $1/cL$, $c\bar{s}/2\pi$, and $\Omega/2\pi$, which in general will be incommensurate. Such solutions are constructed using perturbation methods in Chapter 5. Note however that the modulus of the amplitude remains periodic of period L in both space and time.

CHAPTER 3

Phase Space Structure of the 4-dimensional Duffing System

We consider the equations describing the spatial dependence of quasi-steady solutions

$$\begin{aligned} u' &= p \\ v' &= q \\ p' &= -\delta_1 u + \beta v + (\delta_2 u - \gamma v)(u^2+v^2) - c_1(p + a_0 q) \\ q' &= -\beta u - \delta_1 v + (\gamma u + \delta_2 v)(u^2+v^2) + c_1(a_0 p - q). \end{aligned} \tag{3.1}$$

which were derived in Chapter 2 from the complex damped Duffing equation. The only fixed points of the system for (u, v, p, q) are the origin for all values of the coefficients (corresponding to the undisturbed state) and the ring of fixed points

$$u^2 + v^2 = \frac{\beta}{\gamma} \qquad \text{when} \qquad \Delta \equiv \delta_1 - \frac{\delta_2 \beta}{\gamma} \equiv \frac{d_r \Omega - d_i \sigma_r}{a_i d_r - a_r d_i} = 0$$

for all c. Recall that the existence of the rotational symmetry (2.10) implies that solutions in this phase space are only unique up to an arbitrary rotation. This ring of solutions occurs when the periodic plane wave orbits (2.2) of the GL equation coalesce to the spatially uniform state in a saddle-node bifurcation. For the Poiseuille flow coefficients this will occur for a particular value of the frequency Ω provided $\sigma_r < 0$. In the 4-dimensional space the travelling waves are given by

$$u = {r_T}^{1/2} \cos(s_T x + \theta) \qquad v = {r_T}^{1/2} \sin(s_T x + \theta) \tag{3.2}$$

where r_T and s_T are functions of the parameters as given in equation (4.6) below and θ is arbitrary.

The linearization about zero in the (u, v, p, q) phase space gives two eigenvalues satisfying

$$\lambda^2 + c_1(1 - ia_0)\lambda + \delta_1 + i\beta = 0 \tag{3.3}$$

with the other pair their complex conjugate. If we consider $\sigma_r \neq 0$ as fixed, then δ_1 and β cannot vanish as we vary Ω, and the origin will be a double spiral point in general. Therefore the only bifurcations that can occur from the origin will be of Hopf type, at which a pair of eigenvalues become pure imaginary ($\lambda = \pm i\omega$) and a branch of periodic solutions is possibly shed.

By setting $\lambda^2 = -\omega^2$ with ω real we find that

$$\omega^2 = (\beta/c_1)^2 = \delta_1 - a_0\beta \equiv \sigma_r/a_r$$

so a Hopf bifurcation occurs on the lines

$$\beta = \pm\sqrt{\frac{\sigma_r}{a_r}}c_1$$

or equivalently

$$\Omega = a_0\sigma_r \pm \sqrt{\frac{\sigma_r}{a_r}}c \quad \text{provided } \sigma_r > 0 \text{ and } c \neq 0. \tag{3.4}$$

These two lines in parameter space correspond to the place where each of the plane waves (3.2) bifurcates from zero amplitude for supercritical Reynolds numbers, thus confirming the predictions of the Hopf bifurcation theorem.

With somewhat more algebra, one may consider the real parts of the eigenvalues in equation (3.3) as a function of the two parameters. It is found that the origin is a stable fixed point of the 4-dimensional system in the region bounded by the lines (3.4) and $c > 0$. As σ_r approaches zero these lines coalesce and for $\sigma_r < 0$ the origin is always a spiral saddle.

Normally the determination of the (spatial) stability of the periodic orbits bifurcating in a Hopf bifurcation would require a lengthy calculation. However we know the branches of bifurcating plane wave solutions analytically and thus can infer their stability. Furthermore, by making use of the 3-dimensional reduced representation for Φ in which these solutions are simply represented by fixed points, we are also able to determine secondary bifurcations from these plane waves. These results will be discussed in the next chapter.

In the special case $c = 0$ and $\sigma_r > 0$, a double Hopf resonance occurs at $\Omega = a_0\sigma_r$ when Ω is varied due to the presence of symmetry. From equation (3.3), when $c = 0$ one complex conjugate pair of eigenvalues lies in the the right half-plane and the other in the left half-plane. These eigenvalues coalesce on the imaginary axis when $\beta = 0$ ($\Omega = a_0\sigma_r$), noting that $\delta_1 > 0$ at the bifurcation. This type of bifurcation is a topic of current interest in the literature (e.g. Golubitsky and Stewart 1985). Although the general analysis of this situation is still incomplete, we may expect periodic orbits (besides the plane waves) if not more complex dynamics, to exist nearby in parameter space.

Accordingly, we have found a third spatially periodic branch $P0$ of quasi-steady solutions bifurcating from the origin for fixed $c = 0$ and small $\beta > 0$ which displays the odd and even symmetries of Section 2.3 . Also a family of quasi-periodic solutions (2-tori) bifurcates from the trivial state if we vary c away from zero for small β. These 2-tori lie on a surface in the space of quasi-steady solutions which connects the plane wave solutions and the symmetric branch $P0$. This situation is analyzed using perturbation theory in Chapter 5 and is found in the numerical continuation of quasi-periodic orbits in Chapter 6.

CHAPTER 4

Phase Space Structure of the 3-dimensional Reduced O.D.E. System

In this chapter we study the properties of the reduced system

$$r' = 2wr \tag{4.1a}$$

$$s' = -\beta + \gamma r - 2sw - c_1(s - a_0 w) \tag{4.1b}$$

$$w' = -\delta_1 + \delta_2 r + s^2 - w^2 - c_1(a_0 s + w) \tag{4.1c}$$

which describes the spatial structure of quasi-steady solutions of the GL equation whose amplitude is bounded away from zero for finite $X = x - ct$. This 3-dimensional phase space is geometrically far easier to work with than the 4-dimensional space derived directly from the complex Duffing equation, and reveals several aspects of the dynamics of the Duffing equation more readily than the 4-dimensional representation.

Recall that we consider $\gamma > 0$ and $\delta_2 < 0$ as fixed, β and δ_1 are proportional to the undetermined temporal frequency Ω, and c_1 is proportional to the undetermined speed correction c.

When $c_1 = 0$ the above system is the same as that studied by Sirovich and Newton (1986) and in a slightly different forms by C. Holmes and Wood (1985) and P. Holmes (1986). The first two authors concentrated on studying a single branch of periodic solutions. P. Holmes (1986) studies small perturbations from the Hamiltonian case when $\beta = \gamma = 0$ (the nonlinear Schrödinger equation limit), and proves the existence of spatially periodic and quasi-periodic solutions. An analysis of the case $\delta_2 > 0$ has been carried out by Kopell and Howard (1981) and arises in the analysis of reaction diffusion equations.

We are interested in bifurcations from the laminar and plane wave states in Poiseuille flow. As each of these states is represented by a pair of fixed points in the reduced system, we consider the phase space structure of the 3-dimensional equations in order to find their stability in phase space, thereby giving us information about bifurcations to more complex spatial states. Also of interest are solutions describing spatial transition from the laminar and plane wave states, and thus we seek solutions to the equations (4.1) which tend to these fixed points at spatial infinity ($X = x - ct \to \pm\infty$).

The purpose of this chapter is therefore to discuss the existence and stability properties of the fixed points. This information will be important in the following chapters where we find periodic, quasi-periodic and solitary waves solutions of the GL equation for Poiseuille flow.

4.1 The invariant plane $r \equiv 0$ and the fixed points of laminar flow

An interesting aspect of the system (4.1) is that the plane $r \equiv 0$ is an invariant subspace. In this way the single fixed point of the 4-dimensional system is transformed into a singular plane in the polar representation.

If we consider the reduced system in this subspace

$$s' = -\beta - 2sw - c_1(s - a_0 w) \tag{4.2a}$$

$$w' = -\delta_1 + s^2 - w^2 - c_1(a_0 s + w), \tag{4.2b}$$

then it is possible to find an analytic solution by creating the complex variable

$$z = w + is$$

as introduced in Section 2.2 . The equations (4.2) reduce to

$$z' = -K_1 - K_2 z - z^2 \tag{4.3}$$

with solution

$$z = -\tfrac{1}{2}K_2 - \sqrt{\zeta}\tan(\sqrt{\zeta}X + i\rho) \tag{4.4}$$

where

$$K_1 = \delta_1 + i\beta \qquad K_2 = c_1(1 - ia_0), \qquad \zeta \equiv K_1 - \tfrac{1}{4}K_2^2 = \xi + i\eta,$$

and

$$\xi(\Omega, c) = \delta_1 - \tfrac{1}{4}c_1^2(1 - a_0^2) \qquad \eta(\Omega, c) = \beta + \tfrac{1}{2}a_0c_1^2.$$

ρ is a real constant of integration and the arbitrary shift in the origin of X is implicit.

There are two fixed points of the form $(0, s_0, w_0)$ which we call D_+ and D_-, corresponding to solutions of the quadratic (4.3) set equal to zero. It is interesting to note that this quadratic is identical to the eigenvalue equation (3.3) for the zero amplitude solution in 4 dimensions. Hence both values of w_0 must be negative if and only if the 4-dimensional fixed point is stable. These fixed points have coordinates

$$D_\pm : \quad \begin{aligned} s_0 &= \frac{a_0c_1}{2} \mp \mathrm{sgn}(\eta)\sqrt{\frac{|\zeta| + \xi}{2}} \\ w_0 &= \frac{-c_1}{2} \pm \sqrt{\frac{|\zeta| - \xi}{2}} \end{aligned} .$$

Both fixed points exist for all values of the parameters, except when they coalesce at $\xi = \eta = 0$. A branch cut in parameter space has to be chosen in order to continuously and unambiguously represent these fixed points. We have chosen this cut to be $\eta = 0$ when $\xi \leq 0$, which corresponds to the parabolic segment

$$\Omega = a_0\sigma_r - \frac{a_ic^2}{2|a|^2}, \qquad \Omega \geq -a_0\sigma_r.$$

On crossing this cut by varying Ω and c, D_+ and D_- swap identities.

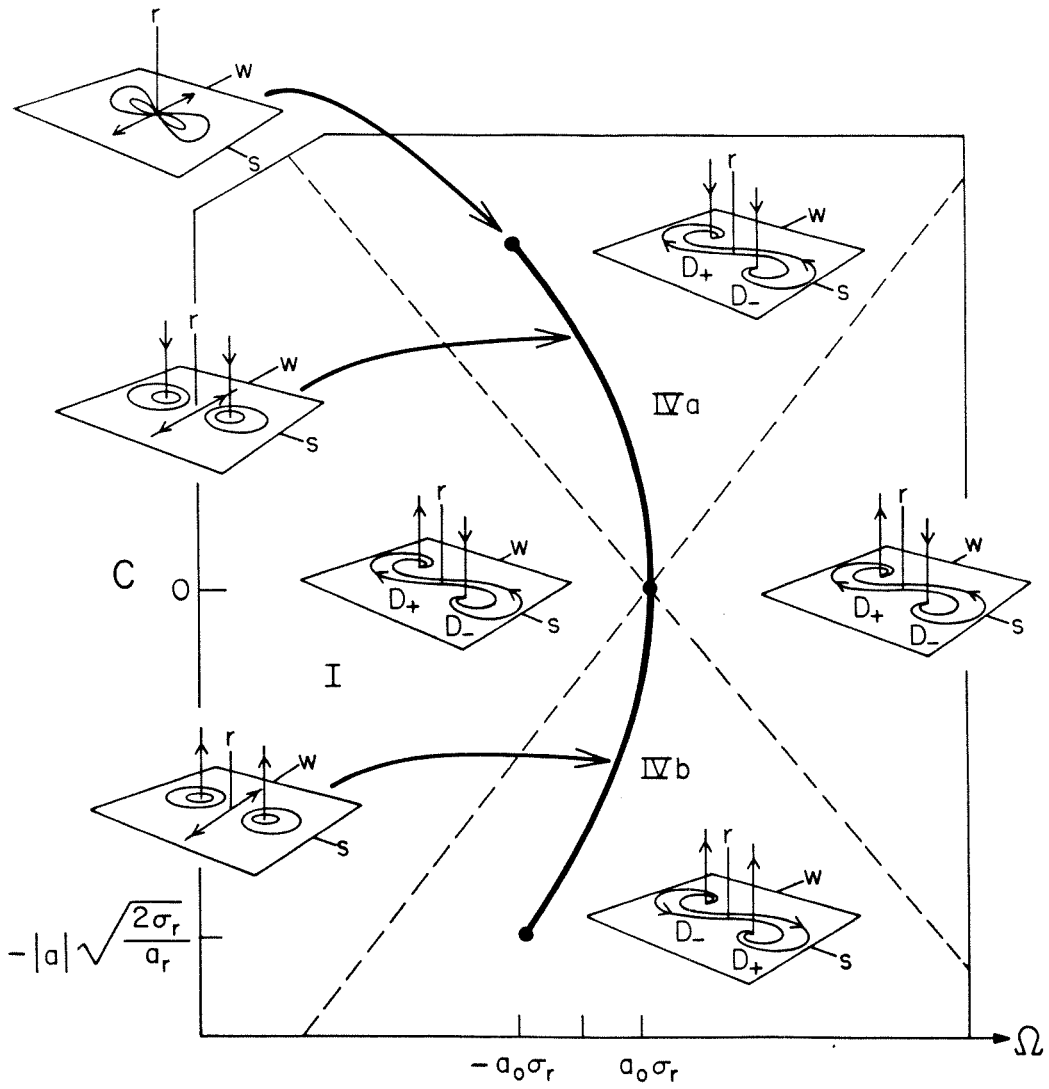

FIGURE 4.1. Phase portraits of the invariant plane for $\sigma_r > 0$.

As $\sigma_r \to 0$ the regions IV disappear and only phase portrait I persists for $\sigma_r < 0$.

The stability of these fixed points for the full 3-dimensional system is determined from the eigenvalues

$$\lambda_1 = 2w_0 \qquad \lambda_{2,3} = -(2w_0 + c_1) \pm i(2s_0 - a_0c_1).$$

By considering the real part of the complex conjugate eigenvalues we find that D_+ is a stable point of the invariant plane and D_- is unstable, except on the branch cut

where both points are marginally stable, the complex conjugate eigenvalues having their eigenspaces lying entirely in the invariant plane.

In Figure 4.1 we illustrate the stability results for $D_\pm$ in the 3-dimensional phase space. As we can expect the stability of the $\Phi = 0$ solution depends only on the real eigenvalue λ_1 at D_+ and D_- because λ_1 is proportional to the real part w_0 of z. Our results for the eigenvalue equation (3.3) therefore carry directly over and we find that D_+ is stable in the region bounded by the lines (3.4) and $c > 0$ and D_- is unstable in the region bounded by these lines and $c < 0$, provided $\sigma_r > 0$. Elsewhere in parameter space these fixed points are saddles, as is always the case when $\sigma_r < 0$.

In general then, from (4.4), all orbits within the plane are bounded with the exception of at most two unbounded separatrices on which w is singular for finite X, which occurs when $\rho = 0$. The bounded orbits are heteroclinic between the spiral points D_- and D_+. For parameter values on the branch cut, however, a change of stability occurs at these fixed points, and a "vertical" Hopf bifurcation takes place. All orbits in the plane are periodic except for a single separatrix on which $w \to \pm\infty$.

One may ask what is the significance of a continuum of zero amplitude solutions represented by the orbits in the $r \equiv 0$ plane. Firstly the fixed points $D_\pm$ represent the exponential decay of solutions that tend to zero at plus and minus infinity, which is given by linearization of the GL equation for small amplitude. Thus solutions decaying to the laminar state at infinity must correspond to the orbits of the 1-dimensional stable or unstable manifold of D_- or D_+ associated with the eigenvalue λ_1.

The singularities for finite X represent solutions whose amplitude approaches zero, due to the algebraic singularity of equation (4.4) which to leading order is of

the form

$$\left.\begin{aligned} w + \frac{c_1}{2} &\sim \frac{1}{X - X_0} \\ s - \frac{a_0 c_1}{2} &\sim -\frac{\beta}{3}(X - X_0) \end{aligned}\right\} \text{ as } X \to X_0 \,. \tag{4.5a}$$

This singularity in the invariant plane is accompanied in the third dimension by a decay of the amplitude to zero such that

$$r \sim r_1 (X - X_0)^2 \qquad \text{as } X \to X_0 \tag{4.5b}$$

where X_0 and r_1 are undetermined. We note that this may still correspond to bounded motion for a solution of the GL equation, and that our choice of polar coordinates with $w = r'/2r$ fails to satisfactorily describe such solutions whose amplitude is zero at a point. In general this restricts our study in the reduced (r, s, w) space to solutions whose amplitude remains bounded away from zero for finite X.

The remainder of heteroclinic orbits in the invariant plane joining the fixed points D_- and D_+ are associated with the $\Phi \equiv 0$ solution and seem to be an artifact of the mathematical construction.

4.2 **The fixed points of the plane wave solutions**

The second pair of fixed points of the system (4.1) are of the form $(r_T, s_T, 0)$ and correspond to the plane waves which were periodic solutions in the 4-dimensional representation. These are given by

$$T_\pm : \quad \begin{aligned} r_T &= \frac{\beta}{\gamma} + \frac{c_1^2 d_r}{2 a_r \gamma^2} \pm \frac{c_1}{\gamma} \sqrt{\frac{c_1^2 d_r^2}{4 a_r^2 \gamma^2} + \delta_1 - \frac{\delta_2 \beta}{\gamma}} \\ s_T &= \frac{c_1 d_r}{2 a_r \gamma} \pm \sqrt{\frac{c_1^2 d_r^2}{4 a_r^2 \gamma^2} + \delta_1 - \frac{\delta_2 \beta}{\gamma}} \\ w_T &= 0. \end{aligned} \tag{4.6}$$

Hence the corresponding GL solutions become

$$A = r_T^{1/2} e^{is_T x} e^{-i(\Omega + s_T c)t},$$

recalling that a wave of given wavenumber $k = s_T$ lies on a line in parameter space given by equation (2.7).

In order for T_+ or T_- to exist we require that these fixed points be real and that $r_T > 0$. When $c = 0$ these points are images of each other under the reflection symmetry and exist provided both

$$\Delta \equiv \delta_1 - \frac{\delta_2 \beta}{\gamma} \qquad \text{and} \qquad \frac{\beta}{\gamma}$$

are nonnegative.

The characteristic equation of the linearization about these plane wave fixed points is given by

$$\begin{aligned} \lambda^3 + 2c_1\lambda^2 + \left[c_1^2 + (2s_T - a_0 c_1)^2 - 2\delta_2 r_T\right] \lambda \\ - 2r_T \left[c_1 \delta_2 + \gamma(2s_T - a_0 c_1)\right] = 0. \end{aligned} \tag{4.7}$$

In studying the stability of the plane wave fixed points we shall refer to regions of parameter space shown for the Poiseuille coefficients in Figures 4.2 and 4.3 and the Table 4.1. Figure 4.2 illustrates the regions relevant in studying the existence and stability of both pairs of fixed points as a function of the two parameters for $\sigma_r = -1$, and similarly for Figure 4.3 when $\sigma_r = 1$. Recall that we can always scale nonzero $|\sigma_r|$ to 1 by the invariance (2.6), so these diagrams are representative of sub- and super-critical Reynolds numbers respectively. Table 4.1 indicates the number of positive and negative eigenvalues associated with each of the four critical points $T_\pm$ and $D_\pm$ in the different regions of parameter space. This table and figures were constructed by solving (4.7) numerically for the Poiseuille parameters as well as by considering bifurcations from the fixed points as described below. In general we

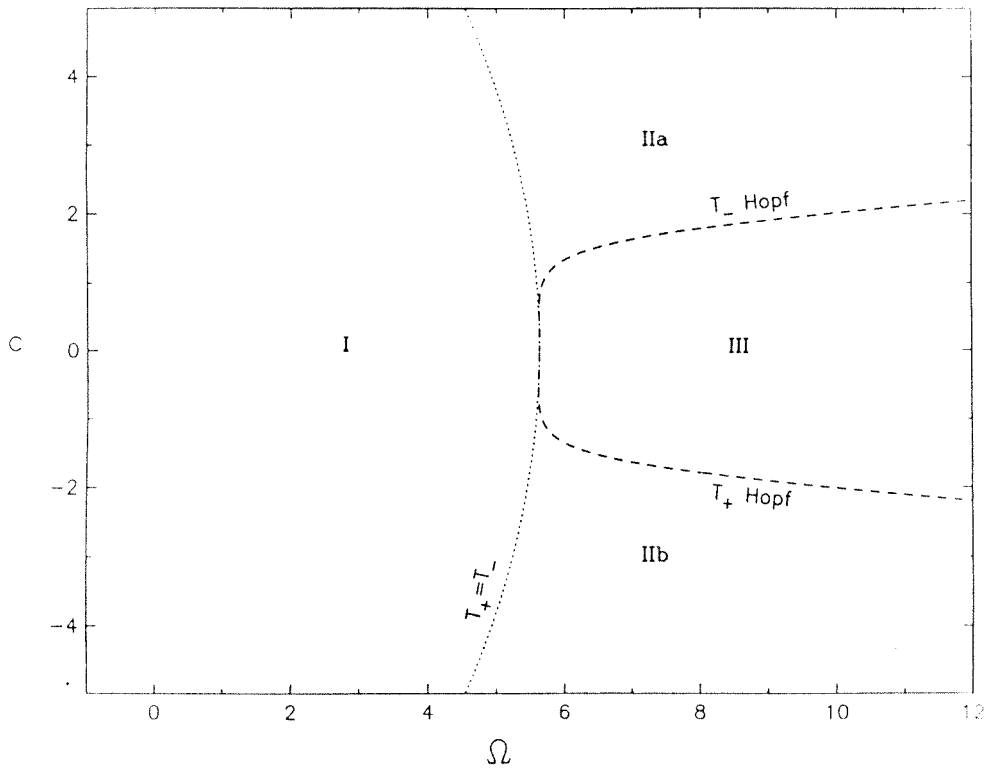

FIGURE 4.2. Stability diagram for the fixed points of the reduced system, $\sigma_r = -1$.

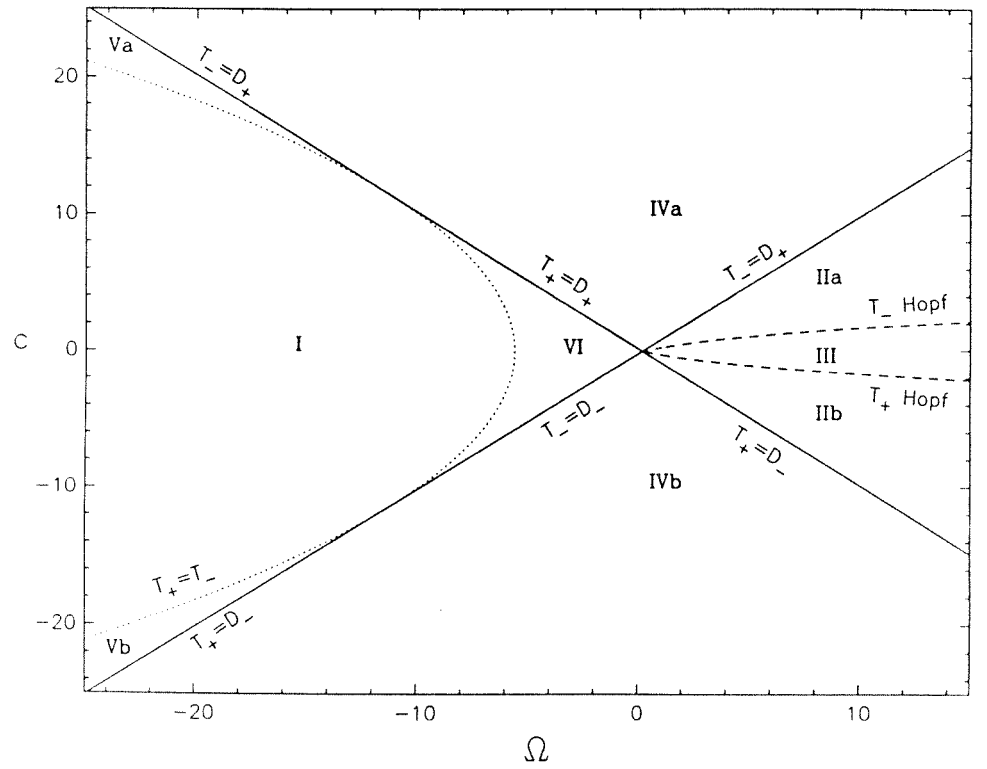

FIGURE 4.3. Stability diagram, $\sigma_r = 1$.

	Critical Point Stability Eigenvalues: (−ve, +ve)			
Region	T_+	T_-	D_+	D_-
I	–	–	$(2,1)$	$(1,2)$
IIa	$(2,1)$	$(3,0)$	$(2,1)$	$(1,2)$
IIb	$(0,3)$	$(1,2)$	$(2,1)$	$(1,2)$
III	$(2,1)$	$(1,2)$	$(2,1)$	$(1,2)$
IVa	$(2,1)$	$r_T < 0$	$(3,0)$	$(1,2)$
IVb	$r_T < 0$	$(1,2)$	$(2,1)$	$(0,3)$
Va	$(2,1)$	$(3,0)$	$(2,1)$	$(1,2)$
Vb	$(0,3)$	$(1,2)$	$(2,1)$	$(1,2)$
VI	$r_T < 0$	$r_T < 0$	$(2,1)$	$(1,2)$

TABLE 4.1. Critical point stability of the reduced system.

The table displays the number of stable and unstable eigenvalues in each region of Ω-c parameter space. The regions in the bottom half of the table exist for $\sigma_r > 0$ only.

find one pair of the eigenvalues of $T_\pm$ is complex conjugate, although in segments of region IV when $\sigma_r > 0$ and region II when $\sigma_r < 0$ all the eigenvalues can be real, but this has no bearing on the stability properties which we discuss here.

In order to determine bifurcations from the plane wave fixed points we examine when an eigenvalue is zero or when there is a pure imaginary pair of eigenvalues. There are two cases for a zero eigenvalue. The first occurs when a plane wave bifurcates from zero amplitude so that $r_T = 0$. At this point one of the T fixed points coalesces with a D fixed point which occurs on the lines (3.4). In this way the Hopf bifurcation describing this phenomenon in the 4-dimensional system has been reduced to a regular bifurcation of steady solutions in the reduced system. The second case of a zero eigenvalue occurs when the square root in (4.6) vanishes and T_+ and T_- coalesce in a so-called saddle-node bifurcation, although this is really a

limit point and no new branches are created there. The locus of this limit point gives the region for the existence of $T_\pm$ which is given by

$$\Omega \geq d_0\sigma_r - \frac{d_r c^2}{4\gamma|a|^2}$$

Thus no plane waves exist in region I of parameter space. Ensuring that $r_T > 0$ also excludes region VI and we find only one plane wave solution exists in the regions IV when $\sigma_r > 0$.

If we seek Hopf bifurcations by setting $\lambda^2 = -\omega^2$ with ω real in (4.7), a cubic equation in c_1^2 results after eliminating ω, s_T and r_T, which is given by

$$\begin{aligned} & c_1^2\,[c_1^2(1+a_0^2) + 6\delta_1 - \beta(a_0 + 7\delta_2/\gamma)]^2 \\ & \quad + c_1^2 \frac{d_r}{\gamma a_r}[c_1^2(1+a_0^2) + 6\delta_1 - \beta(a_0 + 7\delta_2/\gamma)][2\beta + c_1^2(a_0 - 7\delta_2/\gamma)] \\ & \quad - [\delta_1 - \delta_2\beta/\gamma][c_1^2(a_0 - 7\delta_2/\gamma) + 2\beta]^2 = 0. \end{aligned} \tag{4.8}$$

We have solved this equation numerically and find a locus of Hopf bifurcations from T_+ and T_- occurs in Ω–c space for σ_r either side of critical. From the Hopf bifurcation theorem, given that we are not in a degenerate situation, branches of periodic orbits must exist in a neighborhood of these fixed points. These have been found perturbatively as described in Chapter 5. It is interesting that returning to the original representation for Φ this locus of secondary bifurcations is to spatially quasi-periodic solutions, which are 2-tori in the 4-dimensional phase space. This follows from the discussion in Section 3.4 as $c \neq 0$ for these solutions. This bifurcation to a 2-torus was also found by C. Holmes (1985), in a study of the temporal stability of the plane waves of the GL equation (see Section 8.1). By comparing Figures 2.2 and 4.3 we observe that each plane wave of a given wavenumber undergoes such a secondary bifurcation. The situation is also true when $\sigma_r < 0$, where a given plane wave may undergo either one or three bifurcations. This situation is discussed

further in Chapter 8, where we relate these bifurcations to the sideband instabilities of plane waves for the GL equation.

We now summarize the most important features of our stability results when $c > 0$. We find that T_- is an attracting fixed point in regions IIa and Va of parameter space, as is the zero amplitude fixed point D_+ in region IVa. Region IV exists only for $\sigma_r > 0$, and diminishes in size as $\sigma_r \to 0$, when regions II and V coalesce. Otherwise all the critical points are saddles. Regions IV, V and VI are the only sectors of parameter space which are unique to $\sigma_r > 0$. When $c < 0$, from the invariance (2.15), the results are analogous by reversing stabilities and swapping the subscripts $+$ and $-$ of the critical points.

CHAPTER 5

Construction of Spatially Quasi-periodic Solutions by Perturbation Methods

From the stability considerations of the previous chapters, various bifurcations from the known exact solutions can occur, and thus we should be able to find new bifurcating quasi-steady solutions. By searching for periodic solutions of the complex Duffing systems numerically, a complex structure of such bifurcations to quasi-steady spatially periodic and quasi-periodic solutions of the GL equation for plane Poiseuille flow has been found, as is described in Chapter 6. In order to gain a better understanding of the structure of these solutions, we have found that perturbation methods can be employed to describe many of them analytically. In particular, when $\sigma_r > 0$ we can describe a family of quasi-periodic solutions which connect the plane wave solutions to symmetric periodic solutions, all of which bifurcate from the undisturbed state. Furthermore, when $\sigma_r < 0$ there is a family of solutions bifurcating from the non-trivial subcritical spatially uniform state.

In seeking temporally and spatially quasi-periodic solutions of the form $A = e^{-i\Omega t}\Phi(x - ct)$, we first consider necessary conditions on the undetermined parameters Ω and c for their existence. We consider integrals over the motion, and the case $c = 0$ first. Defining

$$\langle|\Phi|^2\rangle = \int_{x_1}^{x_2} |\Phi|^2 dx,$$

we multiply the complex Duffing equation (2.4) with $c = 0$ through by Φ^* and integrate the real and imaginary parts to get

$$-\delta_1\langle|\Phi|^2\rangle + \delta_2\langle|\Phi|^4\rangle = -\langle|\Phi'|^2\rangle + \mathrm{Re}\{\Phi'\Phi^*\}\Big|_{x_1}^{x_2} \qquad (5.1a)$$

and

$$-\beta\langle|\Phi|^2\rangle + \gamma\langle|\Phi|^4\rangle = \mathrm{Im}\{\Phi'\Phi^*\}\Big|_{x_1}^{x_2}. \qquad (5.1b)$$

A first observation is that the boundary term in (5.1a) equals $\frac{1}{2}|\Phi|^{2\prime}$ which must vanish for some $x_2 > x_1$ on any bounded orbit. Thus the boundary term vanishes and the right hand side is negative. It follows then that both $-\delta_1$ and δ_2 cannot be positive if a spatially bounded orbit exists.

Secondly, on a periodic orbit both the boundary terms vanish where the period is $x_2 - x_1$. Similarly these terms can be made arbitrarily small on a quasi-periodic orbit in phase space. It follows then that for any quasi-periodic orbit

$$\beta\gamma \geq 0 \qquad \text{and} \qquad \Delta \equiv \delta_1 - \frac{\delta_2\beta}{\gamma} \geq 0. \qquad (5.2)$$

To achieve this result for periodic solutions we have essentially repeated Holmes and Wood's (1985) argument, although they claim (erroneously) that the result holds for all bounded solutions.

Two simple conclusions can be made for the original Poiseuille flow GL coefficients when the boundary terms vanish in equations (5.1). We find that

$$\Omega > a_0\sigma_r \quad \text{if} \quad \sigma_r > 0$$

$$\Omega > d_0\sigma_r \quad \text{if} \quad \sigma_r < 0$$

in order to find quasi-steady spatially quasi-periodic solutions (with $c = 0$). This is in agreement with the analytic and numerical findings presented below and in Chapter 6 respectively.

When $c \neq 0$, performing the integrals analogous to equations (5.1) does not lead to conditions for existence as above, and we are unable to find conditions to restrict the parameter space in which to find quasi-periodic orbits for general c.

5.1 Small amplitude branches of periodic solutions, $\sigma_r > 0$.

In Chapter 2 we discussed that the GL equation possesses a family of spatially periodic plane wave solutions

$$A = \sqrt{\frac{a_r k^2 - \sigma_r}{d_r}} \exp i[k(x - ct) - \Omega t] \tag{5.3}$$

of wavenumber k, where Ω and c satisfy the relation

$$\Omega + kc = (a_i - d_0 a_r)k^2 + d_0 \sigma_r. \tag{5.4}$$

When $\sigma_r > 0$, plane waves of opposite wavenumber bifurcate from the trivial solution. This can be viewed as a Hopf bifurcation in (u, v, p, q) space, where these waves appear as periodic orbits. Alternatively the plane waves correspond to a pair of fixed points in (r, s, w) phase space at which $w = 0$. In this formulation the bifurcation from the trivial solution occurs when these fixed points bifurcate from the pair of fixed points lying in the plane $r \equiv 0$. In any case the bifurcation is of degenerate type in the case $c = 0$, when an extra symmetry is present in the complex Duffing equation. As was described in Chapter 4, in the 4-dimensional formulation a double complex conjugate pair of eigenvalues sits on the imaginary axis, a situation that is not in general well understood.

In addition to the plane wave solutions, the GL equation is known to possess a branch of periodic solutions for $c = 0$ with both odd and even symmetry in x, provided $\sigma_r > 0$. This was found by C. Holmes (1985) and independently through our numerical computations described in the next chapter, and with a perturbation approach described here. Holmes considered the case $c = 0$ only, and deduced the normal form for the bifurcation at $\Omega = a_0$ when $\sigma_r = 1$, which shows that a third branch of solutions exists at small amplitude in addition to the pair of plane waves.

Because $\Phi(X)$ has zeroes on this branch, the solution cannot be described analytically in the reduced (r, s, w) formulation and we must use the full complex Duffing equation. We consider small amplitude solutions of the GL equation that exist for $\sigma_r > 0$ and bifurcate from the laminar state. Using perturbation techniques for small β (a small perturbation of Ω from its critical value $a_0\sigma_r$) we will construct this symmetric branch of periodic solutions for $c = 0$ and γ positive and finite (as applies in Poiseuille flow), in addition to the plane waves above.

In the following sections we will assume also that the GL coefficients a_r, d_r and σ_r have been scaled to unity as given in (1.10). From (5.2) we know that periodic orbits can only exist for $\beta \geq 0$, and consider the equation (2.4)

$$\Phi'' = -(\delta_1 + i\beta)\Phi + (\delta_2 + i\gamma)\Phi|\Phi|^2 \qquad \beta \ll 1. \tag{5.5}$$

In order to construct small amplitude periodic solutions, we find that it is appropriate to use the scaling

$$\Phi = \beta^{1/2}\phi \qquad \tilde{x} = x(1 + \beta\omega_1 + \beta^2\omega_2 + \cdots)^{1/2}$$

which is standard for Hopf bifurcation problems using the Lindstedt's method of strained coordinates (Kevorkian and Cole, 1981). The problem becomes

$$(1 + \beta\omega_1 + \cdots)\ddot{\phi} + \phi = \beta\left[-i(1 - ia_0)\phi + (\delta_2 + i\gamma)\phi|\phi|^2\right]$$

where the double dots denote derivatives with respect to the stretched variable $\tilde{x}$. Expanding ϕ as

$$\phi = \phi_0 + \beta\phi_1 + \cdots$$

we get at lowest order the harmonic oscillator

$$\ddot{\phi}_0 + \phi_0 = 0.$$

At present we do not impose any boundary conditions except those of periodicity. The general solution at lowest order is thus

$$\phi_0 = Be^{i\tilde{x}} + Ce^{-i\tilde{x}}$$

with B and C complex constants. At next order we must solve the equation

$$\ddot{\phi}_1 + \phi_1 = (\omega_1 - i(1 - ia_0))\phi_0 + (\delta_2 + i\gamma)\phi_0|\phi|_0^2. \tag{5.6}$$

The cubic nonlinearity introduces inhomogeneous secular terms, whose coefficients must be set to zero giving the equations

$$\begin{aligned} (\omega_1 - i(1 - ia_0))B - (1 - i\gamma)\left[B|B|^2 + 2B|C|^2\right] &= 0 \\ (\omega_1 - i(1 - ia_0))C - (1 - i\gamma)\left[C|C|^2 + 2C|B|^2\right] &= 0. \end{aligned} \tag{5.7}$$

Note that these equations are solved subject to ω_1 being real. In the case $B = 0$ only the second equation remains and we find

$$\omega_1 = |C|^2 = \frac{1}{\gamma}.$$

Similarly if $C = 0$ we get

$$\omega_1 = |B|^2 = \frac{1}{\gamma}.$$

In these cases no harmonics are generated on the right hand side of (5.6) and the solutions are therefore exact. We find we have constructed the travelling wave solutions (2.2) which are asymmetric (i.e., not invariant to the $x \to -x$ symmetry).

We now consider the solution of the equations (5.7) when $BC \neq 0$. In this case it follows that

$$|B|^2 = |C|^2 = \frac{\omega_1}{3} = \frac{1}{3\gamma}.$$

Due to the phase and translation invariance of the complex Duffing equation, we may choose B and C real and positive without loss of generality. We thus find that

only one distinct periodic solution results which may be written to lowest order as

$$\phi_0 = 2B_r \cos\tilde{x}, \qquad B_r = \frac{1}{\sqrt{3\gamma}}.$$

Solving for ϕ_1 one finds

$$\phi_1 = -\tfrac{1}{4}B_r^3(\delta_2 + i\gamma)\cos 3\tilde{x} + B_r(D_r + \tfrac{1}{4}iB_r^2\gamma)\cos\tilde{x}$$

and we must consider the equation at order β^2 to determine ω_2 and D_r. Due to the rotational invariance each periodic orbit is really a surface of solutions in 4-dimensional phase space. To remove this degeneracy and the arbitrary shift in space we have applied periodic boundary conditions with the extra conditions $v(0) = v'(0) = 0$ where $\Phi = u + iv$.

On removing the secular terms at order $\beta^{3/2}$ we find

$$\omega_2 = -\frac{1}{72}(1 + \delta_2^2/\gamma^2) \qquad D_r = \frac{\delta_2}{18\gamma}.$$

The resulting bifurcating solution (which we call $P0$) is given then to second order by

$$\begin{aligned} u =& \beta^{1/2}\frac{2}{\sqrt{3\gamma}}\cos\tilde{x} + \beta^{3/2}\frac{\delta_2}{6\gamma\sqrt{3\gamma}}[\tfrac{1}{3}\cos\tilde{x} - \tfrac{1}{2}\cos 3\tilde{x}] + O(\beta^{5/2}) \\ v =& \beta^{3/2}\frac{1}{6\sqrt{3\gamma}}\sin\tilde{x}\sin 2\tilde{x} + O(\beta^{\frac{5}{2}}) \end{aligned} \tag{5.8}$$

with period in x given by

$$L = 2\pi\left[1 - \frac{\beta}{2\gamma} + \frac{\beta^2}{\gamma^2}\left(\tfrac{3}{8} + \tfrac{1}{576}(\gamma^2 + \delta_2^2)\right) + O(\beta^3)\right],$$

recalling that $A = (u + iv)e^{-i\Omega t}$ and $\beta = (\Omega - a_0)/|a|^2$. Note that this branch $P0$ possesses odd and even symmetry in $\tilde{X}$, which would make it singular in the 3-dimensional representation. We were able to numerically compute and continue this branch for finite β, as will be described in Chapter 6. The analysis has therefore revealed 3 branches of solutions emanating form the degenerate Hopf bifurcation,

each describing small amplitude solutions of the GL equation which are spatially and temporally periodic.

5.2 Small amplitude expansion for bifurcating 2-tori

In addition to the above three periodic branches found in the 4-dimensional phase space, our numerical results lead us to seek a perturbation procedure whereby we can describe the periodic solutions in the reduced (r, s, w) phase space which also exist for small amplitude for non-zero speed correction c near the bifurcation point at $\beta = c = 0$ when $\sigma_r > 0$. In general these solutions lie on 2-tori in the 4-dimensional space and thus correspond to spatially and temporally quasi-periodic solutions of the GL equation. Although the underlying linearization in amplitude r leaves us with a nonlinear equation for s and w, we are able to solve the perturbation procedure analytically because we can solve the lowest order equation exactly using complex formulation (2.13).

We find that these 2-tori solutions exist in region III of parameter space (see Figure 4.3) and lie on a surface in parameter space bounded by the Hopf bifurcation loci of T_+ and T_-. As $|c| \to 0$ this family of solutions is singular in the 3-dimensional representation due to the presence of the odd symmetry, but we have constructed the limiting branch $P0$ of spatially periodic solutions for $c \equiv 0$ in the previous section using the full 4-dimensional representation.

Recall that at the bifurcation point $c = \beta = 0$ ($\Omega = \sigma_r a_0$) the plane wave fixed points coalesce with the fixed points in the $r \equiv 0$ plane. The continuum of solutions in the plane are all of period π except for the singular $s = 0$. What we find by both numerical continuation and the following perturbation expansion is that, by varying β and c away from zero along a ray in parameter space, just one of these periodic orbits persists outside of the invariant plane. Thus for fixed $0 < \beta \ll 1$ the family

of periodic solutions that was in the plane at the bifurcation point persists at finite amplitude and may be parametrized by c.

We start by considering the orbits in the $r \equiv 0$ invariant plane at the bifurcation point. From Figure 4.1, the bifurcation point is on the branch cut in Ω-c parameter space, and the degenerate fixed points in the plane are marginally stable in all three directions. From Section 4.1 the orbits in the plane may be described as

$$w + is = z = -\tan(x + i\rho). \tag{5.9}$$

On expanding the right hand side into real and imaginary parts, we find we can eliminate x to get an parametrized representation of the orbits in the invariant plane as

$$s^2 + w^2 + 1 = -2s \coth 2\rho.$$

ρ is thus found to be a natural way of parametrizing the periodic orbits, where as $|\rho| \to \infty$ the fixed points $D_- = T_+$ and $D_+ = T_-$ are approached and as $|\rho| \to 0$ the norm of the periodic orbits tends to infinity and the singular separatrix is approached.

We now seek small amplitude periodic orbits in the 3-dimensional phase space by perturbing the solutions in the invariant plane. We retain the complex z representation for s and w and study the equations (2.13)

$$\begin{aligned} r' &= 2rw \\ z' &= -(1 + i(1 - ia_0)\beta) + (\delta_2 + i\gamma)r - c_1(1 - ia_0)z - z^2. \end{aligned} \tag{5.10}$$

where the independent variable is $X = x - ct$, and we have assumed the scaling $\sigma_r = a_r = d_r = 1$. We find that the appropriate expansion for (r, s, w) is regular in $0 < \beta \ll 1$. We also expand the parameter c_1 in β and stretch the independent

variable X, the latter due to the fact that a shift in the period π is expected for finite β. i.e.,

$$\begin{aligned} r &= \beta(r_0 + \beta r_1 + \cdots) \qquad z = z_0 + \beta z_1 + \cdots \\ c_1 &= \beta(b_0 + \beta b_1 + \cdots) \qquad \tilde{X} = (1 + \omega_1\beta + \omega_2\beta^2 \cdots)X. \end{aligned} \tag{5.11}$$

For small β, b_0 is an order one parameter that determines small c_1, and thus given b_0, Ω and c vary along a fixed ray in parameter space.

Substituting (5.11) into (5.10) we find at lowest order that we recover the solution (5.9) for z_0. Taking the real part w_0 of z_0, we are able to find r_0 as

$$r_0 = R\exp\Big\{2\int^X w_0 dx\Big\} = R(\cos 2X + \cosh 2\rho)$$

where R is an amplitude yet to be determined, and we have dropped the tildes on X, so

$$X = x[1 + \omega_1\beta + O(\beta^2)] - t[b_0\beta + O(\beta^2)].$$

At order β in the z equation we find

$$\ddot{z_1} + 2z_0 z_1 = f_1$$

where

$$f_1 = \omega_1(1 + z_0^2) - (1 - ia_0)(i + b_0 z_0) + (\delta_2 + i\gamma)r_0$$

and

$$z_0(X) = -\tan(X + i\rho).$$

The solution for z_1 is

$$z_1 = \sec^2(X + i\rho)\int^X f_1 \cos^2(x + i\rho)dx. \tag{5.12}$$

In order that z_1 be of period π (in the stretched variable $\tilde{X}$), we must impose the solvability condition that the mean of the integrand is zero over one period, or

$$\int_0^\pi f_1 \cos^2(x + i\rho)dx = 0. \tag{5.13}$$

Of the three terms in f_1 to be integrated, the first two are easily evaluated by moving the contour parallel to the real axis in the complex X-plane, noting that

the trigonometric functions are periodic on any such contour. The integral over the term in r_0 is conveniently evaluated in the complex plane by converting the line integral of trigonometric functions to one of an algebraic function around the unit circle, i.e.,

$$\begin{aligned}
&\int_0^{\pi} (\cos 2x + \cosh 2\rho) \cos^2(x + i\rho)\ dx \\
&\qquad = \frac{1}{4} \int_0^{2\pi} (\cos x + \cosh 2\rho)\,[1 + \cos(x + 2i\rho)]\, dx \\
&\qquad = \frac{1}{16i} \oint_C (\xi^2 + 1 + 2\xi \cosh 2\rho)(2\xi + \xi^2 e^{-2\rho} + e^{2\rho})\ \frac{d\xi}{\xi^3} \\
&\qquad = \frac{3\pi}{4} \cosh 2\rho.
\end{aligned}$$

This method of evaluation is used later on integrals where methods of direct real integration seem inapplicable.

The solvability condition (5.13) yields two real equations with solution

$$\omega_1 = \frac{1}{2}(a_0 - \frac{\delta_2}{\gamma}) \equiv \frac{1}{2\gamma}$$

and

$$R = \frac{2}{3\gamma} \operatorname{sech} 2\rho.$$

The first order shift in period is therefore independent of the parameter ρ, and at this stage b_0 is undetermined.

At second order for r we find

$$r_1 = 2r_0 \int^X (w_1 - \omega_1 w_0) dx.$$

Once again we must ensure that the mean of the integrand vanishes over a period so that r_1 is periodic. w_0 is symmetric so that the resulting condition becomes

$$\operatorname{Re} \int_0^{\pi} z_1 dx = 0.$$

This condition requires the explicit calculation of z_1 from equation (5.12), namely

$$z_1 = \tfrac{1}{4}\sec^2(x+i\rho)\Big[-(1-ia_0)[b_0\cos 2(x+i\rho)+i\sin 2(x+i\rho)] \\ + R(\delta_2+i\gamma)[\cosh 2\rho\sin 2(x+i\rho)+\sin 2x+\tfrac{1}{16}\sin 2(2x+i\rho)]\Big].$$

The subsequent integration of z_1 is performed with several contour integrations of trigonometric integrands similarly as above, and on carrying out these details the real part of the integral is set to zero. After considerable algebra we find the simple result that

$$b_0 = \frac{1}{3}\tanh 2\rho.$$

In this way ρ and thus b_0 parametrizes a family of periodic orbits in phase space. $|b_0| \to 0$ recovers the symmetric periodic branch of the previous section (which is now a singular orbit in the 3-dimensional space), and $|b_0| \to \frac{1}{3}$ recovers the plane waves.

Putting these results together, to leading order the amplitude of the full solution is

$$A \sim \beta^{1/2} r_0^{1/2}(\tilde{X}) \exp\left[i\int_0^{\tilde{X}} \mathrm{Im}\{z_0(x)\}\, dx - i\Omega t\right]$$

$$\tilde{X} = x(1+\beta/2\gamma) - \beta b_0 t + O(\beta^2)$$

with $\beta = (\Omega - a_0)/|a|^2$. This describes a quasi-periodic family in space and time due to the fact that the mean of $\mathrm{Im}\{z_0\}$ over one period in $\tilde{X}$ is in general non-zero. The modulus of such solutions is periodic, however, and is given by

$$|A|^2 = \frac{2\beta}{3\gamma}\left[1+\sqrt{1-9b_0^2}\cos 2\tilde{X}\right] + O(\beta^2).$$

Figure 5.1 is a diagram of the solution surface as a function of the free parameters Ω and c (both linear in β) for asymptotically small amplitude.

We have therefore determined the lowest order terms in amplitude, speed correction c and period shift with a perturbation procedure in the reduced 3-dimensional

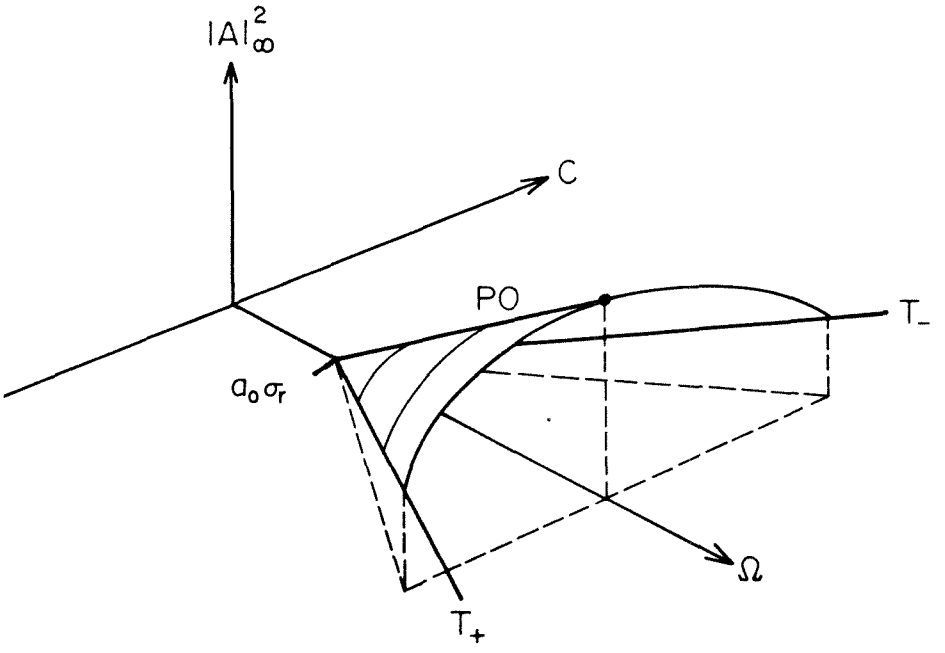

FIGURE 5.1. Solution surface representing quasi-periodic solutions of small amplitude for $\sigma_r > 0$.

The surface connects the plane waves via the symmetric periodic branch $P0$.

formulation, and one may proceed to gain higher order terms if so desired. Alternatively one may also use a two variable expansion procedure with fast and slow space variables for the amplitude Φ in the full 4-dimensional system to construct the corresponding 2-tori solutions. With the above reduced procedure, however, the solutions are periodic in (r, s, w) space and we can confirm the correctness of the perturbation approach by numerical continuation of the periodic orbits. In fact we have checked these asymptotics with such numerics using the program AUTO (see the following chapter) and the agreement is excellent. This confirmation of the existence of 2-tori is not readily available if we had used the full 4-dimensional system.

5.3 Subcritical quasi-periodic solutions

When $\sigma_r < 0$ (corresponding to $Re < Re_c$) and the parameters $c = 0$ and $\Omega = d_0\sigma_r$ there is a spatially uniform solution of the GL equation which comes about when travelling waves of oppositely signed wavenumber coalesce. At this value of the parameters there is a zero eigenvalue and a pair of pure imaginary eigenvalues at the fixed point $(1, 0, 0)$ in the 3-dimensional phase space. The normal form analysis of the analogous situation when $\sigma_r > 0$ and $d_r < 0$ is discussed by C. Holmes and Wood (1985) based on the work of Broer (1983), and they suggest the existence of invariant tori and chaotic motions in a neighborhood of this fixed point although this behaviour may not be structurally stable. There is however a structurally stable periodic orbit bifurcating from this point as Ω is varied, and they point out that it may be constructed by perturbation methods. A perturbation expansion constructing this spatially periodic solution was carried out by Newton and Sirovich (1986a). The small parameter was taken as the perturbation to the critical wavenumber at which temporal instability sets in (their study also considered the case $d_r = -1$ and $\sigma_r = 1$ only).

In this section we develop an expansion for the periodic solution, as well as a family of tori (quasi-periodic solutions in time and space) which exists near the bifurcation point in Ω–c parameter space for the Poiseuille case when $d_r > 0$. Our analysis perturbs both the frequency Ω and also the speed c and works with the 3-dimensional reduced equations. With these two parameters we are able to construct a surface of 2-tori solutions locally about the bifurcation point. These 2-tori bifurcate from the plane wave solutions and connect them via a symmetric periodic branch $S1$, which is a situation similar to that for $\sigma_r > 0$ of the previous section.

All of these solutions are small modulations of the subcritical spatially uniform solution. Continuation of these solutions is done numerically in Section 6.1, where the primary periodic branch is labeled $S1$.

We know that periodic orbits can only exist if $c = 0$ for $\beta \geq \gamma$ ($\Omega > -d_0$) from (5.2) given the scaling $a_r = d_r = 1$ and $\sigma_r = -1$. We let ϵ be our small parameter perturbing the system away from the uniform solution $|A|^2 = 1$, and expand the frequency such that

$$\beta - \gamma \equiv (\Omega + d_0)/|a|^2 = \Omega_1\epsilon + \Omega_2\epsilon^2 + \cdots.$$

We find that in order to construct bounded solutions the appropriate scaling for the variables (r, s, w) given in (2.11) is

$$r = 1 + \epsilon^{1/2}R(\tilde{X}, \epsilon) \qquad s = \epsilon^{1/2}S(\tilde{X}, \epsilon) \qquad w = \epsilon^{1/2}W(\tilde{X}, \epsilon)$$

with a stretched spatial coordinate

$$\tilde{X} = X(1 + \epsilon^{1/2}\omega_1 + \epsilon\omega_2 + \cdots),$$

recalling that $X = x - ct$. As we also want to vary c, we find that for consistency it must be expanded in a series of the form

$$c_1 = c/|a|^2 = b_1\epsilon^{1/2} + b_2\epsilon + \cdots.$$

From the 3-dimensional equations (4.1) we then obtain

$$\begin{aligned}
(1 + \epsilon^{1/2}\omega_1 + \cdots)\dot{R} =& 2W + 2\epsilon^{1/2}RW \\
(1 + \epsilon^{1/2}\omega_1 + \cdots)\dot{S} =& \gamma R - 2\epsilon^{1/2}SW + (\beta - \gamma) - c_1(S - a_0W) \\
(1 + \epsilon^{1/2}\omega_1 + \cdots)\dot{W} =& \delta_2 R + \epsilon^{1/2}(S^2 - W^2) + a_0(\beta - \gamma) - c_1(a_0S + W)
\end{aligned} \tag{5.14}$$

which we solve by expanding R as

$$R = r_0 + \epsilon^{1/2}r_1 + \epsilon r_2 + \cdots$$

and similarly for S and W. At lowest order we find

$$r_0 = B\cos\alpha X, \qquad s_0 = \frac{\gamma B}{\alpha}\sin\alpha X + E_0, \qquad w_0 = -\frac{\alpha B}{2}\sin\alpha X,$$

where $\alpha = \sqrt{-2\delta_2}$, we have removed the tildes on X for convenience, and B and E_0 are undetermined constants. At each successive order we must solve a system of the form

$$\frac{d}{dX}\begin{pmatrix} r_n \\ s_n \\ w_n \end{pmatrix} = \begin{pmatrix} 0 & 0 & 2 \\ \gamma & 0 & 0 \\ \delta_2 & 0 & 0 \end{pmatrix}\begin{pmatrix} r_n \\ s_n \\ w_n \end{pmatrix} + \begin{pmatrix} f_1 \\ f_2 \\ f_3 \end{pmatrix}.$$

In order to have spatially bounded solutions, we must suppress secularity by removing any periodic resonant terms forcing r_n and w_n and the forcing terms with nonzero mean in the s_n equation. These solvability conditions imply that

$$\int_0^{2\pi/\alpha} (f_1' + 2f_3)\begin{Bmatrix} \sin\alpha x \\ \cos\alpha x \end{Bmatrix} dX = \int_0^{2\pi/\alpha} (\gamma r_n + f_2) dX = 0.$$

At order $\epsilon^{1/2}$ in (5.14) the first integral condition gives that

$$\omega_1 B\delta_2 = 0 \qquad \text{and} \qquad B\left[2\gamma E_0 - b_1(1+2\delta_2)\right] = 0 \tag{5.15}$$

In the case $B = 0$ we carry the calculation out to next order and find we have recovered the plane wave solutions for $T_\pm$ given by (4.6). In this case s_0=E_0 and we find

$$\gamma s_0^2 - b_1 s_0 - \Omega_1 = 0$$

from the second integral condition. Continuing with the plane solutions to next order gives $r_1 = s_0^2$ as would be expected, so that the amplitude of the plane waves is $|A|^2 = r = 1 + O(\epsilon)$.

The alternative solution to the equations (5.15) gives rise to the 2-tori solutions and a symmetric periodic branch, all of amplitude $|A|^2 = r = 1 + O(\epsilon^{1/2})$. At first order we find

$$E_0 = \frac{b_1}{2}(1 + 2\delta) \qquad \text{and} \qquad \omega_1 = 0,$$

and on calculating r_1, the second integral condition determines the amplitude B such that

$$B^2 = \frac{\delta_2}{\gamma^2(\gamma^2 + \delta_2^2)} \left[b_1^2(4\delta_2^2 - 1) - 4\gamma\Omega_1 \right].$$

This describes a family of periodic solutions for (r, s, w) which correspond to quasi-periodic (2-tori) solutions in space for the full amplitude A. This is because the phase function $s(X)$ has non-zero mean when $b_1 \neq 0$. When $c = 0$ s has mean zero and a truly periodic solution is recovered, corresponding to the primary symmetric branch which we label $S1$, which is analogous to that studied by other authors (as discussed above).

Note that this family exists provided $B^2 > 0$, and that when $B = 0$,

$$\Omega_1 = \frac{b_1^2}{4\gamma}\left(4\delta_2^2 - 1\right) \tag{5.16}$$

at which point the solution reduces from being $O(\epsilon^{1/2})$ in amplitude to a plane wave of $O(\epsilon)$. The curve (5.16) is the local approximation to the bifurcation locus (4.8) at which point the plane waves undergo a Hopf bifurcation, producing the above surface of periodic solutions.

We can now write down the amplitude of the bifurcating solutions to first order on removing the small parameter ϵ. We get that

$$|A|^2 = r \sim 1 + \frac{1}{|a|\gamma}\sqrt{\frac{\delta_2}{(\gamma^2 + \delta_2^2)}} \left[c^2(4\delta_2^2 - 1) - 4\gamma(\Omega + d_0) \right]^{1/2} \cos\sqrt{-\delta_2}(x - ct)$$

where $c^2 = O(\Omega + d_0) \ll 1$. Figure 5.2 illustrates the surface of subcritical 2-tori solutions found, which connect the plane waves to the symmetric periodic branch.

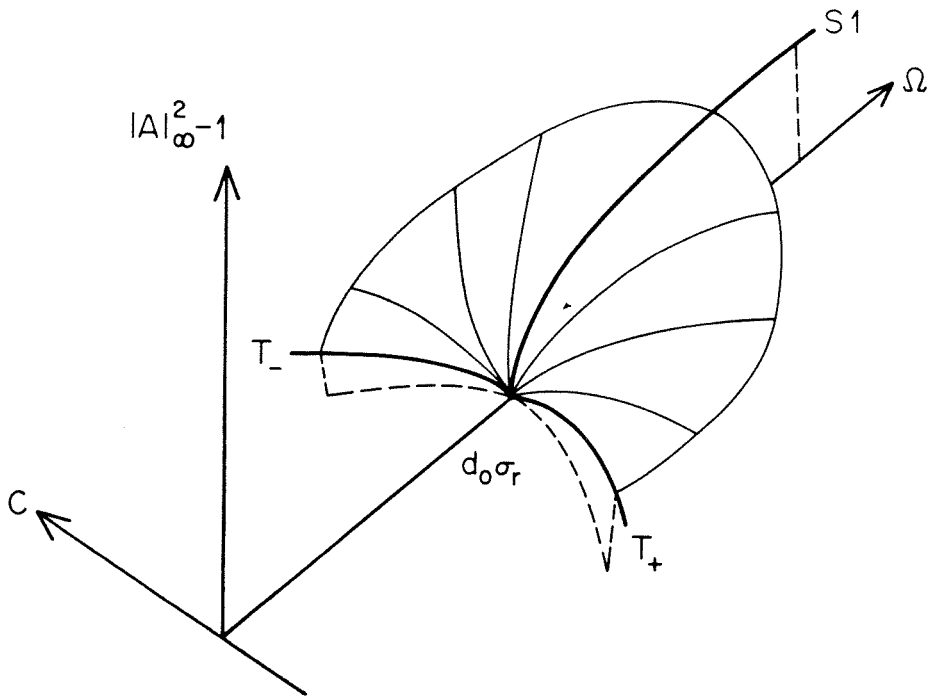

FIGURE 5.2. Solution surface representing quasi-periodic solutions of finite amplitude for $\sigma_r < 0$.

The surface connects the plane waves via the symmetric periodic branch $S1$.

The calculation can now be carried out systematically to higher orders. We have determined the terms r_1, s_1 and w_1 in order to find the highest order period shift ω_2. We omit the details which are straightforward but lengthy. We find that the numerical value of this constant is $\omega_2 \approx 100$ for the Poiseuille coefficients, indicating that the expansion has a very limited region of validity. This is revealed in our numerical calculation of the branch $S1$ in Section 6.1.

In the Poiseuille problem the 2-tori solutions corresponds to a slow modulation to the amplitude of the most unstable Tollmien-Schlichting wave for Re less than critical. We have thus been able to construct finite amplitude subcritical solutions which are spatially and temporally quasi-periodic, which are modulations of the previously known plane wave solutions.

CHAPTER 6

Numerical Continuation of Spatially Periodic and Quasi-periodic Solutions

In this chapter we describe our numerical results concerning periodic solutions of the 4-dimensional and 3-dimensional Duffing systems. A complex bifurcation structure has been found, many new branches bifurcating from the solution branches described analytically in the previous chapter. We concentrate primarily on those aspects which are relevant to our later discussion of solitary wave-type solutions of the GL equation.

6.1 Periodic orbits of the reduced system: $\sigma_r < 0$

In the study of the 3-dimensional system (4.1) with $c = 0$, both Newton and Sirovich (1986) and C. Holmes and Wood (1985) discuss a branch of periodic orbits that exists for a range of the parameters in the phase space (r, s, w) and bifurcates from the spatially uniform solution, which occurs when the pair of plane wave solutions (2.2) coalesce in the limit of vanishing wavenumber. If the $|\delta_i|$ are scaled to unity they consider having $\delta_1 = \delta_2 = -1$, in which case the uniform solution $(r, s, w) = (\beta/\gamma, 0, 0)$ exists only when $\beta/\gamma = 1$. As they consider that $\sigma_r > 0$ in the GL equation, this implies that $d_r < 0$ for this bifurcation to occur. Holmes and Wood continued the branch and deduced that it is most likely created in a heteroclinic bifurcation from the analytically known solitary wave solution which we describe in Section 7.2. This solution is of the form of a breather, in that it decays to zero at plus and minus infinity, connecting D_+ and D_- in the reduced phase space.

The bifurcation from the uniform solution also occurs for the Poiseuille case $d_r > 0$ if we consider $\sigma_r < 0$. The exact solitary wave solution does not exist for subcritical σ_r and thus we continued the branch numerically in Ω away from the

bifurcation point ($\Omega = -d_0$ for $\sigma_r = -1$) to see where it leads. Starting from an initial guess found by analytically perturbing $r = \beta/\gamma$ for small β as described in Section 5.3, we continued the branch using the program AUTO developed by Doedel and Kernevez (1985). This software is able to perform accurate continuation and bifurcation analysis for solution branches of systems of O.D.E's by a collocation method on an adaptive mesh. In particular the program is able to follow periodic orbits and generate the Floquet multipliers. For the reduced system one multiplier σ_0 is always at 1 due to the translation invariance on a periodic orbit. The other multipliers $\sigma_{1,2}$ satisfy

$$\sigma_1\sigma_2 = \exp(-2c_1L) \tag{6.1}$$

where L is the period.

The Floquet multipliers indicate a normal pitchfork bifurcation (including symmetry breaking) when an exponent passes through 1; a period doubling bifurcation when it crosses -1; and if the exponents cross the unit circle as a parameter is varied the possibility of bifurcations to orbits of higher multiples of the period L and invariant 2-tori (two frequency motion) and perhaps spatial chaos. When both multipliers lie inside the unit circle the orbit is stable. In the case $c = 0$, the two nontrivial multipliers can be either real and reciprocals of each other or complex conjugate and on the unit circle.

Figure 6.1 is a diagram of two of the branches $S1$ and $S2$ of periodic solutions that we have found when $\sigma_r = -1$. Branch $S1$ is the primary branch which bifurcates from the uniform solution at $\beta = \gamma$ ($\Omega = -d_0$), described analytically in Section 5.3. The modulus of the amplitude of the solutions on these branches remains essentially near unity and slowly varying, and they have the even symmetry. The resulting solutions suggest the existence of symmetric periodic envelope solutions in plane Poiseuille flow at Reynolds numbers less than Re_c that only slightly modify

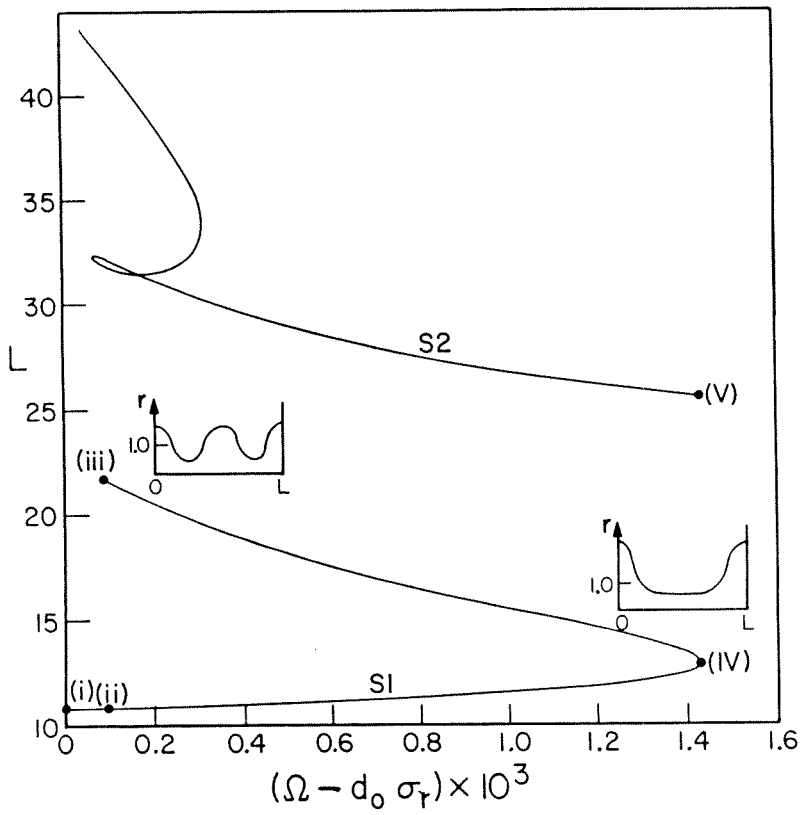

FIGURE 6.1. 2 branches of symmetric periodic orbits, $\sigma_r = -1$.

Point (i) is the uniform solution where $T_- = T_+$.

the form of the Tollmien-Schlichting wave. We have found others of higher period and all of these lie in a small neighborhood of the critical value of Ω as do the ones of lower period shown.

By monitoring the Floquet multipliers and plotting out the solutions along the branches we find that $S2$ is born in period doubling bifurcations from $S1$. We have marked points where such bifurcations occur in Figure 6.1 . Point (i) is the primary bifurcation from the uniform solution. Period doublings occur from (ii) to (iii) and (iv) to (v). In fact we suspect there is at least one period doubling cascade occurring which may lead to the existence of chaotic orbits close to the uniform state at $\beta = \gamma$. This behavior is in accordance with the more detailed local analysis performed by

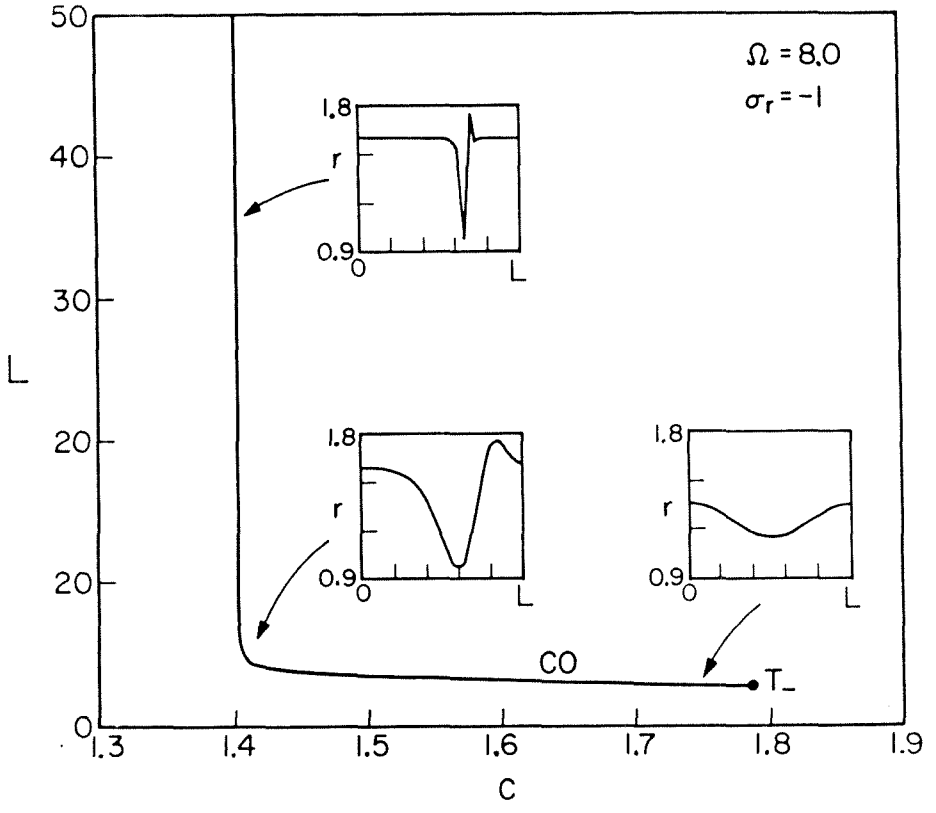

FIGURE 6.2. Branch $C0$ of periodic orbits in region III, $\Omega = 8.0$ and $\sigma_r = -1$.

The branch bifurcates from the fixed point T_-, and approaches a homoclinic orbit as c is decreased.

Holmes and Wood (1985), whose normal form analysis and numerical work suggests the local existence of quasi-periodic and perhaps chaotic orbits.

In any case we find that for the Poiseuille coefficients the bounded solutions found for $c = 0$ exist only in a small neighborhood of the bifurcation point. Also unlike the cases discussed by other authors, for the Poiseuille parameters the uniform state is subcritical and temporally unstable, as is the bifurcating periodic branch (as discussed in Section 8.2).

We can continue solutions in the parameter c, and thus search for (spatially) stable periodic orbits which correspond to 2-tori of the GL equation in space and time. Such quasi-periodic solutions were constructed by perturbation methods near

the bifurcation point in Section 5.3. We show an example of a computation when we decreased c for $\Omega = 8.0$ from the Hopf bifurcation point of the fixed point T_-, and the resulting branch $C0$ is shown in Figure 6.2. We find that the bifurcation is supercritical, and the stable periodic orbit that is shed has a continuation to orbits of period tending to infinity. This differs from the situation described perturbatively near $\Omega = 5.62$, when the analogous branch to $C0$ approaches the symmetric periodic branch $S1$, because $S1$ no longer exists at $\Omega = 8.0$. $C0$ is stable up to at least period 8 when we can no longer accurately compute the Floquet multipliers. We have been able to compute orbits of period greater than 10^6, providing good evidence that the branch converges to a homoclinic orbit of the plane wave fixed point. In this way it appears that there is a curve in Ω-c parameter space at which this homoclinic orbit exists (see Chapter 7 for a discussion of homoclinic and heteroclinic orbits).

6.2 Periodic orbits of the reduced system: $\sigma_r > 0$

We start once again with a discussion of the periodic solutions in the 3-dimensional phase space for $c = 0$, and can set $\sigma_r = 1$ for the general supercritical case. We found symmetric periodic orbits initially using a shooting method. Once a solution was converged to at a particular value of Ω we could then continue it using the code AUTO. We have been able to find 5 symmetric branches with this procedure, the number limited by our relatively primitive starting procedure.

Figures 6.3 and 6.4 display a set of solution branches for the system (4.1) with vertical axes period and L^2 norm for (r, s, w) respectively, and horizontal axis Ω. All possess the reflection symmetry (2.15). These solutions represent families of spatially symmetric periodic envelopes of Tollmien-Schlichting waves and travel downstream at the group velocity for $Re > Re_c$.

The left hand end of each branch shown corresponds to the formation of a singularity in the periodic orbit. In each case the amplitude of w tends to infinity

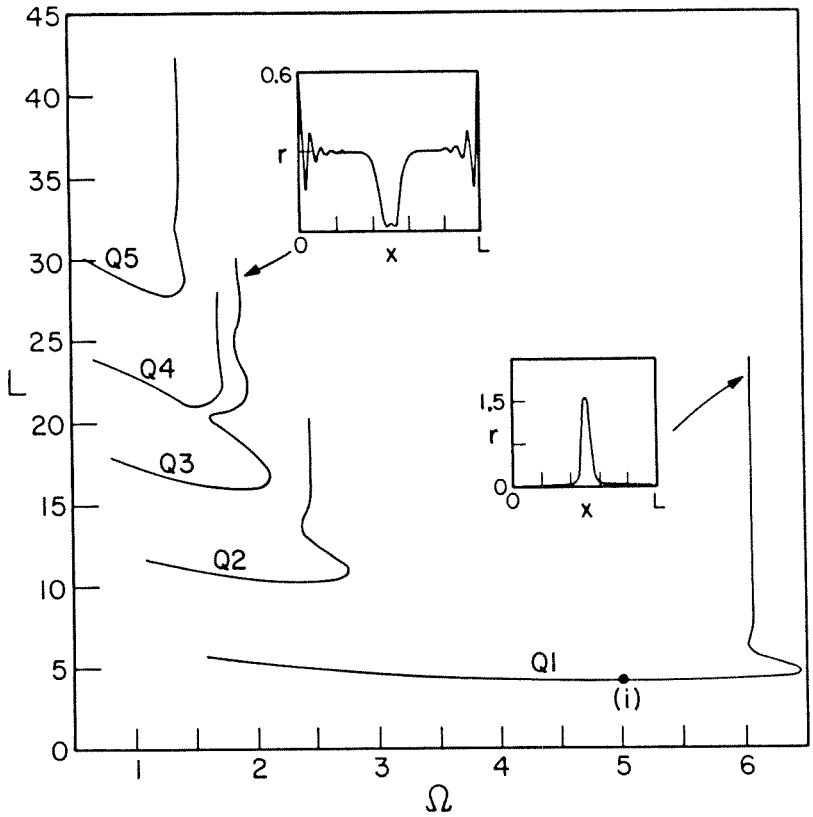

FIGURE 6.3. Period versus Ω for symmetric Q branches, $c = 0$ and $\sigma_r = 1$.

and r and s tend to zero simultaneously. We find that the solution is tending to have the asymptotic form (4.5) which indicates the amplitude of the solution is passing through zero as Ω is varied. This reflects the shortcoming of the polar representation of the amplitude that we use. In order to continue these branches it is necessary to use the full 4-D system (2.8) for the amplitude, and in fact we will find that they all bifurcate from the periodic branch $P0$ with odd symmetry where $\Phi(0) = \Phi(L/2) = 0$, which we constructed in Section 5.1.

At the right hand end of each branch in Figure 6.3 the period is becoming large, and in each case the numerical evidence suggests that the branch is being created in a heteroclinic bifurcation. Our conclusions are drawn from the examination of the periodic orbits of large period, and the further numerical work of Section 7.3 .

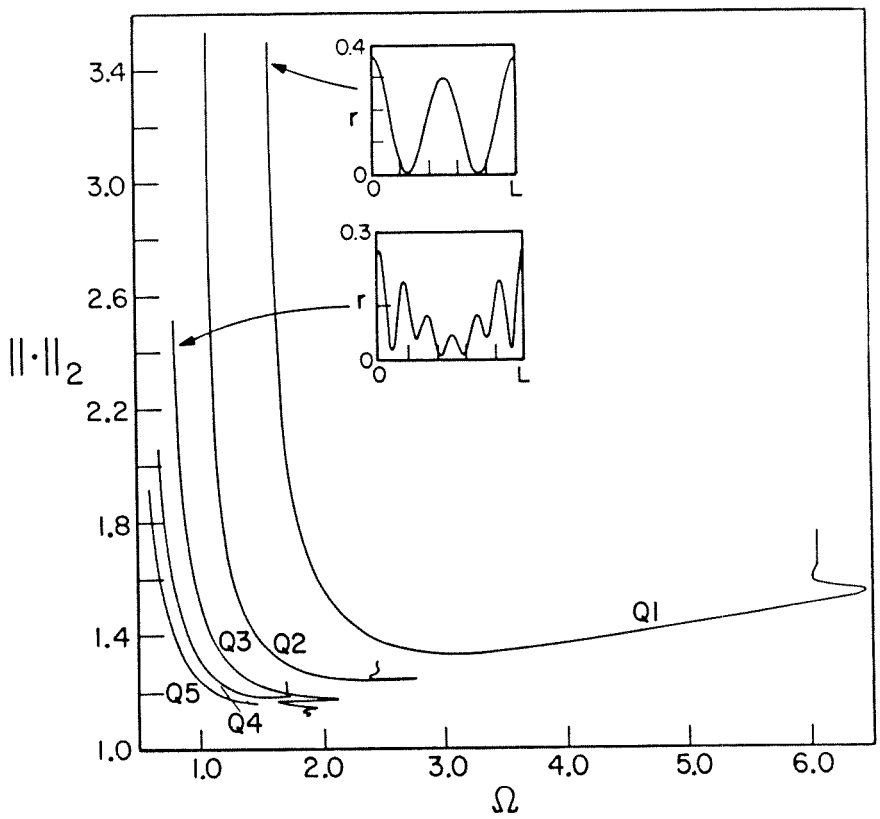

FIGURE 6.4. L^2 norm versus Ω for the Q branches, $c = 0$ and $\sigma_r = 1$.

Firstly, the evidence is strong that the branch $Q1$ is created in the bifurcation of the breather solitary wave known analytically (see Section 7.2). In particular the value at which this exact solution exists is $\Omega = 6.058$ in agreement with our continuation to very high period using the program AUTO. Similarly, the branches $Q2$, $Q4$ and $Q5$ consist of solutions for which the amplitude approaches zero for an increasingly large proportion of their period. In this way it appears that these periodic orbits are also approaching a pair of heteroclinic connections between D_+ and D_-, one lying in the $r \equiv 0$ plane and the other lying above it. Such solutions become solitary envelopes of the Tollmien-Schlichting waves for plane Poiseuille flow and travel at the group velocity. We recompute these and more solutions connecting D_+ to D_- in Section 7.3 .

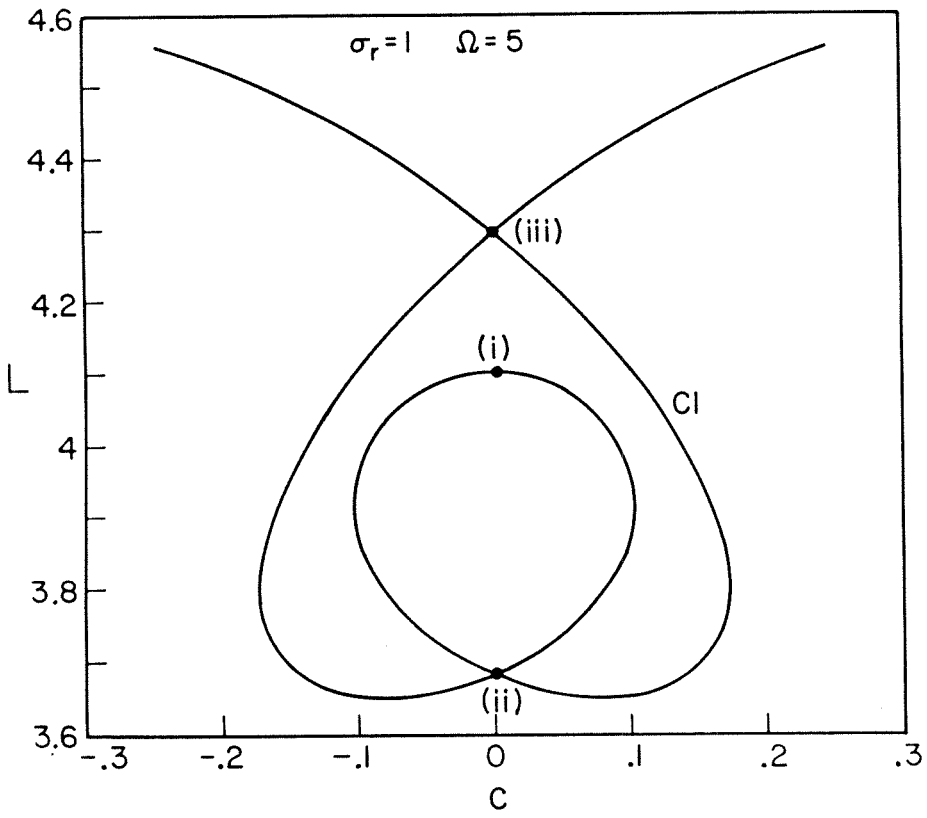

FIGURE 6.5. Continuation of point (i) on branch $Q1$ in c for fixed $\Omega = 5.0$.

The fate of branch $Q3$ is quite distinct from the others, however. It comes very close to the plane wave fixed points T_+ and T_- and has amplitude modulus always staying bounded above zero, which strongly suggests at this value of $\Omega \approx 1.85$ a heteroclinic loop exists between the plane wave fixed points.

We now briefly discuss continuation of periodic orbits by varying c. Starting at the orbit on the symmetric branch $Q1$ at $\Omega = 5.0$ (point (i) in Figure 6.3), we fixed Ω and continued in c for the equations (4.1). Figure 6.5 shows the branch $C1$ that results. We find that for this value of Ω there are 4 more periodic orbits with $c = 0$, at points labelled (ii) and (iii). These solutions are non-symmetric and the mean of s over one period is nonzero, indicating the corresponding GL solution is quasi-periodic as discussed in Section 2.3. Thus the branch $C1$ lies on a surface of 2-tori solutions in the product space of quasi-steady solutions and the 2-dimensional

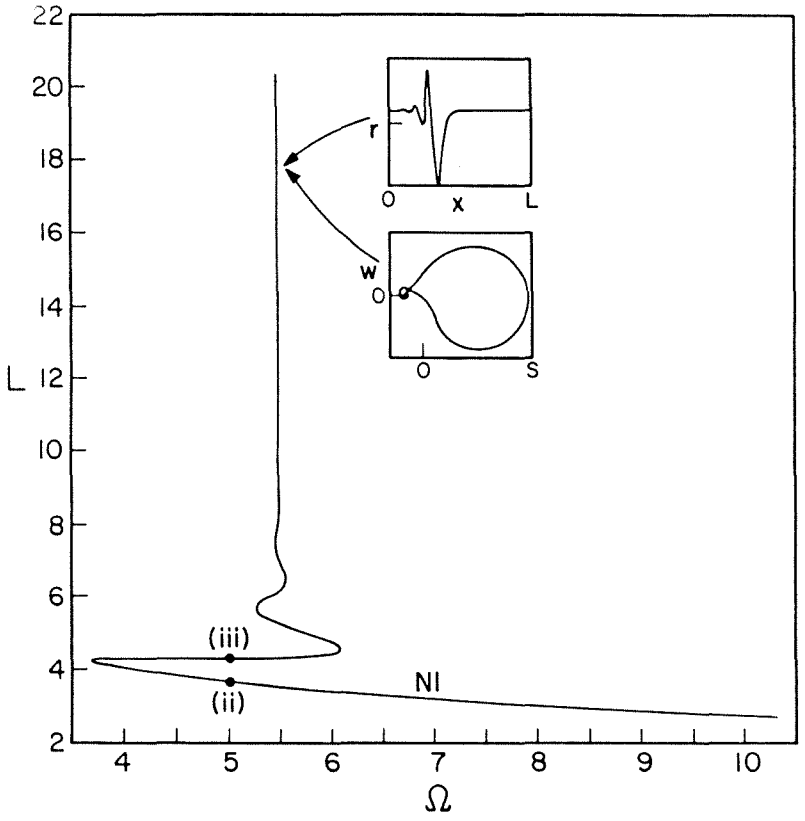

FIGURE 6.6. Branch $N1$ of nonsymmetric periodic solutions, $c = 0$.

parameter space. By monitoring Floquet multipliers, even though $c > 0$ on part of this branch, all solutions on $C1$ are not stable, as must be true for the Q branches when $c = 0$.

At each of the points (ii) and (iii) there is a pair of solutions which are reflections of each other. We have continued these solutions in Ω with fixed $c = 0$ and show one of the resulting non-symmetric branches $N1$ in Figure 6.6. Note that a twin branch to the one shown must also exist under the reflection symmetry. We find that along this branch $\bar{s}$ is nonzero as defined in equation (2.18) so that the solutions on this branch, although periodic in the reduced phase space, are quasi-periodic when the spatial form of the corresponding Ginzburg-Landau solution is obtained.

We find that the solutions at the right hand end of $N1$ are becoming singular which suggests that this branch, like the symmetric Q branches, is bifurcating from

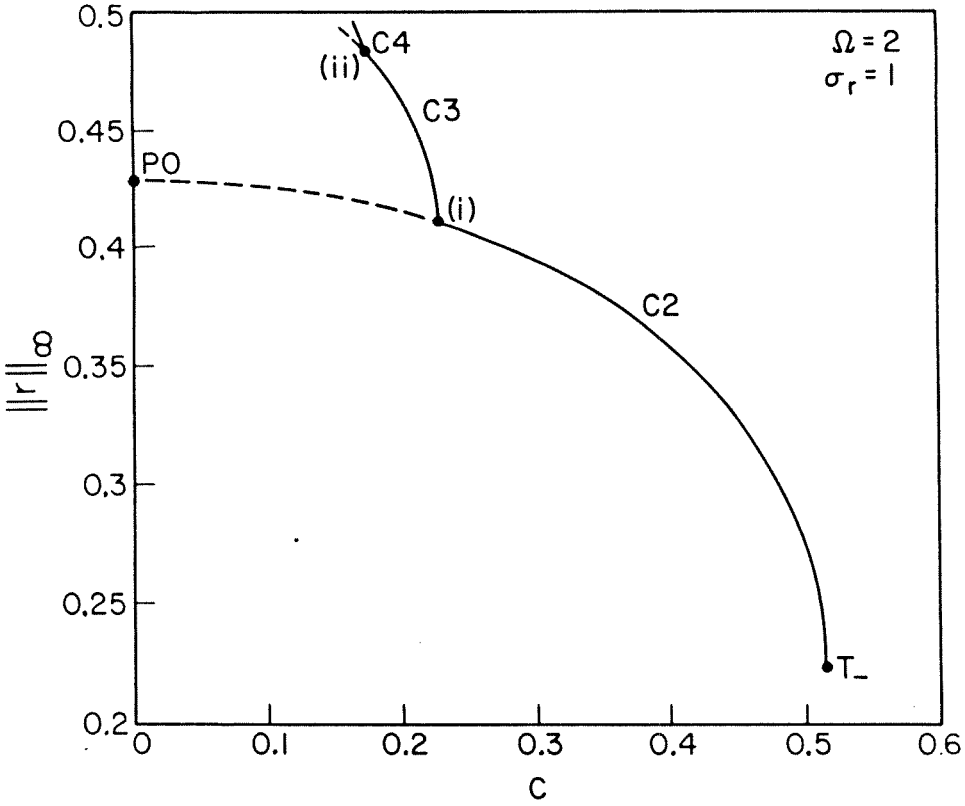

FIGURE 6.7. Continuation in c of Hopf-bifurcating branch into region III.

Solid lines are stable periodic orbits. Supercritical period doubling bifurcations occur at (i) and (ii).

a branch with odd symmetry at $\Omega \approx 10.4$. It is also interesting that the left hand end of $N1$ increases to very large period and on inspecting such solutions as in the insets of Figure 6.6 we find that this branch seems to bifurcate in a homoclinic bifurcation from the plane wave T_-, as does its reflection from T_+. In this way we have strong evidence that homoclinic orbits to the plane wave fixed points exist for $c = 0$ at a value of $\Omega \approx 5.49$.

Now we consider the continuation of periodic orbits bifurcating from the plane wave fixed point T_- at the boundary of the regions II and III in parameter space for $\sigma_r = 1$ and fixed Ω. In Figure 6.7 we show the maximum modulus squared (maximum of r) versus c for the $C2$ branch at $\Omega = 5.0$. The branch undergoes at

least two supercritical period doubling bifurcations, the first one to branch $C3$. The behavior differs from the case $\sigma_r = -1$ in Figure 6.2 in that the primary branch extends to $c = 0$ where it becomes singular though the period and amplitude remains bounded, due to bifurcation from a periodic solution $P0$ with odd symmetry as for the Q branches. In this way such a branch and its twin for $c < 0$ connect the plane wave solutions with a family of 2-tori through the periodic orbit $P0$ at $c = 0$. Hence the situation described analytically in Section 5.2 for Ω near 0.147 holds qualitatively at much larger Ω.

6.3 Periodic orbits in the 4-dimensional phase space for $\sigma_r > 0$.

From the results of the last section we are led to search for a branch of quasi-steady spatially periodic solutions of the GL equation with odd symmetry for $c = 0$ and $\sigma_r = 1$. Such a branch is singular in the reduced system due to the amplitude vanishing at a point, thus forcing us to consider the 4-dimensional complex Duffing system.

Using perturbation theory we have been able to find a small amplitude expansion for a periodic orbit bifurcating from $\beta = 0$ ($\Omega = a_0\sigma_r$), which has both odd and even symmetries (see Section 5.1). With this as a starting point, we continued to finite amplitude numerically. Because of the rotation symmetry in the 4-dimensional system, a standard continuation procedure for periodic solutions fails due to this causing a singular Jacobian. By adding the artificial perturbation parameter ϵ in the periodic boundary condition on u, where

$$u(0) = u(L)(1 - \epsilon),$$

we could continue the branch satisfactorily as a boundary value problem using the code AUTO. In addition to the above boundary condition and periodicity for v, p and q, we imposed two integral constraints to fix the translation and phase invariances,

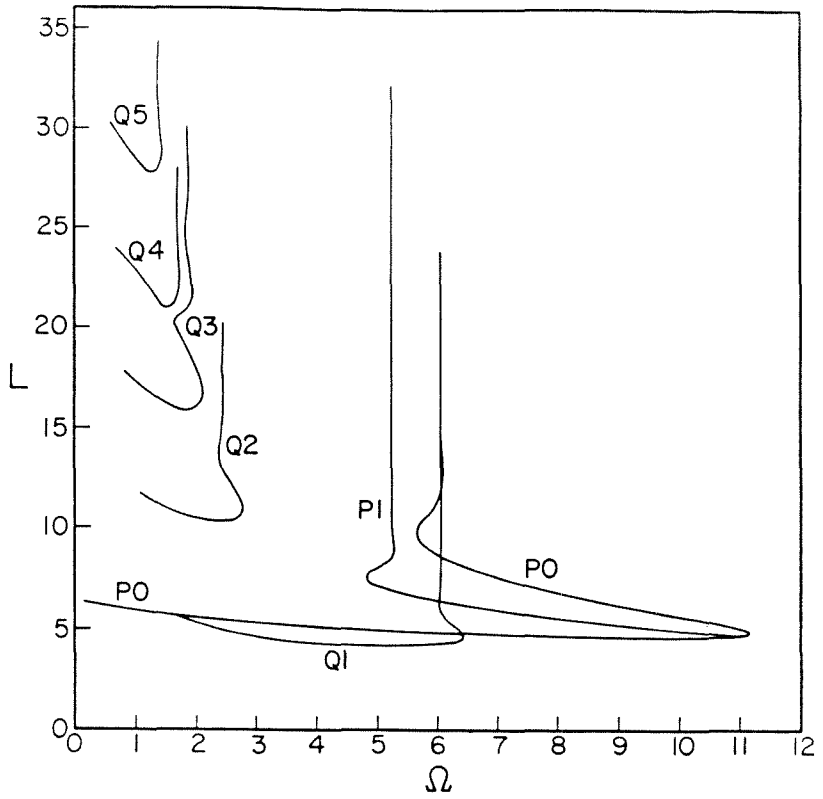

FIGURE 6.8. Bifurcation diagram for the period of solutions in the 4-dimensional complex Duffing phase space, $c = 0$.

and continued in the three free parameters Ω, the period L and ϵ. During the continuation we insisted that $\epsilon < 10^{-8}$, so that accurate solution to the actual periodic problem was ensured. We were also able to monitor the Jacobian of the extended system to find bifurcations.

Apart from the primary branch which we call $P0$, we have found a new branch $P1$ bifurcating from it in a spontaneous symmetry breaking. $P1$ has odd symmetry so is still singular in a 3-dimensional representation, but no longer preserves the reflection symmetry. We were also able to recompute the symmetric Q branches using the 4-dimensional code. In Figures 6.8 and 6.9 we show the bifurcation diagrams for all these solutions as a function of period L and maximium modulus of the amplitude $\|\Phi\|_\infty$ respectively. The latter is a convenient choice as one can also

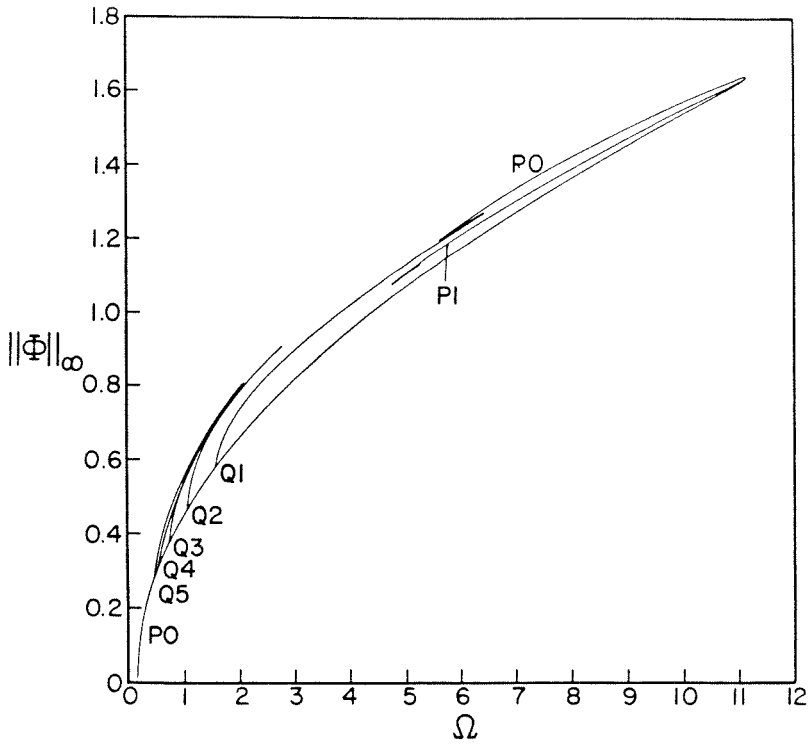

FIGURE 6.9. Bifurcation diagram for the maximum modulus of solutions in the 4-dimensional complex Duffing phase space, $c = 0$.

plot quasi-periodic solutions on such a bifurcation diagram, whose period is strictly infinite.

We can now directly observe that the Q branches all bifurcate from $P0$ with loss of odd symmetry. Although we have been unable to compute Floquet multipliers in the 4-dimensional continuation, the two nontrivial multipliers satisfy equation (6.1) and thus $\sigma_1\sigma_2 = 1$ when $c = 0$. We expect that the multipliers are at $+1$ when $Q1$ bifurcates, -1 when $Q2$ bifurcates in a period doubling, and that they move around the unit circle back to $+1$ for decreasing $\Omega > a_0\sigma_r = 0.147$. We thus conjecture that an infinite number of branches bifurcate from $P0$ of period nL/m when the multipliers lie at $\exp(\pm 2\pi mi/n)$.

We have already commented on the large period limits of the Q branches. We see that for large period branches $Q1$ and $P0$ appear to coalesce. This is a particularly

interesting bifurcation as $P0$ possesses odd and even symmetries whereas $Q1$ is even only. We conclude that there is a "period doubling at infinity", where $Q1$ is a single hump tending to a breather solitary wave (in fact an exact solution shown in Figure 7.3a) and $P0$ is a two hump solution approximating two $Q1$ humps of opposite phase. See Figure 6.10. The large period limit of the branch $P1$ also yields a breather solution but with odd symmetry only, as shown in Figure 6.11.

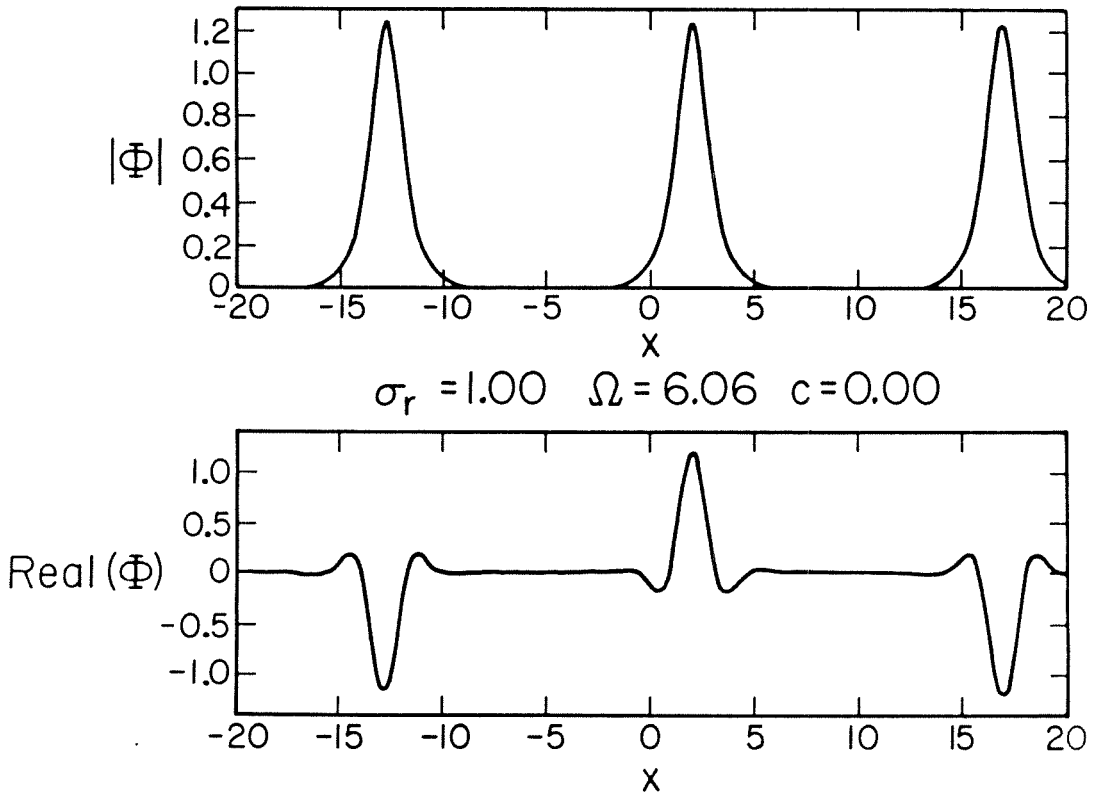

FIGURE 6.10. $1\frac{1}{2}$ periods of an orbit of high period on branch $P0$, approaching a pair of $Q1$ breather solitary waves.

Although we cannot continue periodic solutions to non-zero c in the 4-dimensional space as they become quasi-periodic, as with the case of the Q branches we can interpolate between the results of the 3- and 4-dimensional complex Duffing representations which complement each other. We are able to conclude that the continuation of $P0$ in c is the surface of 2-tori solutions mentioned earlier which

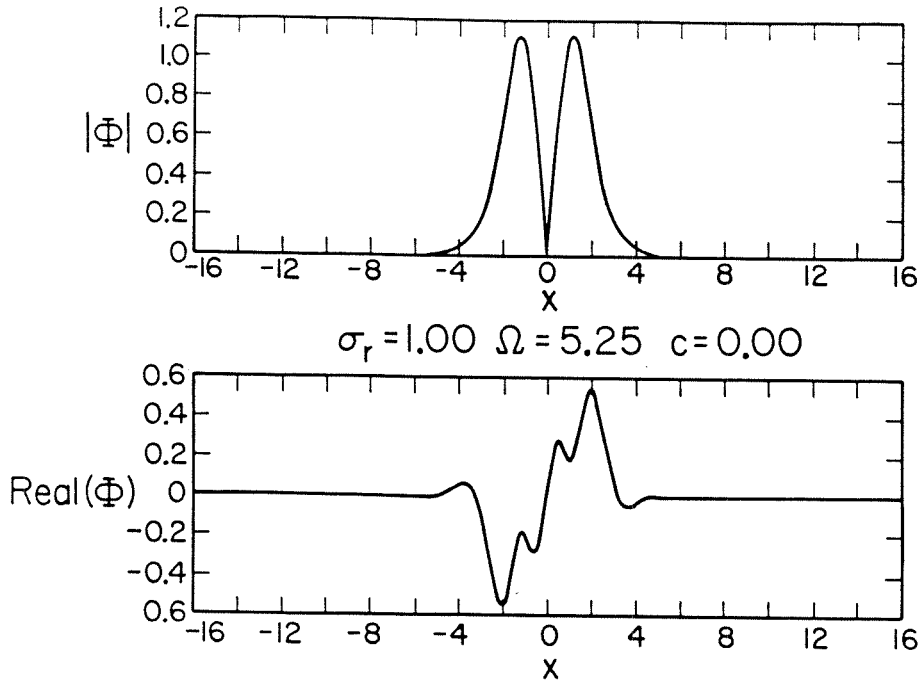

FIGURE 6.11. A single period of a solution of large period on branch $P1$, approaching a breather solitary wave of odd symmerty.

bifurcates from T_+ and T_- in a Hopf bifurcation, as is confirmed by the perturbation theory of Chapter 5.

In conclusion to this section, we have been able to find a complicated structure of periodic solutions for the systems (2.8) and (4.1) using the parameter values (2.5) appropriate to Poiseuille flow. This structure is much richer than that which we can describe with perturbation theory. The solutions of the GL equation that result are periodic or quasi-periodic in space and simply periodic in time, provided one is moving in a frame of reference of speed c. For $c = 0$ we appear to have found a large class of solitary wave solutions for $\sigma_r > 0$. For $c > 0$ we have also found (spatially) stable quasi-periodic solutions for σ_r either side of critical.

The complexity of the structure of periodic solutions is somewhat typical in that complicated dynamics (in this case spatial) may occur in continuous systems with simple nonlinearities in only three dimensions. The symmetries in the GL equation

also play an important role in determining the structure of the periodic solutions. We stress that due to the complexity of this structure our classification of periodic orbits is far from complete. One reason we have not pursued this further is that due to the discovered nonuniqueness and lack of any selection criterion for the free parameters Ω and c, it is unclear which of the branches of periodic orbits, if any, are physically relevant.

CHAPTER 7

Solitary Wave Solutions and Transition from the Laminar and Plane Wave States

In this chapter we consider quasi-steady solutions of the GL equation which are asymptotic at either plus or minus infinity to the trivial laminar state or plane wave states. Hence we study orbits in the 3-dimensional reduced phase space which are the stable or unstable manifolds of the critical points $D_\pm$ and $T_\pm$. In particular we are interested in homoclinic and heteroclinic orbits connecting these critical points which result in solitary wave solutions. Recall that $T_\pm$ and $D_\pm$ have physical significance in the Poiseuille problem and that connections between these points in phase space may indicate similar connections between travelling waves and the undisturbed state in the fluid equations from which the GL equation is derived. In addition we numerically find solutions that are asymptotic from the laminar state and plane waves to some of the attracting quasi-periodic solutions described in the previous chapter and also to apparently spatially chaotic states. In so doing we are able to find a large class of quasi-steady solutions describing a transition from the laminar state to a finite amplitude disturbance, which exist for the Reynolds number parameter σ_r either side of critical.

7.1 **Classification of solitary wave connections in phase space**

We now discuss the possible heteroclinic and homoclinic connections that could exist for the system of three O.D.E.'s under consideration as the parameters Ω and c are varied. Some of these solutions have been found previously in analytic form by other authors, and our numerical work of Section 6.3 gives strong evidence for the existence of many others.

In the light of the stability calculations for the critical points $D_\pm$ and $T_\pm$, we can expect solitary wave solutions to exist for either a continuum or discrete values of Ω and c by considering the dimensionality of the fixed points' stable and unstable manifolds.

Homoclinic orbits can exist only at the fixed points $T_\pm$, which we label

$$H0: \qquad T_+ \to T_+ \quad \text{and} \quad T_- \to T_-.$$

However there are four main types of heteroclinic orbits joining distinct fixed points, illustrated in Figures 7.1 and 7.2 . First we know a continuum of connections exists of the type

$$H1: \qquad D_- \to D_+$$

in the $r \equiv 0$ plane for almost all values of the 2 parameters Ω and c, although these represent the trivial $A \equiv 0$ solution. A connection of the type

$$H2: \qquad D_+ \to D_-$$

for which the modulus of the amplitude is positive was shown to exist by Hocking and Stewartson (1972) for a discrete value of Ω and $c = 0$, who simply wrote down this breather type solitary wave solution in closed form, which we will discuss in Section 7.2. Note that a heteroclinic orbit of type $H2$ corresponds to a homoclinic orbit of $(0,0,0,0)$ for the 4-D system (2.8). Any connection to or from the laminar state in the reduced representation must consist of the 1-dimensional stable or unstable manifolds of D_- and D_+ respectively. When $c = 0$ the connection of type $H2$ must be symmetric and such a solution would in general not be expected for a continuum of Ω. We have numerical findings that strongly suggest that many more if not an infinite number of symmetric breather solutions exist for a discrete spectrum of Ω, which we discuss in Section 7.3. When $c \neq 0$ one would expect breather solutions to exist for discrete values of the two parameters only (i.e., a codimension-2 situation).

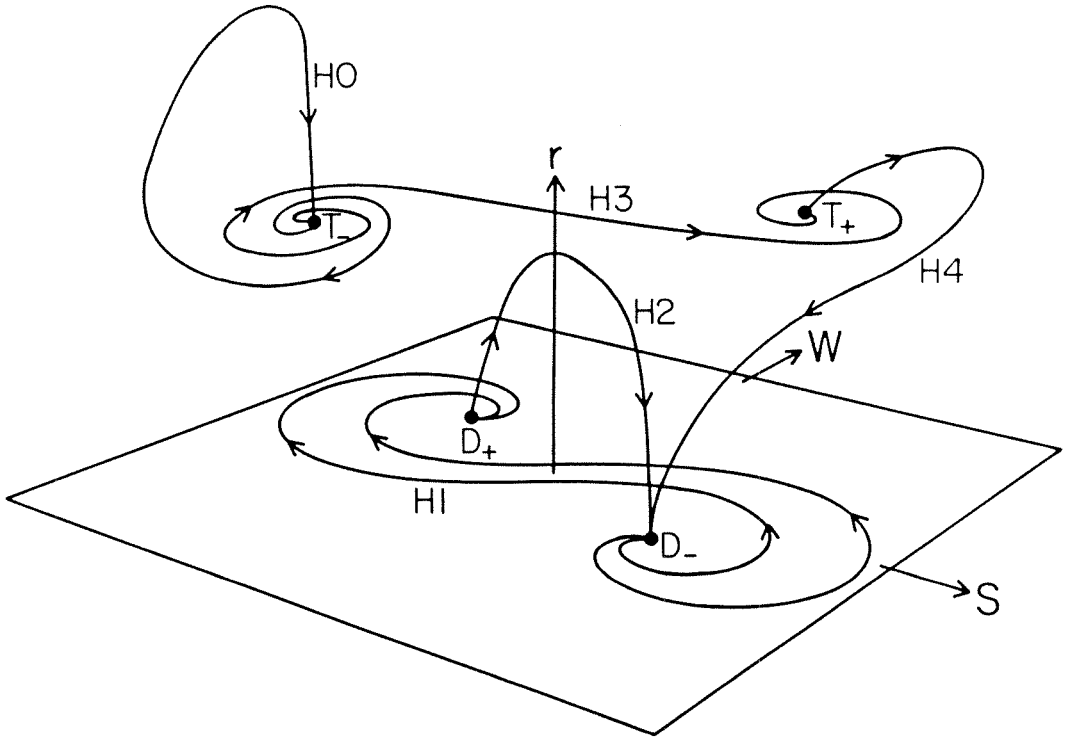

FIGURE 7.1. Orbits in the reduced phase space as examples of homoclinic ($H0$) and heteroclinic connections ($H1$–$H4$).

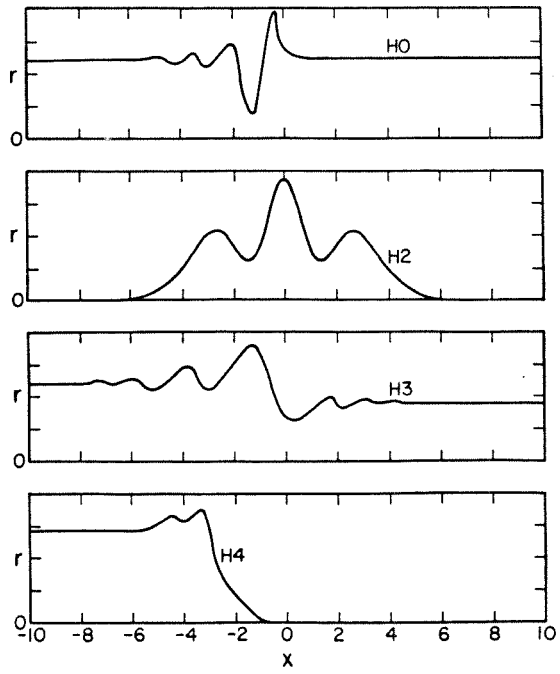

FIGURE 7.2. Modulus versus X for solitary wave solutions resulting from homoclinic and heteroclinic orbits of Figure 7.1.

$H0$ and $H3$ are hole type solutions, $H2$ a breather and $H4$ a front or shock.

The hole type connections

$$H3: \qquad T_- \to T_+ \qquad \text{and} \qquad T_+ \to T_-$$

may take various forms due to the different stability properties of these fixed points in different parameter regimes according to Table 4.1 . In region III of Figures 4.2 and 4.3 for instance we might expect the $T_- \to T_+$ connection to exist continuously as the parameters are varied due to the likely transverse intersection of two 2-manifolds in 3-space. Our numerical work for $c = 0$ supports this conjecture.

The possible connections

$$H4: \qquad D_+ \to T_\pm \qquad \text{and} \qquad T_\pm \to D_-$$

are of particular interest in describing transitional fronts from the undisturbed state. Once again these may also take various forms depending on the stability properties of the fixed points.

Referring to the results of Chapter 4, in regions IIa and IIb of parameter space the plane wave solutions T_- and T_+ are asymptotically stable and unstable respectively. We are thus motivated to seek solutions of type $H3$ and $H4$ in these regions which, if existing at all, would exist for a continuum of parameter values. Similarly in regions Va and Vb where the stability properties are identical.

In regions IVa and IVb the points D_+ and D_- are stable and unstable respectively so that we can also seek solutions of type $H4$ for those values of Ω and c. Such investigations are carried out in Section 7.3.

7.2 Some solitary wave exact solutions

It is somewhat surprising that three analytic solutions are known which describe heteroclinic orbits for the reduced O.D.E. system (4.1). It is also interesting to observe that these three solitary wave solutions are of the form of the breather, front (shock or kink) and hole solutions which arise in the study of the sine-Gordon equation. Their forms become particularly simple when cast in the framework of the reduced form of the complex Duffing equation.

The first referenced above as the solitary wave of type $H2$ was first written down by Hocking and Stewartson as a solution of the GL equation

$$A = \lambda L e^{-i\Omega t}(\operatorname{sech} \lambda x)^{1+i\nu} ,$$

where the parameters in the equation are uniquely determined by the GL coefficients. For the reduced system (4.1) this solution is of the form

$$r = \lambda^2 L^2 \operatorname{sech}^2 \lambda x, \qquad w = -\lambda \tanh \lambda x, \qquad s = \nu w. \tag{7.1}$$

We find that

$$\lambda^2 = \frac{\delta_1}{\nu^2 - 1}, \qquad L^2 = -\frac{3\nu}{\gamma}, \quad \text{and} \quad \frac{\beta}{\delta_1} = \frac{2\nu}{1-\nu^2}.$$

In this and the other solutions which follow ν is given by a root of the appropriate sign of the equation

$$\nu^2 + 3\nu\frac{\delta_2}{\gamma} - 2 = 0. \tag{7.2}$$

This breather solution always exists if $\delta_2 < 0$ (the Poiseuille case), but when $\delta_2 > 0$ this breather exists only for $\delta_1 > 0$. For the Poiseuille flow parameters (2.5) we must have $\sigma_r > 0$ and we find that when $\sigma_r = 1$, $\Omega = 6.058$.

This solution and another two heteroclinic orbits were found by Nozaki and Bekki (1984). These authors extended the direct method of Hirota (1976) for finding solitary wave solutions of the cubic Schrödinger equation to the GL equation, which is based on the fact that these partial differential equations may be written in terms of bilinear differential operators. They assumed that $\sigma_r d_r < 0$ in the GL equation, though we find that this is an unnecessary restriction.

A solution that we find most interesting has the form of a front, where the solution tends to a travelling wave at minus infinity and to zero at plus infinity. In this case which is $H4$ above, the GL solution is

$$A = Le^{i[k(x-ct)-\Omega t]}\,[1 - \tanh\lambda(x-ct)]\,[\mathrm{sech}\,\lambda(x-ct)]^{i\nu}$$

or the solution to the ordinary differential equations (4.1) is of the form

$$r = L^2(1-\tanh\lambda X)^2, \qquad s = k - \nu\lambda\tanh\lambda X, \qquad w = -\lambda(1+\tanh\lambda X).$$

On solving the 6 simultaneous equations which result in our 3-dimensional representation we get

$$\lambda^2 = \frac{\delta_1}{8-9a_0^2} \qquad L^2 = \frac{3\nu\lambda^2}{\gamma} \qquad \frac{\beta}{\delta_1} = \frac{18a_0}{9a_0^2-8}$$

$$c_1 = 6\lambda \qquad k = \lambda(3a_0+\nu)$$

This shock solution exists for a large range of GL coefficients and for unique values of Ω and c. For the Poiseuille case, on returning to the original parameters we find that σ_r must be supercritical and the solution exists for $\sigma_r = 1$, $\Omega = -0.183$ and $c = 2.14$, and thus is a heteroclinic orbit between T_+ and D_- existing in region IVa of parameter space. This solution is codimension-2 due to the coincidence of two 1-dimensional manifolds. In this way it is a special case of the connection $H4$. Note

that due to the reflection symmetry (2.15) a reverse shock also exists but for a value of c of the opposite sign from that given above.

The hole solution found by Nozaki and Bekki is of the form

$$A = \lambda L e^{-i\Omega t} \tanh \lambda x (\operatorname{sech} \lambda x)^{i\nu}.$$

Cast in the 3-dimensional dynamical system form we find

$$r = \lambda^2 L^2 \tanh^2 \lambda x, \qquad s = -\nu\lambda \tanh \lambda x, \qquad w = \frac{2\lambda}{\sinh 2\lambda x},$$

where for existence one must satisfy

$$\lambda^2 = \frac{\delta_1}{2}, \qquad L^2 = \frac{3\nu}{\gamma}, \quad \text{and} \quad \frac{\beta}{\delta_1} = \frac{3\nu}{2}.$$

For Poiseuille parameters we find that the hole solution exists only for supercritical σ_r, and when $\sigma_r = 1$, $\Omega = 3.45$. This solution requires the symmetry of $c = 0$ and exists for a discrete value of Ω only as it occurs due to the coincidence of two 1-dimensional manifolds. Notice that the solution tends to the travelling waves T_- and T_+ at plus and minus infinity and there is a singularity in w where the solution passes through amplitude zero. This solution exposes the weakness of the 3-dimensional phase invariant formulation of the problem, in which it has a singularity of the form (4.5). The solution is analytic in the original variables, however, where in the 4-dimensional formulation it corresponds to an orbit of odd symmetry tending to the plane wave periodic orbits at plus and minus infinity.

7.3 Numerical results

We first describe the family of symmetric breather solitary wave solutions of type $H1$ that we have found for $c = 0$. The shooting method used solves the initial value problem in x for the reduced system from close to D_+ on the linearization of its 1-dimensional unstable manifold and shoots to a point $(r_1, 0, w_1)$ on the

Poincaré plane $s \equiv 0$. All our numerical integrations were performed using the Sandia ODE package. Newton's method with a numerical Jacobian was then used to solve $w_1(\Omega) = 0$. On Newton convergence the resulting orbit approximates half of a symmetric breather solution at a value of Ω determined by the iteration procedure. Our method recovered the known exact solution (7.1) to greater than 6 digit accuracy. It also converges to a large number of other previously unknown breather-type solutions, provided $\sigma_r > 0$. These solutions possess a discrete spectrum of frequencies for $\Omega > a_0\sigma_r$. This lower bound for Ω when $c = 0$ follows from the relation

$$\int_{-\infty}^{\infty} r(\gamma r - \beta)dx = rs\Big|_{-\infty}^{\infty}.$$

which is derived from the dynamical equations (4.1) by integration by parts. The boundary term vanishes on a breather solution and thus β must be positive for such a solution to exist. Although we cannot prove the existence of these other heteroclinic orbits in the (r, s, w) phase space, we believe the numerical evidence for their existence is very strong.

In our shooting method we may choose the number of times n_s the orbit is to pass through the $s \equiv 0$ Poincaré plane before hitting the r axis. When $n_s = 0$ we converged to 10 breather type solutions, the number limited by the set of initial Ω values in the Newton procedure. Two breather solutions found with $n_s = 0$ are shown in Figure 7.3*a* and *b*. Similarly we find more breather-type solutions with $n_s \geq 1$, two of which are plotted in Figure 7.3*c* and *d*. No solutions were found for $\sigma_r < 0$.

We expect that an infinite number of breathers exist, each one the infinite period limit of a branch of periodic orbits. This is based on our conjecture that an infinite number of periodic branches bifurcate from the branch $P0$ which behave similarly to $Q1$, $Q2$, $Q4$ and $Q5$ of Figure 6.3. All of these solitary wave envelopes are steady

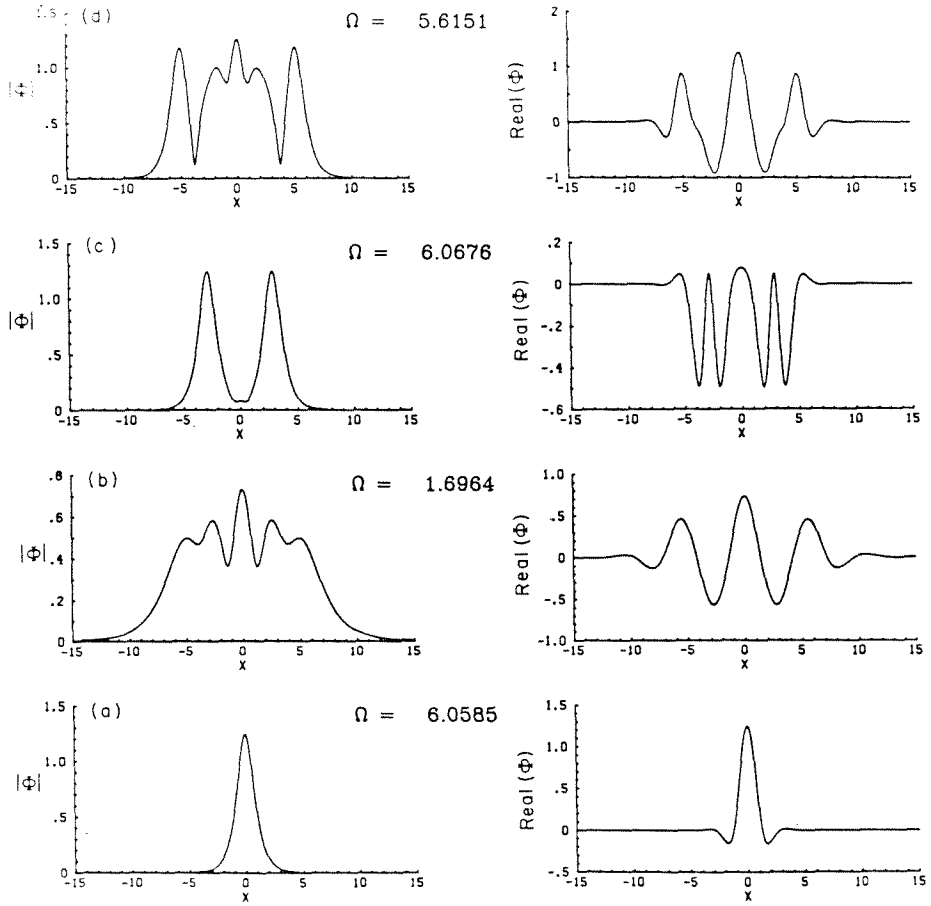

FIGURE 7.3. Real part and modulus of some breather solutions, $c = 0$ and $\sigma_r = 1$.

(a) is the exact solution (7.1) on branch $Q1$.

in the group velocity frame for Poiseuille flow but have distinct temporal frequencies of oscillation.

Our attempts to find nonsymmetric solitary waves decaying at plus and minus infinity were unsuccessful. We used a Newton procedure in which shooting was performed from the 1-dimensional unstable and stable manifolds of D_+ and D_- respectively to the plane $w \equiv 0$. Both c and Ω were shooting parameters, and there was no convergence except to the symmetric breathers when $c = 0$.

We also know from continuing the branch $P1$ in the 4-dimensional phase space that at least one breather solution exists which has the odd symmetry, which is

singular in the reduced representation. Again we might expect a discrete spectrum of these solutions in Ω for $c = 0$. Similarly the continuation of branch $Q3$ suggests that at least one pair of hole-type solutions $H3$ exists for a discrete spectrum of Ω and $c = 0$.

The heteroclinic connection $H3$ joining the plane waves $T_{\pm}$ is known to exist for $c = 0$ when the two fixed points are "close" to where they coalesce and disappear in a saddle-node bifurcation. Kopell and Howard (1981) have some general results on the existence of this connection when the distance between T_+ and T_- is small and P. Holmes (1986) has a similar result for small β and γ. We have numerical results that suggest that this symmetric connection persists for varying Ω whenever the plane wave fixed points exist (and $c = 0$), and occurs due to the intersection of two 2-dimensional invariant manifolds in 3-space. Again we used a Newton-Poincaré plane method to shoot from the point T_- to get to a point on the r-axis in phase space. The initial condition was chosen on an arbitrarily small circle about T_- lying in its planar unstable eigenspace, the shooting parameter being the position of the initial condition on this circle. In this way a family of symmetric hole-type solitary waves was found to exist connecting the distinct plane wave solutions either side of the critical value of $\sigma_r = 0$. We also expect these solutions to exist as c is perturbed from 0 provided the plane wave fixed points remain as saddle points in phase space (i.e., in region III of phase space). Such nonsymmetric heteroclinic orbits would thus connect plane waves of different amplitudes, as illustrated in Figure 7.2 .

We now discuss a class of solitary wave-type solutions describing a transition from the laminar state or plane wave states. These solutions have the common feature that they exist for nonzero c and are structurally stable in that they persist under perturbations in both Ω and c. This is because the orbit in the reduced phase space corresponding to each solution approaches a stable attractor as $X \to \infty$, or by symmetry a repellor as $X \to -\infty$. In what follows our remarks will refer only

to solutions with $c > 0$, recalling that for each such solution there corresponds a reflected quasi-steady solution of the GL equation with speed correction $-c$.

We are interested in determining orbits which lie in the basins of attraction of any bounded attractors. As we are concerned with solutions on the infinite interval, the initial conditions were chosen on the unstable manifolds of the fixed points $D_\pm$ and $T_\pm$, provided they exist. We shoot from a given initial condition in (r, s, w) phase space close to a fixed point in the direction of the appropriate eigenvector, and observe whether the trajectory approaches a bounded attractor. In all cases when this did not occur, the trajectory diverged to infinity. We have already discussed that singular behavior may correspond to a manifestation of the coordinate singularity of zero amplitude with asymptotic behavior (4.5). Numerically another form of singularity almost always appears, however, and analytically we can find its asymptotic form. The algebraic terms describing the behavior as X approaches some finite value X_0 are determined uniquely to all orders, with leading terms

$$\begin{aligned} r &\sim \left(\frac{2-\nu^2}{\delta_2}\right)\frac{1}{(X-X_0)^2} \\ s &\sim -\frac{\nu}{X-X_0} \qquad\qquad \text{as } X \to X_0 \\ w &\sim -\frac{1}{X-X_0} \end{aligned} \tag{7.3}$$

with ν given by equation (7.2). The resulting singularity for the full spatial part of the amplitude is

$$\Phi \sim \sqrt{\frac{2-\nu^2}{\delta_2}}|X-X_0|^{-(1+i\nu)} \qquad \text{as } X \to X_0 \ ,$$

which gives a spatial singularity at some finite value of $X = x - ct$ for given Ω and c (note that only the leading terms are independent of c). Such solutions are not of interest here as we require solutions to remain bounded, but these may be relevant in determining singularities that may arise in space and time in the initial

value problem of GL equation. Numerically, almost all initial conditions in phase space lead to the behavior (7.3) when $c = 0$, there being no bounded attractors in phase space. Also such singular orbits are found if $c \neq 0$ when integrating both forward and backward in X, when bounded attractors can exist. In this way Ω and c must often be varied over an appropriate region of parameter space until a bounded trajectory, if any, is found.

From our discussions so far, there are two main sectors of parameter space to search for bounded attractors. When $\sigma_r > 0$ we seek solutions in region IVa tending to D_+ as $X \to \infty$, the only possible initial condition of the above type being on the 1-dimensional unstable manifold of T_+. The second case occurs for σ_r of either sign when there can exist stable attractors in regions IIa, Va and III. In IIa (and similarly Va for $\sigma_r > 0$) the fixed point T_- is stable, and in region III there is at least one family of periodic orbits which are stable. We find that there is also the possibility of a strange attractor in this region of parameter space, as we describe below. In regions IIa, III and Va we can shoot from the 1-dimensional unstable manifolds of either T_+ or D_+. In addition in region III we can also shoot from the 2-dimensional unstable manifold of T_-.

Our numerical computations of front-like solutions of type $H4$ ($T_+ \to D_+$) when $\sigma_r > 0$ suggest that these solutions exist for all values of the parameters Ω and c in region IVa. Two such solutions are shown in Figure 7.4 , where we display both the modulus and the real part of the solution $\Phi(X)$ reconstructed from (r, s, w) via the transformation (2.11). Such front-like solutions can exist with a positive speed correction c only for supercritical Reynolds numbers ($\sigma_r > 0$).

In regions IIa (and similarly Va) the plane wave solution T_- is spatially stable. Figures 7.5 and 7.6 illustrate that hole $H3$ ($T_+ \to T_-$) and front $H4$ ($D_+ \to T_-$) solutions exist for σ_r either sign. Figure 7.7 also shows a series of front solutions with Ω and c fixed and σ_r varying between sub- and super-critical Reynolds numbers.

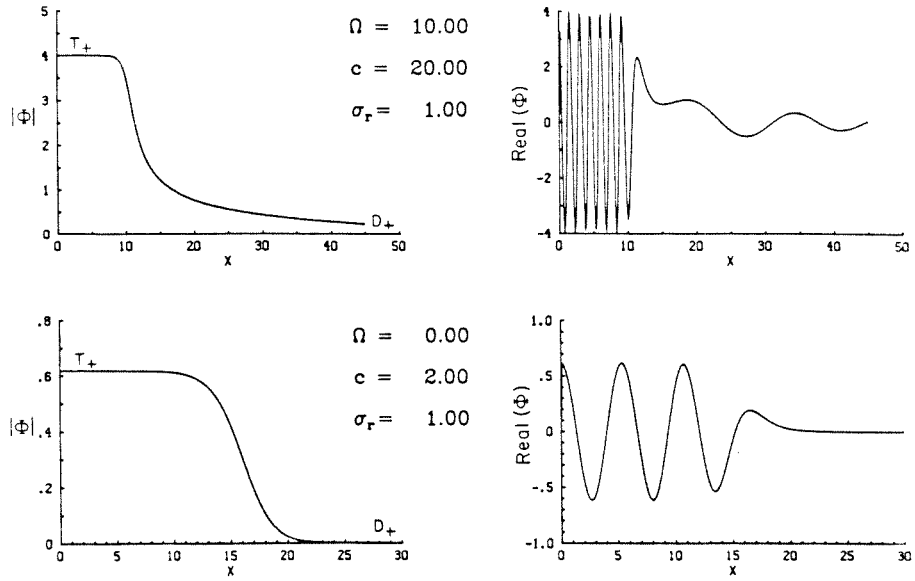

FIGURE 7.4. Front solutions ($T_+ \to D_+$) in region IVa of parameter space.

These fronts with $c > 0$ exist for $\sigma_r > 0$ only.

As far as we can tell from a limited search of parameter space these two types of heteroclinic orbits exist for a large proportion of the regions II and V, although the unstable manifold of D_+ is sometimes found to be spatially unbounded with behaviour (7.3). The hole and front solutions in region Va which we have found are similar to those shown in Figure 7.6 although their spatial scale is much larger and the phase oscillates rapidly due to the larger values of coordinate s involved.

In region III there are no stable fixed points, however from our numerical continuation of Chapter 6 we know that there exist attracting periodic orbits in the reduced phase space corresponding to 2-tori for the complex amplitude. The dynamics in phase space for this sector of parameter space is extremely complex, and our studies are limited. Here we will describe some of the behavior for $\sigma_r = 1, \Omega = 2$ fixed and varying $0 < c < 0.515$, the latter being the value at which T_- loses stability in a supercritical Hopf bifurcation. Recall that the periodic orbit on branch $C2$ shed in this bifurcation (see Figure 6.7) is stable until it undergoes a series of period

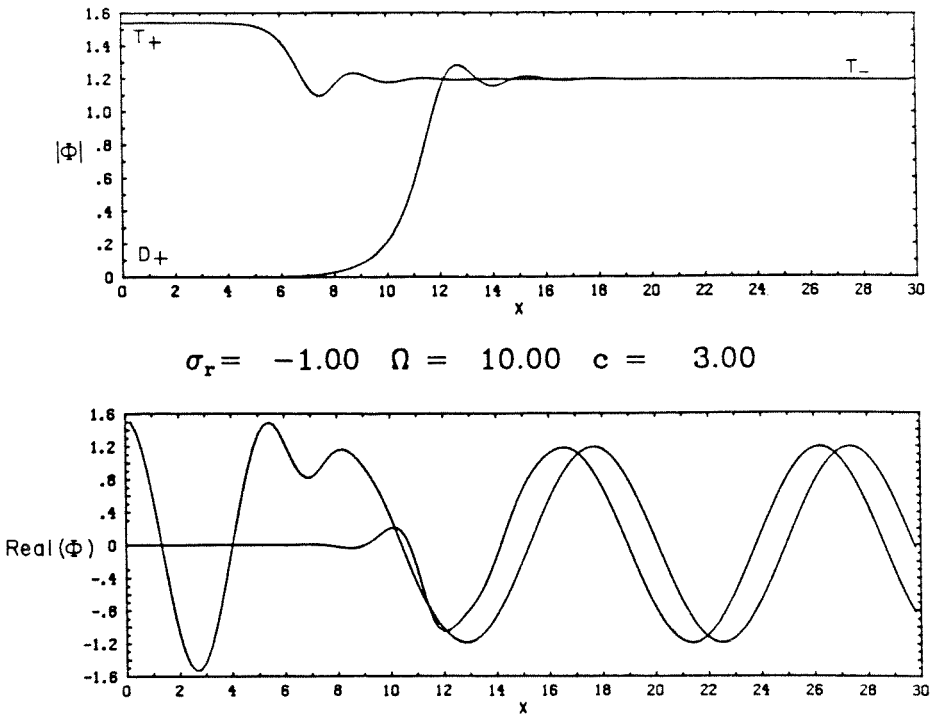

FIGURE 7.5. Real part and modulus of hole and front solutions in region IIa, $\sigma_r < 0$.

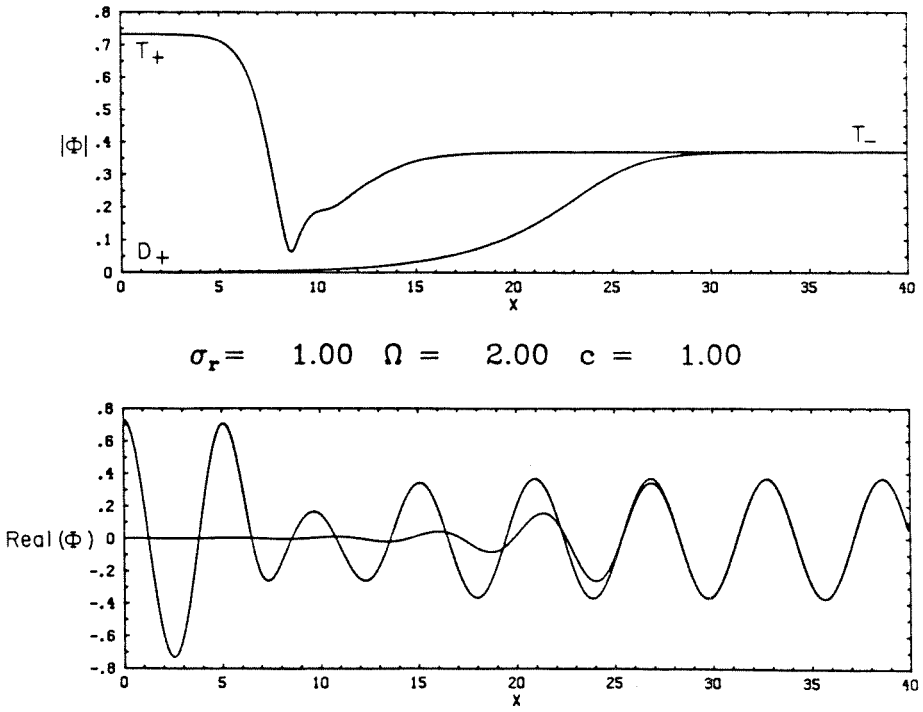

FIGURE 7.6. Real part and modulus of hole and front solutions in region IIa, $\sigma_r > 0$.

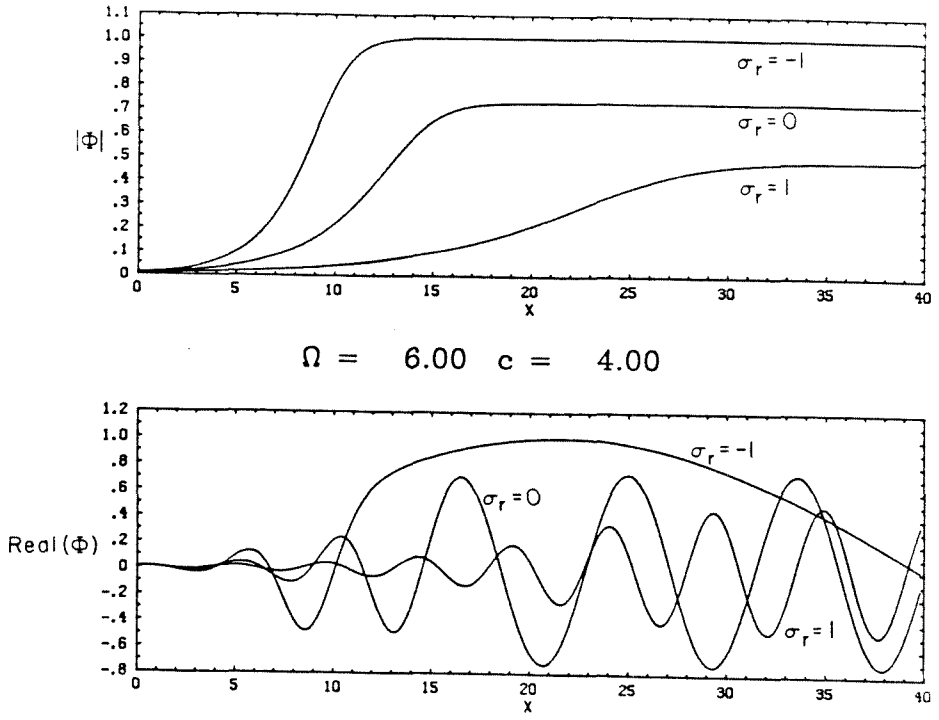

FIGURE 7.7. Front solutions ($D_+ \rightarrow T_-$) for σ_r either side of critical for fixed Ω and c.

doublings as c is decreased. Figure 7.8 shows the modified front and hole solutions at $c = 0.3$ where this periodic orbit is stable, which result from shooting from D_+ and T_+ respectively. Similar behavior results from shooting from T_-, although there is a one parameter family of solutions attracted to $C2$ from this plane wave as this fixed point is 2-dimensionally unstable. When $c = 0.2$ the unstable manifold of T_+ is attracted to the period doubled orbit on $C3$ as shown in Figure 7.9 . However a nonuniqueness is seen to arise as the front solution emanating from D_+ is attracted to a different periodic orbit.

Decreasing c further we find attractors of higher period and perhaps chaotic attractors. In Figure 7.10 we show the pair of solutions from D_+ and T_+ for $c = 0.14$. By inspection of these and other orbits for c in a neighborhood of this value, it appears that these solutions are nonperiodic. It is possible that they are very long transients to a periodic or quasi-periodic state, but are most likely chaotic, indicating

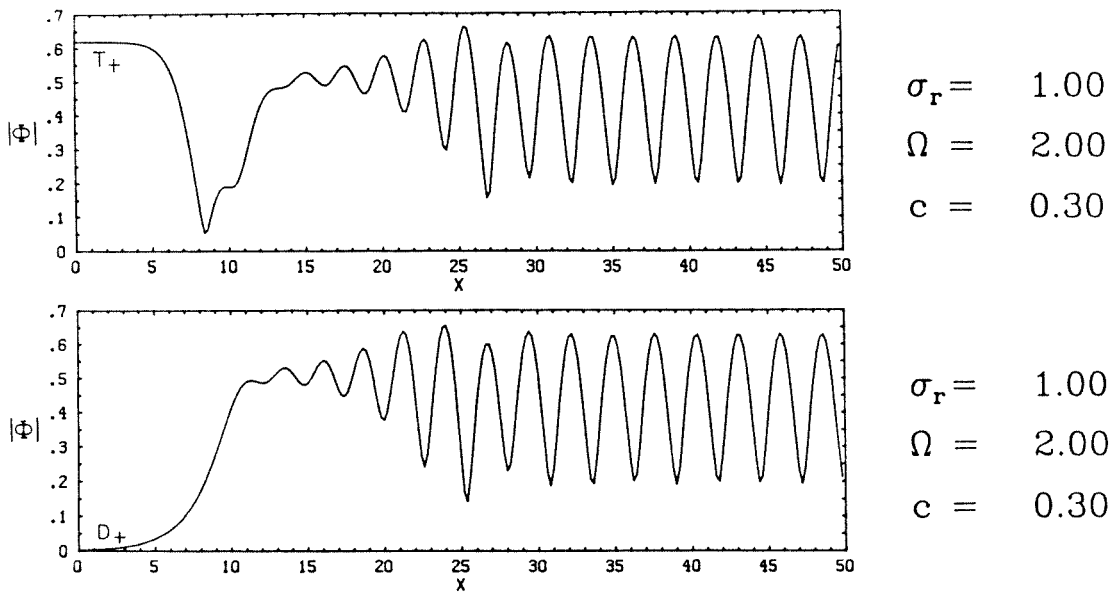

FIGURE 7.8. Transition from plane wave (a) and laminar solution (b) in region III to the stable periodic orbit on branch $C2$.

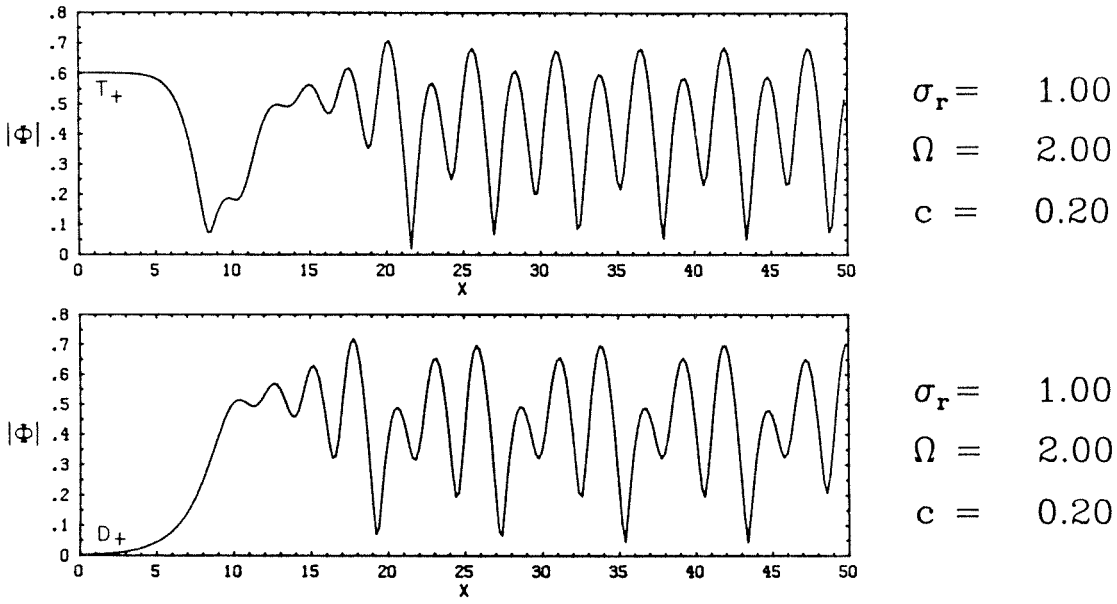

FIGURE 7.9. Transition from plane wave (a) and laminar solution (b) in region III to distinct periodic orbits.

(a) approaches the period doubled branch $C3$ and
(b) approaches a previously undiscovered stable orbit.

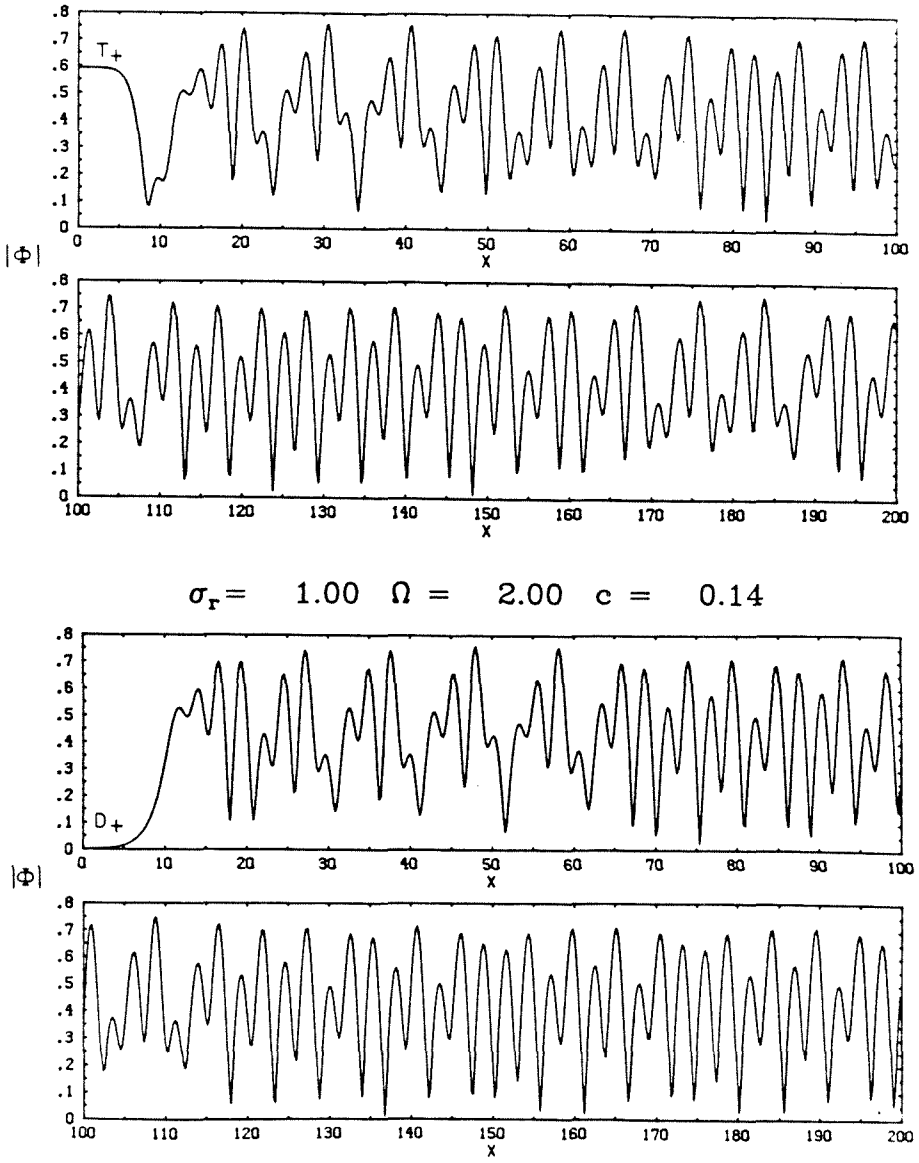

FIGURE 7.10. Transition from plane wave (a) and laminar solution (b) in region III to apparently chaotic states, $\sigma_r > 0$.

the existence of a strange attractor in phase space persisting for a continuum of values of Ω and c. In any case they illustrate a transition from the laminar and plane wave solutions to a finite amplitude spatially complicated state. Lastly for $\Omega = 2$ and c less than about 0.1 the orbits from D_+ and $T_\pm$ become spatially unbounded.

When shooting from these three fixed points in region III for $\sigma_r = -1$ and fixed Ω, only periodic branches of type $C0$ of Figure 6.2, corresponding to spatially quasi-periodic solutions of the GL equation, are found to be attracting. Recall that such solutions which bifurcate from T_- do not appear to undergo period doubling bifurcations as is possible when $\sigma_r > 0$. Figure 7.11 illustrates the modulus of the amplitude of the unstable manifolds of D_+ and T_+ for one set of parameters in this region where such a periodic orbit is attracting. From our limited numerical search we find that for fixed Ω the unstable manifolds become unbounded before the periodic branch becomes homoclinic as c is decreased. We have been unable to find any other more complex bounded behavior for subcritical σ_r other than the connection between laminar and plane wave states. These solutions are of great interest, however, illustrating that a transition from undisturbed to finite amplitude states does exist for $\sigma_r < 0$, corresponding to Reynolds numbers less than critical.

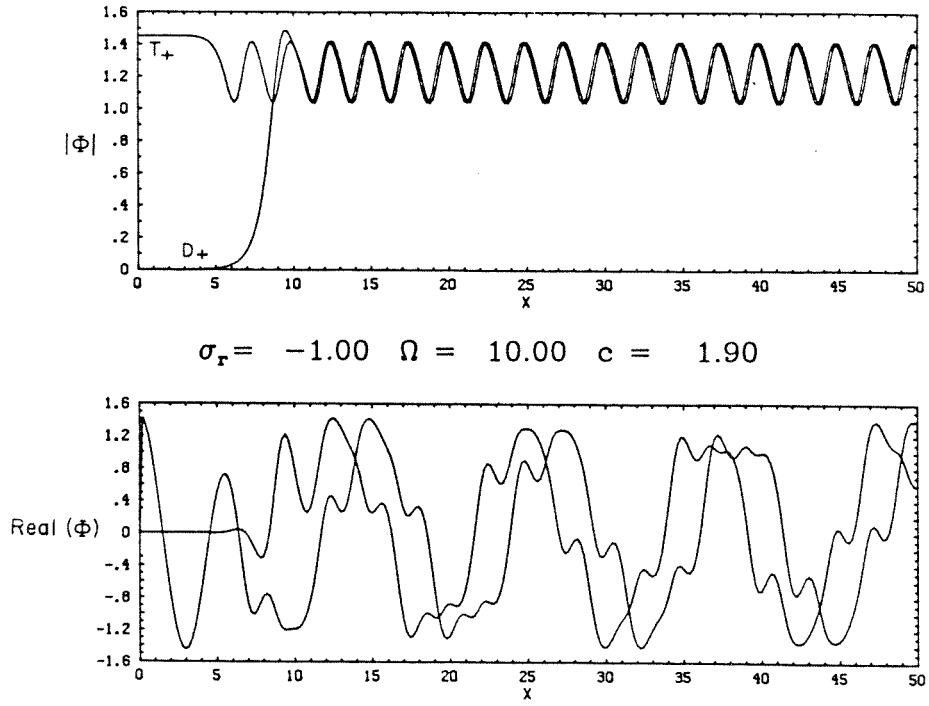

FIGURE 7.11. Transition from plane wave (a) and laminar solution (b) to a quasi-periodic solution in region III for $\sigma_r < 0$.

CHAPTER 8

Time Dependent Stability of Quasi-steady Solutions

It is of interest to determine the stability of many of the solutions of the GL equation described above, particularly due to the existence of one or more periodic orbits over a large range of values of the undetermined parameters c and Ω. The evidence we present here strongly suggests that all quasi-steady solutions are unstable if the GL nonlinearity d_r is positive, although stable spatially periodic solutions are known to exist for d_r negative. There is a possibility that some of the transition solutions may appear as transients in time, however, as suggested by the simulations of Nozaki and Bekki (1983), which we discuss in the last part of this chapter.

8.1 Stability of plane waves

It is well known that the whole family of plane wave solutions (2.2) is unstable in the case when the nonlinearity of the GL equation has the sign such that $d_r > 0$, which is the relevant case for Poiseuille flow (C. Holmes, 1985). The instability is a manifestation of the side-band instability, where the waves are unstable to long wave modulations. We will briefly demonstrate how this instability operates, as it can be compared with our bifurcation analysis of quasi-steady solutions described in Chapter 4. In so doing, we will be able to show that the quasi-steady quasi-periodic solutions of the GL equation which exist for σ_r either sign are formed as a consequence of the side-band instability.

In order to establish the side-band instability, the solution A of the GL equation is perturbed from a plane wave such that

$$A = \left[1 + \epsilon B_1 e^{iqx+\sigma t} + \epsilon B_2^* e^{-iqx+\sigma^* t}\right] B e^{i(kx-\Omega t)}. \tag{8.1}$$

On substitution into the GL equation (1.9) and linearizing for infinitesimal ϵ, the eigenvalue relation

$$\sigma^2 + 2\alpha_1\sigma + \alpha_2 = 0 \tag{8.2}$$

results, where

$$\begin{aligned}\alpha_1 =& a_r(q^2 - k^2) + \sigma_r + 2ia_i kq \\ \alpha_2 =& |a|^2 q^2(q^2 - 4k^2) + 2|a|^2|B|^2[\delta_2 q^2 - 2i\gamma kq].\end{aligned}$$

C. Holmes considers the stability boundaries in the k–q plane, and for $d_r = 1$ (Poiseuille flow) finds that for any k, there is a set of destabilizing sidebands of wavenumber q such that $\mathrm{Re}\{\sigma\} > 0$.

Her analysis is for $\sigma_r = 1$ only (supercritical Reynolds number), and on repeating the analysis for $\sigma_r = -1$ we find that the same is true. Her paper goes on to deal mostly with $d_r < 0$ and the bifurcations that arise as a plane wave loses stability as one eigenvalues moves into the right half plane. It is important to note, however, that even though a plane wave may already possess one eigenvalue with $\mathrm{Re}\{\sigma\} > 0$, the second eigenvalue may pass through the imaginary axis, and a bifurcation would in general take place with the bifurcating branch also being unstable. This is the scenario for plane Poiseuille flow, and leads to the bifurcations to the periodic and 2-tori solutions, as follows.

In general if one fixes the plane wave by fixing k, and varies q, then an eigenvalue with nonzero imaginary part will cross the imaginary axis and a bifurcation will take place. We seek the locus of bifurcations by putting $\sigma = i\omega$ in the eigenvalue relation (8.2), with ω real. This leads to the cubic equation for $Q = q^2$ where

$$\begin{aligned}Q^3 + Q^2[-4k^2 + 2|B|^2(\delta_2 - d_r/a_r)] + Q|B|^2\left[-8\delta_2 k^2 + |B|^2\frac{d_r}{a_r}\left(\frac{d_r}{a_r} - 4\delta_2\right)\right] \\ +4|B|^4k^2\left[2a_0\gamma\frac{d_r}{a_r} - \frac{d_r^2}{a_r^2} - \frac{|a|^2\gamma^2}{a_r^2}\right] + 2|B|^6\delta_2\frac{d_r^2}{a_r^2} = 0\end{aligned} \tag{8.3}$$

and

$$\omega = -i\sigma = \frac{2kq|B|^2\gamma|a|^2}{a_r(q^2-k^2)+\sigma_r}.$$

At a positive real root of (8.3), in general an eigenvalue with nonzero imaginary part will cross the imaginary axis and a Hopf bifurcation will take place, introducing a second timescale and thus lead to a quasi-periodic solution. A real eigenvalue can cross the axis only if perturbing the spatially uniform solution $k = 0$ when $\sigma_r = -1$; in this case a regular bifurcation occurs at $q^2 = -2\delta_2$ giving rise to the periodic branch $S1$, as described in Sections 5.3 and 6.1 by perturbation methods and numerical continuation respectively. Figure 8.1 illustrates the locus of values at which the real part of an eigenvalue passes through zero for sub- and supercritical values of σ_r. Note that each plane wave undergoes a single bifurcation when $\sigma_r > 0$, and when $\sigma_r < 0$ a wave may undergo one or three bifurcations, which is consistent with the analysis of plane wave phase space stability in Section 4.2.

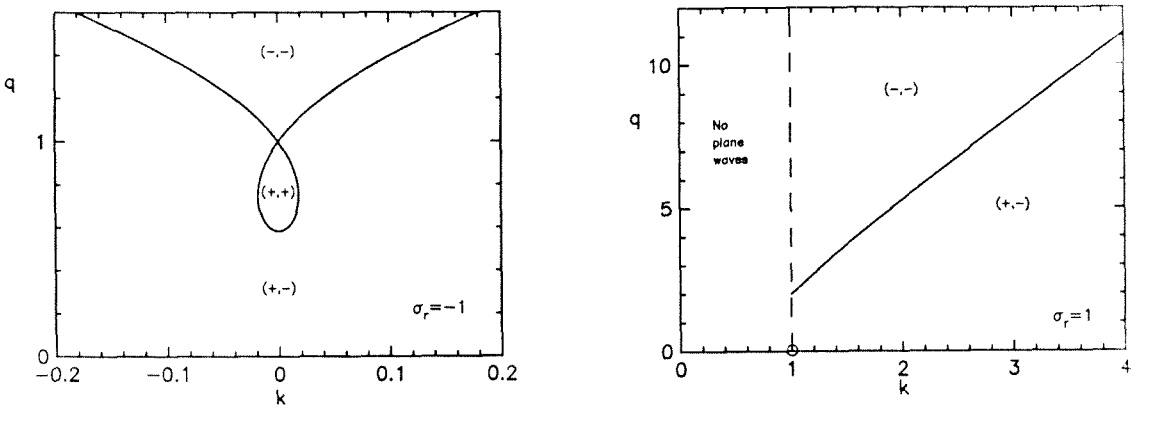

FIGURE 8.1. Bifurcation curves for sideband instability.

a) $\sigma_r = -1$. The signs of the two eigenvalues σ are indicated in parentheses. At $k = 0$, $q = 1$ both eigenvalues pass through zero, leading to the bifurcation of small amplitude 2-tori and the periodic branch $S1$.
b) $\sigma_r = 1$. At $k = 1$, $q = 0$ a degenerate situation occurs, leading to the periodic branch $P0$ and the family of bifurcating 2-tori.

It is now interesting to see how this analysis relates to the quasi-steady analysis of this thesis. In Chapter 4 we linearized about the plane wave fixed points $(r_T, s_T, 0)$ in the 3-dimensional phase space, thus seeking bifurcations to non-trivial quasi-steady solutions. The form of the perturbation was

$$\begin{aligned} A =& e^{i\omega t}[r_T + r(x-ct)]^{1/2} \exp\left[i\int^{x-ct}(s_T + s(\xi))d\xi\right] \\ \sim& Be^{i[kx-(\Omega+kc)t]}\left[1+\epsilon e^{\lambda(x-ct)}\right] \end{aligned} \tag{8.4}$$

on seeking solutions of the form $r, s \sim e^{\lambda(x-ct)}$. On comparing equations (8.4) and (8.1) we can make the identifications

$$\lambda = iq \qquad c = i\sigma/q$$

when $c, q, i\lambda$ and $i\sigma$ are real. In this way the eigenvalue equation (8.2) governing side-band bifurcations reduces to the cubic for λ (4.7) which is the characteristic equation for the spatial stability of the plane waves in phase space, and similarly the locus of bifurcations in k–q space given by (8.3) is equivalent to that in c–Ω space (4.8).

Now, the perturbation or normal form analysis done by C. Holmes about the bifurcations in k–q space reveals only the *asymptotic* nature of the solutions which bifurcate from the plane waves. In our quasi-steady formulation, however, the *exact* form of the bifurcating branches of solutions has been found to be of the form $A = e^{-i\Omega t}\Phi(x-ct)$, where Φ satisfies the complex damped Duffing equation.

8.2 Numerical calculation of stability of spatially periodic solutions

We have computed the stability of quasi-steady spatially periodic branches of solutions for $c = 0$. Consider a small perturbation ψ to a quasi-steady solution

$\phi(x)e^{-i\Omega t}$ of the form

$$A = [\phi(x) + \psi(x,t)]\, e^{-i\Omega t}.$$

Substituting this into the GL equation (1.9) and linearizing about the quasi-steady state gives

$$\begin{aligned} &\frac{\partial \psi}{\partial t} = \mathcal{L}\psi \\ &\mathcal{L}\psi \equiv (a_r + ia_i)\frac{\partial^2 \psi}{\partial x^2} + (\sigma_r + i\Omega)\psi + (d_r + id_i)\left(2|\phi|^2\psi + \phi^2\psi^*\right). \end{aligned} \tag{8.5}$$

In the case of our numerically computed spatially periodic solutions we can consider their stability to sub- and super-harmonic disturbances using Floquet theory and by solving an appropriate linear eigenvalue problem. Sirovich and Newton (1986) considered the superharmonic stability of the branch of periodic solutions which bifurcates from the uniform solution undergoing primary instability for $d_r = -1$. Time dependent calculations of the GL equation (Keefe, 1985) suggest that the periodic solution is stable for a range of the parameters but that a secondary instability occurs as the size of the periodic box is increased. Based on an assumption that the periodic solution loses stability when the equation

$$\mathcal{L}\psi = s\psi \tag{8.6}$$

has a real eigenvalue s passing through zero, they numerically calculated a curve of secondary instability for spatial period L as a function of one of the GL coefficients (they also plot a numerical calculation of the nonlinear dispersion relation for L as a function of Ω for fixed coefficient values). They compare their predicted point of instability with that found by Keefe and there is significant disagreement.

It is not clear to us however that the associated eigenvalue problem for the equation (8.5) is of the form (8.6). We therefore consider perturbations of the form

$$\psi = be^{st} + ce^{s^* t}$$

with b and c complex, or equivalently we split

$$\psi = \bar{u} + i\bar{v}$$

into real and imaginary parts such that the perturbation equation (8.5) becomes analytic. The coupled equations for $\bar{u}$ and $\bar{v}$ are assumed to have the time dependence

$$\bar{u} = e^{st}u \qquad \bar{v} = e^{st}v$$

which follows on taking Laplace transforms assuming a discrete spectrum for the eigenvalue s. As equations for $\bar{u}$ and $\bar{v}$ are real and linear we may always take the real part of any complex solutions that arise due to a complex eigenvalue s to ensure that $\bar{u}$ and $\bar{v}$ are real. We thus get a system of the form

$$\begin{pmatrix} u \\ v \end{pmatrix}_{xx} = \mathsf{A}(x,s) \begin{pmatrix} u \\ v \end{pmatrix} \tag{8.7}$$

where the 2 by 2 matrix A is L-periodic in x and linear in s. From Floquet theory, all bounded solutions of this system are of the form

$$\begin{pmatrix} u \\ v \end{pmatrix} = \mathsf{p}(x,s)e^{2\pi i\lambda x/L} \tag{8.8}$$

with p an L-periodic 2-vector and λ real, or linear combinations thereof. Substitution of (8.8) into the system (8.7) gives a system of the form

$$\mathsf{p}_{xx} + 2i\lambda\mathsf{p}_x - \lambda^2\mathsf{p} + \mathsf{A}(x,s)\mathsf{p} = 0. \tag{8.9}$$

$\mathsf{A}(x,s)$ is linear in s and thus we have a linear eigenvalue problem to solve for s given λ subject to L-periodic boundary conditions. $\lambda = 0$ for superharmonic disturbances to ϕ and $0 < \lambda < 1$ for subharmonic disturbances.

We discretized (8.9) by taking the derivatives using discrete Fourier transforms, usually with between 27 and 45 modes depending on the smoothness of ϕ and the resulting eigenfunctions. The eigenvalues s of the resulting matrix system were then found using a standard generalized eigenvalue solver. We also checked that the eigenvalues of largest real part which are of most interest were stable to the addition of more discretization modes. Another method of checking the accuracy of this procedure is to check the accuracy of the two eigenvalues that must sit at $s = 0$. This occurs due to the fact that the translation and phase invariance of the GL equation leads to the existence of two eigenfunctions such that

$$\mathcal{L}(\phi_x) = 0 \quad \text{and} \quad \mathcal{L}(i\phi) = 0.$$

We repeated the calculation of the stability of the branch considered by Sirovich and Newton for the parameters appropriate to Keefe's simulation which correspond to

$$a_r = 1 \qquad a_i = 4 \qquad d_r = -1 \qquad d_i = 4 \qquad \sigma_r = 1.$$

The branch was found using AUTO by continuing in the parameter β as described in the previous section and then the matrix A was calculated for a range of values of this parameter near the point where a pair of complex conjugate eigenvalues moved into the right half-plane indicating a loss of stability for ϕ. We interpolated the data for $\mathrm{Re}(s)$ versus period L to find the period at which $\mathrm{Re}(s) = 0$.

We find that for Keefe's set of coefficients we agree to 3 significant figures with his value of the period at which secondary instability occurs, which is $L_K = 5.72$. The corresponding value from Sirovich and Newton is $L_{NS} = 5.91$, the explanation for which we believe is due to their incorrect assumption on the eigenvalues s in (8.6). This is especially clear in the light of Keefe's (1985) time dependent simulations where the periodic orbit is seen to lose stability to a 2-torus solution, so that a Hopf

bifurcation introducing a second time scale is responsible for the loss of stability. The instability is thus triggered by a pair of complex conjugate eigenvalues crossing the imaginary axis, as is confirmed by our calculations, and will only be captured by the type of analysis leading to equation (8.9). This scenario is in fact suggested in a later paper by Newton and Sirovich (1986b), who unsuccessfully attempt to predict the point of secondary instability using perturbation methods assuming the unstable eigenvalue is real.

Our stability code was then used to test the stability of the various spatially periodic solutions we have found for the GL equation. We first determined the stability of the primary branch $P0$ described perturbatively for $\sigma_r = 1$ in Section 5.1. By testing residuals the second order approximation was found to be accurate for $0.147 < \Omega \lesssim 0.2$. Within this range three unstable eigenvalues were found, indicating the temporal instability of this branch to superharmonic disturbances.

We then tested the stability of the secondary branches Q1, Q2 and Q3 of symmetric periodic solutions we have found when $\sigma_r = 1$, and which were found using numerical continuation. Each of these was also found to be unstable to superharmonic disturbances. The smoothest branch 1 which approaches the breather solution had at least 2 eigenvalues in the right half-plane. The other branches which have more spatial structure were found to be even more unstable.

Similarly we tested the stability of the primary periodic branch $S1$ bifurcating from the uniform state when $\sigma_r = -1$ and $d_r = 1$. The numerical solution of this branch was used, and it was found to have several eigenvalues with positive real parts. Close to the bifurcation from the uniform state there are 4 eigenvalues in the right half-plane; at the other end of the branch where the orbit undergoes spatial period doubling there are up to 9 unstable modes.

These stability results are not particularly surprising due to the common belief that all integrations of the time dependent GL equation with periodic boundary conditions blow up when $d_r = 1$.

8.3 Stability of other solutions

Given that the quasi-periodic solutions are regular perturbations of the plane waves and the other branches of periodic solutions, it is reasonable to suppose that these are also temporally unstable.

We can also generally argue that the breather type solitary waves found for $\sigma_r > 0$ and $c = 0$ will be unstable to long wave perturbations in space, by noting that for large $|x|$ the amplitude is small and thus the perturbation satisfies

$$\frac{\partial \psi}{\partial t} \sim (a_r + ia_i)\frac{\partial^2 \psi}{\partial x^2} + (\sigma_r + i\Omega)\psi.$$

Small perturbations of the form

$$\psi = e^{st+ikx}$$

will satisfy the dispersion relation

$$s = -(a_r + ia_i)k^2 + (\sigma_r + i\Omega)$$

so that for sufficiently small wavenumber the perturbation will grow in time if $\sigma_r > 0$. This argument is essentially the one that also shows that the laminar state is stable (unstable) at subcritical (supercritical) Reynolds numbers.

We now consider the other solitary wave and transitional solutions found in Chapter 7. Determining the stability of travelling solitary wave solutions of nonlinear parabolic equations is a difficult problem in general. In model problems such as the Fisher equation (Dee and Langer, 1983), a continuum of fronts of speed c

connecting unstable and stable stationary uniform states can be found. In time dependent simulations, a unique front propagating into the unstable state is selected, which is found theoretically to be stable to the largest class of perturbations which decay exponentially at plus and minus infinity in the moving frame.

For the Ginzburg-Landau equation any such stability theory is complicated by the fact that the fronts are of the form $A = e^{-i\Omega t}\Phi(x - ct)$, with the asymptotic state at one end being (in the simplest case) spatially and temporally periodic. At present there is to our knowledge no analytic stability theory for such solutions. When $\sigma_r > 0$ we can argue that as such transition solutions connect states which are both unstable to long wave modulations, these structures will not in general persist. For $\sigma_r < 0$ the undisturbed state is linearly stable, however, and fronts were shown to exist for a continuum of Ω and c which define a transition between this state and (unstable) plane waves or quasi-periodic solutions as in Figures 7.5 and 7.11. As c was found to be negative/positive when the laminar flow is upstream/downstream, a localized plane wave disturbance would shrink in time and thus define only a transient type of structure as the stability of the undisturbed state dominates.

Nevertheless, in time dependent simulations of the GL equation (with nonlinear coefficient $d_r < 0$), Nozaki and Bekki (1983) have found that modulationally unstable plane waves can propagate into the unstable undisturbed state. A further transition to either a stable plane wave of large wavelength or chaotic state then develops behind the initial front. We cannot expect this behavior to carry over to the Poiseuille case of $d_r > 0$ due to the lack of finite amplitude stable states; however we hope that in the future similar numerical experiments will be carried out to ascertain if transition solutions appear at least as transients for the GL equation of Poiseuille flow. We will argue in the final chapter that the above lack of positive stability results for the GL equation does not preclude the existence of similar solutions in the full fluid equations which are stable.

CHAPTER 9

Application to Shear Flows

We believe that the existence of the quasi-steady solutions of the Ginzburg-Landau equation described in this thesis may be relevant to the study of transition in shear flows. In this final chapter we will give evidence to this effect and hypothesize the existence of solutions of the Navier-Stokes equations which have the features of transition from the laminar state.

9.1 The validity of the Ginzburg-Landau equation

The Ginzburg-Landau equation describes the evolution of modulations to the primary linear wave of instability for Poiseuille flow at Reynolds numbers near critical. The Stewartson-Stuart derivation of the GL equation will also apply to other flows for which there is a neutral curve of Orr-Sommerfeld type, and in this sense the GL equation is the generic amplitude equation for fluid problems where a continuum of wavenumbers becomes unstable as the control parameter is increased above a finite threshold.

In order to determine whether the features of the GL equation carry over to the Navier-Stokes equations, one must assess the structural stability of this truncation of the full equations and also its region of validity. This is a difficult question to address and arises whenever an approximation to the full physical model occurs. Presently all we are able to say is that the large class of quasi-steady solutions which we have found will persist under perturbations to the coefficients of the GL equation. This property is essential as we have used values of these coefficients that are approximate, coming from numerical calculation. In addition, the small

magnitude of s_r in the definition of ϵ (1.6) may allow the GL equation to have a relatively large range of validity in amplitude and Reynolds number.

Another question that we have so far not addressed is that of the choice of initial and boundary conditions for the GL equation. The derivation by Stewartson and Stuart (1971) assumes an infinitesimal localized initial condition which initially develops according to linear theory. This leads to localization in space for all finite time and thus the correctly posed boundary conditions for the GL equation are

$$|A| \to 0 \qquad \text{as } x \to \pm\infty \; . \tag{9.1}$$

This approach was taken to ensure that a self-consistent rational theory resulted. With an infinitesimal initial condition, for any fixed $Re < Re_c$ the solution will decay to the laminar state as the effect of the destabilizing nonlinearity of the GL equation will remain negligible. This issue is discussed in Hocking *et al.* (1972), and we agree with their conclusion that the GL equation contains the structure of the subcritical instability which is only revealed if finite amplitude GL solutions are considered. In this way we must relax Stewartson and Stuart's original assumptions in order to allow finite amplitude states for $Re < Re_c$. Similarly we have relaxed the condition (9.1) on almost all of the solutions we have discussed in this paper, with the exception of the breather solutions decaying at infinity. In our study of quasi-steady states it is only reasonable to allow the most general boundary condition possible,

$$|A| < K \qquad \text{for all } x,$$

as we have been studying the structure of the GL equation independent of the evolution of initial conditions. Most often we have found $|A|$ approaches a steady state at plus or minus infinity or is periodic for all x.

The numerical eigenvalue calculations in Chapter 8 for the stability of spatially periodic quasi-steady solutions for sub- and super-critical values of σ_r (and $c = 0$)

suggest that all of these solutions are temporally unstable. This is in agreement with numerical calculations for the time dependent equation. Our experience in solving the initial value problem for the GL equation relevant to Poiseuille flow with periodic boundary conditions is that solutions become unbounded in finite time because the nonlinear term is unable to cause amplitude saturation as it does when the real part of the nonlinearity is negative. In contrast, Hocking and Stewartson (1972) solved the initial value problem with zero end conditions on a finite domain, and their computations revealed solutions that remained bounded but appeared irregular in space and time. Our finite difference calculations are unable to confirm this, however, as we found that a localized initial condition quickly evolved into a spreading structure with increasingly fine spatial scales, so that the limit of spatial resolution is soon reached and numerical accuracy is lost.

In any case there are several motivations for studying the quasi-steady GL equation whose solutions are temporally unstable. The first is that the continuation of an unstable branch of solutions may lead to its stabilization at different parameter values. The canonical example for this is the existence of the plane waves $T_{\pm}$ in the GL equation. These give the existence for small amplitude of the equilibrium branch of travelling waves for Poiseuille flow described in Chapter 2. Although these travelling waves are unstable for both the Ginzburg-Landau and Navier-Stokes equations at small amplitude, they become stable to a general class of 2-dimensional perturbations at large amplitude at Reynolds numbers far less than Re_c of linear theory (Pugh, 1987), and are believed to play an important role in parallel shear flow instability. In this way we might expect other branches of solutions suggested by the GL equation for Poiseuille flow (e.g., fronts connecting a travelling wave to the undisturbed state) to have continuations down to lower Re, where we seek to find solutions indicative of the experimentally observed subcritical threshold (Nishioka,

1985). Secondly, the knowledge of the structure of steady solutions of a differential equation often lends insight into the dynamics of the time dependent problem. Moreover, with the use of dynamic control a physically desirable steady state may be attained which otherwise could never be observed without external forcing.

The many quasi-steady solutions that we have found for the GL equation derived for plane Poiseuille flow are often nonunique and exist for either a discrete or continuous spectrum of the two undetermined parameters Ω and c, the temporal frequency and wave speed correction to the group velocity of linear theory. This degeneracy often arises in parabolic problems where the wave speed is left undetermined. Hence if these periodic solutions are relevant to the unsteady Poiseuille problem one may hope to find an underlying selection mechanism so that only a few of the solutions are realized in the initial value problem.

9.2 Interpretation of the quasi-steady solutions

Given that the above scenario holds and that the solutions for the Ginzburg-Landau equation that we have found are in direct correspondence with solutions of the Navier-Stokes equations, the periodic and quasi-periodic GL solutions seem to describe quasi-periodic packets of instability. A large range of solutions exists for both sub- and super-critical Reynolds numbers, whose modulating envelopes possess different temporal frequencies of oscillation and varying speeds about the group velocity of linear theory. Such weakly nonlinear modulations to Tollmien-Schlichting waves have been observed in the pioneering experiments of Schubauer and Skramstad (1947) in their study of laminar boundary layer transition, as shown in Figure 9.1. These slow modulations appear downstream of the leading edge of the flat plate and persist until 3-dimensional bursts develop. For plane Poiseuille flow experimental work is far more difficult and incomplete than for boundary layers, and it is less clear what the secondary processes of transition from the initial growth of

T-S waves are, although it appears that the onset of 3-dimensional effects occurs much sooner than in the boundary layer (Nishioka, 1985).

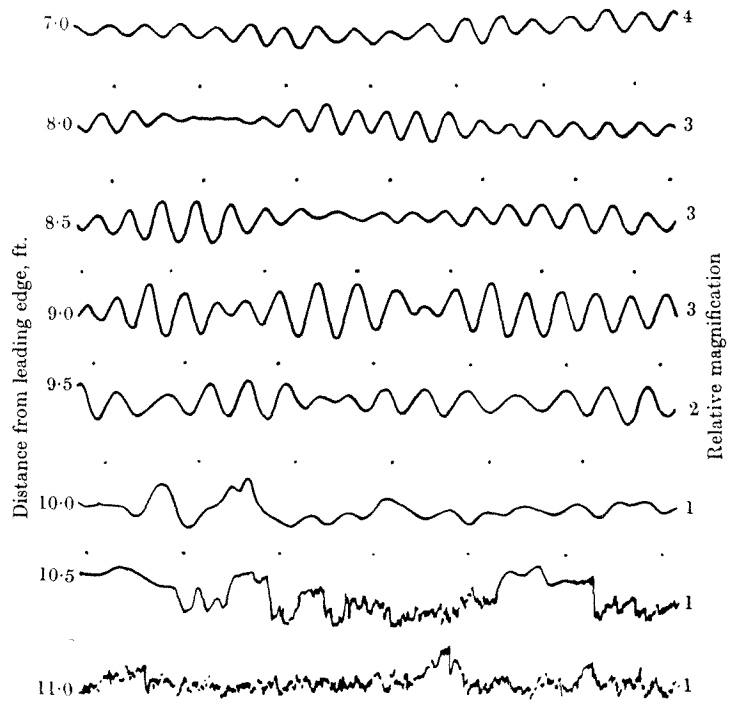

FIG. IX. 13. Oscillograms of u-fluctuations showing laminar boundary-layer oscillations in boundary layer of flat plate. Distance from surface, 0·023 in.; $U_0 = 53$ ft/sec; time interval between dots, 1/30 sec.

FIGURE 9.1. Velocity traces from the boundary layer experiments of Schubauer and Skramstad (1947).

The modulated Tollmien-Schlichting waves suggest that the wave packet develops in a weakly nonlinear manner until breakdown far down the plate.

The periodic envelope solutions are also reminiscent of the slugs and puffs of instability that divide sections of laminar flow in pipe flow. We cannot dwell on this similarity as it is accepted that there is no point of linear instability for circular pipe flow, and thus it is not clear that one can derive an equation of Ginzburg-Landau type for this flow. In circular pipe flow, however, the experimental results suggest that if the laminar solution is perturbed sufficiently, there appears to exist a subcritical instability to a finite amplitude state. It is therefore possible that the

structure of the GL equation, in allowing the description of finite amplitude periodic and quasi-periodic solutions for $\sigma_r < 0$, in some way models these subcritical states.

The solitary wave solutions of the GL equation and their generalizations which correspond to stable and unstable manifolds in phase space are of particular interest because we know that the four fixed points in the reduced phase space we have studied correspond with known solutions of the full 2-dimensional Navier-Stokes equations.

The breather-type solutions are a class of solutions where the envelope of the T-S waves is localized so that the flow is laminar both up and downstream. We expect that there is an infinite number of these solutions moving at the group velocity with a given discrete set of temporal frequencies. These solutions arise as the limiting cases of the periodic solutions when the wavelength tends to infinity.

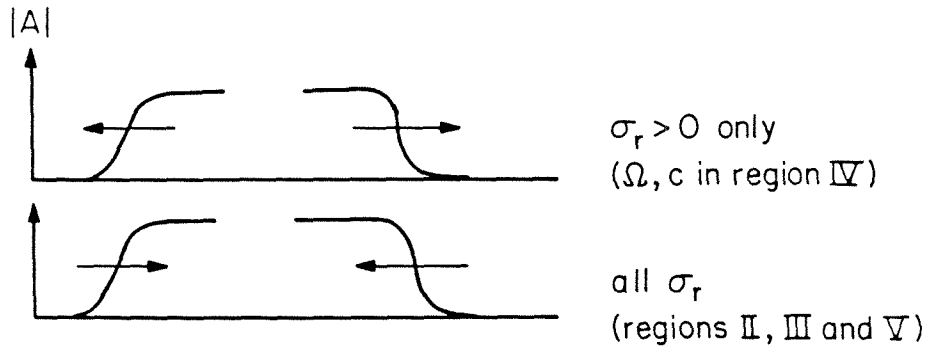

FIGURE 9.2. Schematic diagram of front solutions.
The GL equation supports front solutions moving faster than the group velocity only for supercritical σ_r.

The front solutions describing a sharp transition between undisturbed flow and a plane wave and are found to exist at a given Reynolds number for a continuous spectrum of frequency and speed. A front from wavelike to laminar behavior travelling faster than the group velocity ($c > 0$) exists only for supercritical Reynolds numbers ($\sigma_r > 0$). Similarly, by symmetry, there will also exist a transition from the

laminar to wavelike state travelling slower than the group velocity. See Figure 9.2. If we think of these solutions as approximating the front and rear sections of a fully time dependent section of instability, these results suggest that in a neighborhood of the critical Reynolds number, the instability can spread only for $Re > Re_c$, but can decay for Re on either side of Re_c.

The solutions connecting plane waves of the same or different wavenumber which can exist for a continuum of temporal frequencies or speeds are more difficult to interpret. These, however, may be quite likely to exist in the full fluid equations as connecting solutions between the well established finite amplitude steady waves.

Lastly we have found transition solutions described by the unstable manifolds of the plane waves and laminar state in region III of parameter space either side of critical. The transition from undisturbed flow to a more complex finite amplitude state which is spatially quasi-periodic or chaotic in the moving frame is of particular interest. The former were found to exist for σ_r either side of critical; the latter for a supercritical value only. These finite amplitude complex quasi-steady states are in need of further investigation both in the context of the GL equation and plane Poiseuille flow.

9.3 **Final remarks**

Any reasonably complete theory of laminar-turbulent transition must be able to describe the 3-dimensional structures that are observed in shear flows. Studying 2-dimensional weakly nonlinear models such as that of the GL equation is not irrelevant, however, as experimentally there are many stages in transition, the first of which appears to reveal 2-dimensional modulations of the primary instability of the base flow, in accordance with Squire's theorem for parallel shear flows (Drazin and Reid, 1981). We point out the existence of a 3-dimensional generalization of

the GL equation derived for plane Poiseuille flow by Davey, Hocking and Stewartson (1974), which consists of the 3-dimensional analogue of the GL equation coupled with an elliptic equation for the spanwise pressure gradient. It may be possible to find fully 3-dimensional quasi-steady structures for this equation, and some work on 3-dimensional plane wave stability has recently been carried out by C. Holmes (1985).

An aim for the future is to be able to find quasi-steady solutions to the equations of two-dimensional plane Poiseuille flow that are continuations of those found for the GL equation. The existence of multiple scales in both space and time suggests that the straight forward Galerkin and collocation methods used to find the equilibrium travelling wave solutions would render the discretized problem prohibitively large even on current super-computers. In the future we hope that an application of other approximate but fully nonlinear methods to the Navier-Stokes equations will reveal the fronts and periodic structures described in this thesis.

Bibliography

Broer H. W. (1983),
"Bifurcations of singularities in volume preserving vector fields," Ph.D. thesis.

Davey, A., Hocking, L.M. and Stewartson, K. (1974),
"On the nonlinear evolution of three-dimensional disturbances in plane Poiseuille flow," *J. Fluid Mechs.* **63**, 529-536.

Dee, G. and Langer, J. S. (1983),
"Propagating pattern selection," *Phys. Rev. Letts.* **50** 383-386.

Deissler, R.J. (1985),
"Noise-sustained structure, intermittency, and the Ginzburg- Landau equation," *J. Stat. Phys.* **40**, 371-395.

Doedel, E.J. and Kernevez, J.P. (1985),
"Software for continuation and bifurcation problems," (Applied Math. Tech. Rep., Caltech).

Drazin, P.G. and Reid, W.H. (1981),
Hydrodynamic Stability, Cambridge University Press.

Golubitsky, M. and Stewart, I. (1985),
"Hopf bifurcation in the presence of symmetry," *Arch. Rat. Mech. Anal.* **87**, 107-165.

Herbert, T. (1981),
"Stability of plane Poiseuille flow – theory and experiment," *Fluid Dynamics Transactions* **11**, 77-126.

Hirota, R. (1976),
"Direct method of finding exact solutions of nonlinear evolution equations"' in *Bäcklund Transformations*, ed. R.M.Miura, Lecture Notes in Math. vol. 515, Springer-Verlag 1976, 40-68.

Hocking, L.M. and Stewartson, K. (1972),
"On the nonlinear response of a marginally unstable parallel flow to a two-dimensional disturbance," *Proc. Roy. Soc.* **A 326**, 289-313.

Hocking, L.M. and Stewartson, K. and Stuart, J.T. (1972),
"A nonlinear instability burst in plane parallel flow," *J. Fluid Mech.* **51**, 705-735.

Holmes, C.A. and Wood, D. (1985),
"Studies of a complex Duffing equation in nonlinear waves on plane Poiseuille flow," (preprint, Imperial College London)

Holmes, C.A. (1985),
"Bounded solutions of the nonlinear parabolic amplitude equation for plane Poiseuille flow," *Proc. Roy. Soc.* **A 402**, 299-322.

Holmes, P. (1986),
"Spatial structure of time-periodic solutions of the Ginzburg- Landau equation," *Physica* **23D**, 84-90.

Keefe, L.R. (1985),
"Dynamics of perturbed wavetrain solutions to the Ginzburg-Landau equation," *Studies in Appl. Math.* **73**, 91-153.

Kevorkian, J. and Cole, J. D. (1981),
Perturbation Methods in Applied Mathematics, Springer-Verlag.

Kopell, N. and Howard, L.N. (1981),
"Target patterns and horseshoes from a perturbed central-force problem: some temporally periodic solutions to reaction diffusion equations," *Studies in Appl. Math.* **64**, 1-56.

Moon, H.T., Huerre, P. and Redekopp, L.G. (1983),
"Transitions to chaos in the Ginzburg-Landau equation," *Physica* **7D**, 135-150.

Newell, A.C. and Whitehead, J.A. (1969),
"Finite bandwidth, finite amplitude convection," *J. Fluid Mechs.* **38**, 279-303.

Newton, P.K. and Sirovich, L. (1986a),
"Instabilities of the Ginzburg-Landau equation: periodic solutions," *Quart. J. Applied Math.* **43**, 535-542.

Newton, P.K. and Sirovich, L. (1986b),
"Instabilities of the Ginzburg-Landau equation: part II, secondary instability," *Quart. J. Applied Math.* **44**, 367-374.

Nishioka, M., Iida, S. and Ichikawa, Y. (1975),
"An experimental investigation of plane Poiseuille flow," *J. Fluid Mechs.* **72**, 731-751.

Nishioka, M. (1985),
"Laminar-turbulent transition in plane Poiseuille flow," in *Recent Studies on Turbulent Phenomenon*, 193-203.

Nozaki, K. and Bekki, N. (1983),
"Pattern selection and spatiotemporal transition to chaos in the Ginzburg-Landau equation," *Phys. Rev. Letts.* **51** 2171-2174.

Nozaki, K. and Bekki, N. (1984),
"Exact solutions of the generalized Ginzburg-Landau equation," *J. Phys. Soc. Japan* **53** No. 5, 1581-1582.

Pugh, J. (1987),
"Finite amplitude waves in plane Poiseuille flow," Ph.D. thesis, Caltech (to appear).

Schubauer, G.G. and Skramstad H.K. (1947),
"Laminar boundary-layer oscillations and stability of laminar flow," *J. Aero. Sci.* **14**, 69-78.

Sirovich, L. and Newton, P.K. (1986),
"Periodic solutions of the Ginzburg-Landau equation," *Physica* **21D**, 115-125.

Stewartson, K. and Stuart, J.T. (1971),
"A non-linear instability theory for a wave system in plane Poiseuille flow," *J. Fluid Mechs.* **48**, 529-545.

Zahn J.-P., Toomre, J., Spiegel, E.A. and Gough, D.O. (1974),
"Nonlinear cellular motions in Poiseuille channel flow," *J. Fluid Mechs.* **64**, 319-345.